Improving the classification of different Land and Forest cover types on remotely sensed imagery to support REDD+: A comparative study in the Afram Headwaters Forest Reserve, Ghana.

Torgbor, Adjah Benjamin

March, 2012

Course Title:	Geo-Information Science and Earth Observation for Environmental Modelling and Management (GEM).
Level:	Master of Science (MSc.).
Course Duration:	August, 2010 – March, 2012.
Consortium partners:	Lund University (Sweden). International Institute for Geo-Information Science and Earth Observation (ITC) (The Netherlands).

Improving the classification of different Land and Forest cover types on remotely sensed imagery to support REDD+: A comparative study in the Afram Headwaters Forest Reserve, Ghana.

by

Torgbor Adjah Benjamin

Thesis submitted to the Faculty of Geo-information Science and Earth Observation, University of Twente in partial fulfilment of the requirements for the degree of Master of Science in Geo-information Science and Earth Observation, Specialisation - Environmental Modelling and Management.

Thesis Assessment Board

Chairman:	Dr. Yousif Hussin (ITC – UT, The Netherlands)
External Examiner:	Prof. Petter Pilesjö (Lund University – Sweden)
First Supervisor:	Dr. Michael Weir (ITC – UT, The Netherlands)
Second Supervisor:	Drs. Eduard Westinga (ITC – UT, The Netherlands)

UNIVERSITY OF TWENTE.

ITC FACULTY OF GEO-INFORMATION SCIENCE AND EARTH OBSERVATION

Disclaimer

This document describes work undertaken as part of a programme of study at the Faculty of Geo-information Science and Earth Observation, University of Twente. All views and opinions expressed therein remain the sole responsibility of the author, and do not necessarily represent those of the institute.

Dedicated to:

My wonderful family especially Patricia and Kevis Hugh

Abstract

Tropical deforestation is an issue of global concern and, in recent times, has been noted to be a major driver of climate change due to the release of CO_2 into the atmosphere through the activities of man. There are efforts by the international community to mitigate climate change. One such intervention is the REDD+ programme as proposed under the Kyoto Protocol of the UNFCCC.

Ghana ratified this convention on 26th November, 2002 in order to reduce emissions from deforestation and forest degradation and also qualify for financial incentives by way of the so-called “Carbon Credits”. Important criteria for this are the regular monitoring, verification and reporting on the changes in the landcover of a participating nation. This therefore requires an accurate landcover map of the areas earmarked for the REDD+ programme. However, adequate high resolution multi-temporal optical data is often not available in the tropics where cloud cover is inevitable. In this situation, SAR provides a useful alternative.

This study seeks to develop a suitable method that will improve the classification accuracy of different land and forest cover types by testing the MLC and OBIA techniques on ASTER and SAR data separately and in combination, to support the REDD+ programme in Ghana. A comparative study was conducted in the Afram Headwaters Forest Reserve in the Ashanti Region of Ghana. Previous studies in the area applied only the MLC algorithm on the above datasets and did not attempt to classify the datasets separately and in combination to compare the results either spatially or statistically or both.

When compared spatially, the ASTER alone and combined ASTER+SAR maps showed over 70% agreement between MLC and OBIA. The SAR alone map showed 64% agreement. Statistically, the hypothesis that, there is no significant difference in the classification results (Kappa) between MLC and OBIA was confirmed. Furthermore, there is no significant difference between the kappa of ASTER alone and combined ASTER+SAR maps for both MLC and OBIA. There is, however, a significant difference between the MLC and OBIA classified maps of ASTER /SAR alone and SAR alone/combined ASTER+SAR.

The overall best landcover map of the Afram Headwaters Forest Reserve (AHFR) was produced from the MLC of the combined ASTER+SAR data with an accuracy of 82.09% and a Kappa of 0.74. Five classes (Natural Forest (NF), Plantation (P), Agroforestry (AF), Settlement/Bareground (S) and Fallow/Grassland (FG)) and four classes (NFP, AF, S and FG) were identified on the ASTER and SAR data respectively.

There is a potential for image combination to improve the classification accuracy of SAR. After the combination, the accuracy of SAR improved by 14% and 21% by applying MLC and OBIA respectively.

Acknowledgements

My heartfelt gratitude goes to the Netherlands Fellowship Programme (NFP) for providing a fellowship to enable me to follow this prestigious MSc. programme. My special thanks go to the course coordinators and staff of the GEM programme, both in Lund University, Sweden and ITC, the Netherlands. I wish to also acknowledge the support of the Forestry Commission (FC), Ghana, for offering me the study leave to enrol on this course.

I am highly indebted to Dr. Michael Weir, and Drs. Eduard Westinga, first and second supervisors respectively, for the many ideas you shared and your willingness to discuss anything new I came up with. You really boosted my confidence. I cannot forget your encouragement during my stressful times. To Dr. Yousif Hussin, I say a very big thank you for the suggestion of the topic and your assistance throughout the period of my study. Dr. Hein van Gils and Ir. Louise van Leeuwen, I appreciate your support very much.

I wish to thank all staff of FC-FSD Headquarters, Regional and District offices who supported me directly during my fieldwork especially Mr. H.C.A Brown, Mr. Iddrisu (ADM), Felix Nyantekyi (RS), Francis Brobbey (Forester), Mr. Kwadwo Wireko (FG), Mr. Thomas Agyemang (FG) all of Offinso District. Mr. Yakubu and Mr. D. Baidoo of the RMSC-GIS Unit. I also appreciate the support of Mr. Kojo Fodjour (Manager, MPL) and all the staff of MPL.

I am very grateful to Justice Odoiquaye Odoi, Kwame Botchwey and Stephen Donkor for their support. Thanks to all my friends in ICF, Enschede especially Kathini for your encouragement when things were tough. To all my Ghanaian colleagues especially Yvonne, Georgina, Robert, Sadick and Richard I say thank you for your friendship.

My sincere gratitude goes to all my GEM classmates especially Speeder Lu and Abel Chemura for your friendship. I was privileged to study with you. I managed to learn part of your culture and especially your language. I cannot forget this part of my life I shared with you.

I highly appreciate my parents Mr. David A. Torgbor and Mrs. Patience. K. Torgbor for their love, prayers and the opportunity they gave me to come this far. Sincere thanks to my brothers Obed Torgbor, Isaac Torgbor and Daniel Torgbor for their constant prayers and encouragement. I cannot end without appreciating the love, understanding and patience of my lovely wife Patricia Torgbor and my amazing son, Kevis Hugh Torgbor. You are my source of inspiration. When the oceans rose and thunders roared I held on because of you.

Table of Contents

List of figures

List of tables

1.0 INTRODUCTION

1.1 Background

Forest ecosystems provide a wide variety of services such as the conservation of soil, water, biodiversity and carbon sequestration for climate change mitigation (de Groot *et al*., 2002). The role of forests in the global carbon cycle has become a major concern in recent times (Cramer *et al*., 2004). Forests also offer direct and indirect economic opportunities for rural communities such as sale of non-timber forest products including firewood, snails, mushrooms and chewing stick, particularly in West Africa. They also provide timber for local construction and export.

Ghana is well endowed with natural resources, including forests. In the year 1900, Ghana had a tropical high forest area of approximately 8.2 million hectares. According to the Forestry Commission Ghana (2009c), by the year 2005 this area had reduced to 1.2 million hectares. In concurrence, the FAO (2010) has reported that the annual rate of the country's deforestation was 135,000 hectares per year in 2010. This is twice the rate (65,000 hectares per year) quoted by the Forestry Commission for 2005 (Forestry Commisson Ghana, 2009c). The alarming rate of deforestation has been caused mainly by unsustainable but legal logging, illegal chainsaw operations, legal and illegal gold mining (commonly called "galamsey"), infrastructural development and agricultural practices such as slash and burn (shifting cultivation) methods of land preparation (Metz, 2009). The consequence is a change in landcover and its associated impacts on the proper functioning of ecological, hydrological and atmospheric processes.

On the other hand, forests serve as the main source of livelihood for about 70% of rural communities in Ghana (Birikorang *et al*., 2001). Moreover, about 4% of the country's GDP is contributed by the forestry sector which is the fourth foreign exchange earner, providing 11% of the export earnings (Birikorang *et al*., 2001). Ghana therefore depends on its forest resources to support vital socio-economic and national development. In addition to the local benefits, Ghana's forest constitutes an important part of the global tropical forest system and the country is a major player in the production and trade of tropical timber.

In view of this, Ghana, like many other tropical countries, has ratified the Reduced Emissions from Deforestation and Degradation plus (REDD+) programme under the Kyoto protocol of the United Nation Framework Convention on Climate Change (UNFCCC) to enable it to reduce emission of CO_2 resulting from deforestation and forest degradation (UNEP, 2011). With respect to REDD+, countries that reduce emission of CO_2 and stop forest degradation through rigorous plantation development and halting deforestation, are given financial incentives by way of so-called "carbon credits" (Walker *et al*., 2010). However, to access these funds, there is the need for a proper assessment of the country's carbon stock for an equitable carbon accounting. Another condition under the Kyoto protocol is a regular monitoring (Walker *et al*., 2010) of landcover change in member countries. Producing accurate landcover maps and indicating their associated uncertainty and quality by way of accuracy assessment through a confusion or error matrix as proposed by the Intergovernmental Panel on Climate Change (IPCC) (2003), provides credibility to a country's membership to the Kyoto Protocol. The confusion matrix, in addition to the producer's and user's accuracies computation possibilities it provides, forms the basis for further analyses by way of statistical testing for significance using the Cohen's Kappa statistics (Foody, 2002). This will be discussed further in Chapter 2.

If well done, field (ground-based) methods of landcover mapping and carbon stock measurement are the most accurate (Lu, 2006). However, they are time consuming, destructive, arduous and expensive due to the large areas involved. Remote sensing (RS) based methods provide an efficient way of landcover mapping and carbon stock estimation since it covers a large area with relatively less time and cost (Lu, 2006). Multispectral satellite remote sensing methods are appropriate for this purpose, but require a cloud free condition which is practically impossible in the tropics. This therefore reduces the applicability of multispectral data acquired in tropical conditions for landcover studies. It is therefore important for the RS community to develop RS and Geographical Information Systems (GIS) techniques that can be used in combination with field measurements to accurately map landcover and biomass carbon (Gaston *et al*., 1998).

Several studies have applied different methods and types of satellite data ranging from low to high resolution optical and radar images for landcover classification and mapping (Ainsworth *et al*., 2009; Benz & Pottier, 2001; Chu *et al*., 2007; Mallinis *et al*., 2008; Sun, 2004; Thiel *et al*., 2006). The application of an object oriented image analysis (OBIA) technique (discussed in Section 2.3) on high spatial resolution optical image has given more accurate estimates of carbon stock (Blaschke, 2010; Ouyang *et al*., 2011) than low or medium resolution data. OBIA has also been found to show promising enhancements on classification compared to other pixel-based techniques (Hay & Castilla, 2008) such as Maximum Likelihood Classification (MLC), a technique also discussed in Section 2.2.1. However, high spatial resolution images are very expensive, especially for a developing country like Ghana, and may not be available for a larger area. Other limitations of the high resolution data include the presence of shadows, haze and clouds on the acquired image. Moreover, the OBIA technique cannot be carried out on a large area / datasets due to data processing (software) limitations (Hay & Castilla, 2008). There is therefore a challenge to accurately map landcover, above ground biomass (AGB) and carbon stock over a large area.

Synthetic Aperture Radar (SAR) data has an advantage over optical data (high, medium and low resolution images) in terms of atmospheric disturbances such as cloud and haze. In the tropical ecosystems especially, where cloud cover prevails (Mitchell *et al*., 2010) radar is able to penetrate the clouds and acquire data both day and night (IPCC, 2003) and under all weather conditions (Dostovalov *et al*., 2010). SAR also has the capability of separating forests from other landcover types. Recently, a study (Nguyen, 2010) based on ALOS PALSAR data instead of high resolution multispectral satellite data estimated carbon stock in the Afram Headwaters Forest Reserve (AHFR) in Ghana. The study also identified four main landcover classes in the study area. The focus of this research was to build on previous research in the area by exploring the possibilities of improving the accuracy in classifying and mapping the landcover in the area using the OBIA technique (Lefebvre *et al*., 2008; Riggan Jr. & Weih Jr., 2009; Thiel *et al*., 2006) in addition to the MLC that was used by Dwomoh (2009) and Nguyen (2010) in the Afram Headwaters Forest Reserve (AHFR), to support REDD+ in Ghana.

SAR data has a problem with speckle noise (Figure 1). This causes degradation of the image quality that makes detection of different ground features and classification very challenging (Jarabo-Amores *et al*., 2009). Speckle noise is a bright and dark (salt and pepper) pattern in a SAR image due to the coherent nature of the radar system (Lopez-Martinez & Fabregas, 2003). It is a result of the wide random variation in radar beam as it passes over an extended target. Popular SAR processing techniques, such as filtering and multi-look processing, are noted to reduce speckle noise but end up diminishing the textural information of the SAR data (Fernandez, 2002). Other algorithms based on filtering pixels with homogenous regions have successively been developed (Lee *et al*., 2009; Walessa & Datcu, 2000). Their usefulness lie in their precise measurement of heterogeneity in a scene, thereby preserving the edge and textural information for further processing of SAR data (Jie *et al*., 2009).

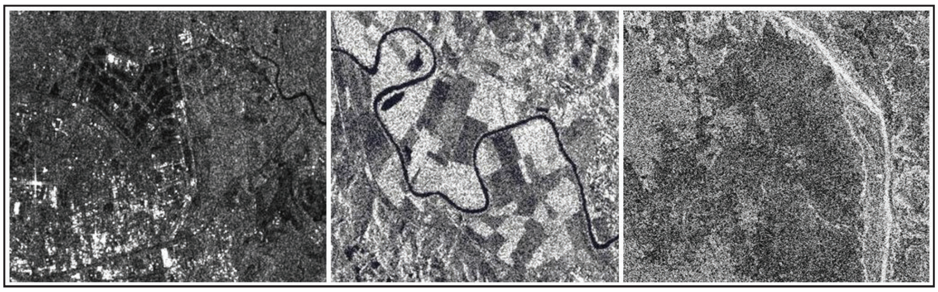

Figure 1: Different SAR datasets showing speckle noise (salt and pepper pattern)
Source: Google images

Although SAR data provides very high spatial and textural information it has less spectral information (Sun, 2004). The IPCC (2003) has recognized SAR data as one of the most important RS data for landcover classification and supports the argument that combining different types of RS data (fusion of optical and SAR) of different spatial and spectral resolution can be used to categorize different landcover types accurately. An image fusion technique provides the opportunity of producing an image that takes advantage of both the spectral and spatial or textural domain of multi-sensor data (e.g. ALOS PALSAR data and a multispectral ASTER data). This therefore improves the separation of different cover classes in landcover classification (Benz *et al*., 2001; Pohl & Van Genderen, 1998). Image fusion can also be very effective in speckle noise reduction (Pohl & Van Genderen, 1998; Youshi *et al*., 2009).

Pohl & van Genderen (1998) argued that fused or combined images enhance interpretation capabilities and produce more reliable results through the combination of characteristics from different data sources. Hence, the classification accuracy of RS data is improved. For instance, some vegetation stands and species (e.g. cocoa) are difficult to separate from forests since their spectral response is similar. However, with the combination of SAR data which introduces shape, surface roughness and moisture content these stands can be differentiated (Pohl & Van Genderen, 1998). Image fusion of optical and SAR data may provide a cost effective approach to continuous landcover monitoring, especially in developing countries.

1.2 Conceptual Framework

The conceptual diagram (Figure 2) below puts the project in perspective. In summary, the REDD+ programme of the UNFCCC requires an accurate forest and landcover map through an improved classification method using remotely (satellite) sensed data covering the forest under consideration. This baseline information is important to relevant agencies and governments of member countries ratifying the Kyoto protocol to regularly monitor the changes in the forest/landcover.

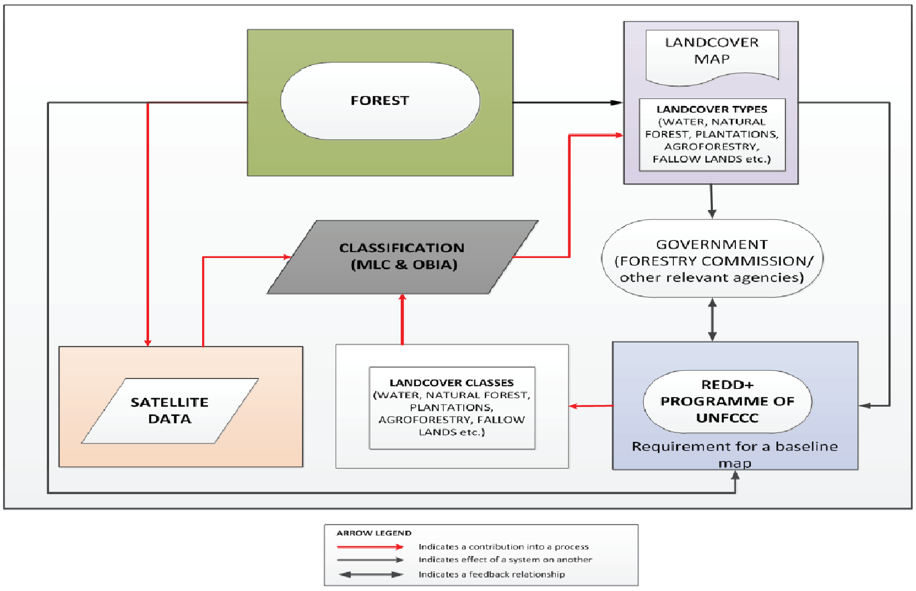

Figure 2: Conceptual diagram of the research

1.3 Problem Statement

The issue of accurate and consistent landcover maps is a challenge to the realization of the goals of the REDD+ programme in Ghana. Low accuracies in landcover maps have mainly resulted from the type of datasets and methods applied in their analyses. For instance, in the tropics, where cloud cover is a major challenge, the applicability of a multispectral data is limited. SAR (which can acquire data at anytime under any weather condition) provides a better alternative source of data but its usage is also limited due to the difficulty associated with its classification and information extraction. Also the quality of SAR data is reduced due to its inherent speckle noise which makes its usage in remote sensing analyses very challenging, though it contains more useful spatial information than other sensor data such as ASTER or Landsat TM alone (Jarabo-Amores *et al.*, 2009; Tupin, 2010). Several methods that exist for SAR data classification and reduction of speckle noise are mainly pixel based image analyses techniques that were originally developed for spectral (and not spatial or textural) domain analyses. Those methods also use different filters for speckle reduction to improve accuracy (Jarabo-Amores *et al.*, 2009). However, the use of these filters eventually results in
the diminishing of vital spatial information in the data (Fernandez, 2002), in most cases resulting in higher uncertainties.

A review of recent previous studies in the AHFR show that only a pixel based classification approach (MLC) was used for mapping the landcover. Dwomoh (2009) classified an ASTER data alone using MLC to produce a landcover map of the AHFR.

In the same study area, Nguyen (2010) combined ASTER and SAR data to produce the landcover map. However, these studies did not attempt to classify SAR alone or even compare the pixel based algorithm with any other approach like an object based image analyses technique. It is important then, to apply a different approach (e.g. OBIA) and systematically compare the outcome with the MLC.

There is therefore the need for the development of a remote sensing based approach that will take advantage of the availability of SAR data by retaining and using its textural and spatial information in combination with an optical data that will provide information on the spectral properties of the scene to be classified for an enhanced image interpretation and improved classification accuracy. Such a method will be useful in the extraction of other information such as landcover types over a large extent for accurate mapping purposes. This approach will be cost effective and less labour intensive (Pohl & Van Genderen, 1998).

1.4 Research Objectives

In view of the above, this research was conducted to develop an appropriate method to extract information and accurately classify different landcover types in the AHFR to support the REDD+ program in Ghana using MLC and OBIA on ASTER, SAR and combined ASTER+SAR data. The success of this research therefore will be the solution to the challenge of obtaining high accuracy and covering a larger area in mapping forest and landcover which will contribute to Ghana's preparation and implementation of the REDD+ programme (Forestry Commisson Ghana, 2009a).

The following **specific objectives** were pursued:

1. To investigate which landcover classes in the study area can be identified from SAR and ASTER images.
2. To compare, statistically and spatially, two different procedures for classifying landcover in the study area namely:
   (i) MLC on SAR, ASTER and combined ASTER+SAR data.
   (ii) OBIA on SAR, ASTER and combined ASTER+SAR data.
3. To evaluate the effects of 3 different filters (3x3, 5x5 and 7x7) and different texture combinations in improving the classification accuracy of ASTER, SAR and combined ASTER+SAR data.
4. To evaluate the potential of image combination in improving classification accuracy.
5. To produce an accurate landcover map of the study area using the best result from the filtered SAR, ASTER and combined ASTER+SAR data classification.

1.5 Research Questions

1. What relevant landcover information (classes) can be identified from the classification of SAR and ASTER data?
2. Are there significant differences (Statistical and Spatial) in the quality of landcover type classification obtained from MLC and OBIA on ASTER, SAR and ASTER+SAR data?
3. Which kind of texture (in OBIA) combination gives the best results in ASTER, SAR and combined ASTER+SAR data classification?
4. Which filter window (in MLC) gives the best result in ASTER, SAR and combined ASTER+SAR data classification?
5. What is the overall best classification accuracy in terms of Kappa obtained from ASTER, SAR and combined ASTER+SAR data classification?
6. What is the quality of the landcover map produced from the overall best classification of ASTER, SAR and combined ASTER+SAR data?

1.6 Research Hypotheses

1. There is no significant difference in the classification results (kappa) between OBIA and MLC.

   [H_O: $\widehat{K}_1 = \widehat{K}_2$] and
   [H_A: $\widehat{K}_1 \neq \widehat{K}_2$]

   Where:
   H_O and H_A are the null and alternative hypotheses respectively, $\widehat{K}_1$ and $\widehat{K}_2$ are the estimate of kappa for MLC and OBIA maps to be compared respectively.

2. There is no significant difference in the classification results between SAR alone and combined ASTER+SAR data for both MLC and OBIA.

   [H_O: $\widehat{K}_1 = \widehat{K}_2$] and
   [H_A: $\widehat{K}_1 \neq \widehat{K}_2$]

3. A better MLC classification accuracy of ASTER, SAR and combined ASTER+SAR data is obtained by using 5x5 instead of 3x3 and 7x7 window filtering.

4. The overall best classification accuracy can be obtained from combined ASTER+SAR data.

1.7 Justification

The experience with radar remote sensing, data analysis and other applications of SAR, particularly landcover classification, in West Africa, for example in Ghana, is not well developed as applications in low and medium resolution optical data. SAR data can be very useful for accurate landcover classification if the appropriate methods can be developed and used. The combined use of SAR data which is difficult to classify due to the problem of speckle noise and low spectral information; and OBIA will present a novel approach to SAR image classification in the study area and Ghana as a whole. OBIA on SAR data especially, is a relatively new area of image classification and this study will contribute to the already ongoing efforts to improve classification accuracy and speckle noise reduction.

The targeted method/approach, when developed, would put Ghana in a better position to benefit from the financial incentives (Carbon credits) that would be given to Countries ratifying and fulfilling the conditions in the REDD+ programme of the Kyoto Protocol under the UNFCCC. Ghana would stand a better chance of benefitting financially because the method will provide regular monitoring capabilities in terms of data source (e.g. ASTER, SAR or combined ASTER+SAR depending on cloud cover conditions prevailing at a given period in the tropics) as well as the use of a robust accuracy assessment approach as required by the UNFCCC.

2. 0 LITERATURE REVIEW

This literature review chapter provides an overview of the various components of this research as summarised in the conceptual framework (Figure 2). It reviews literature on the methods, datasets for this research and the specific management information on the study area.

2.1 Remote Sensing And Forestry

Ground-based tropical forest monitoring and mapping has often been challenging due to the complex nature of the terrain and large areas of forests involved. Remote sensing (RS) thus provides a good platform for tropical forest and other land-based monitoring. Remotely sensed data have been used widely for landcover mapping and other applications in forestry. Historically, landcover classification systems for use with RS data was developed by the United States Geological Survey (USGS) in the mid-1970s (Lillesand *et al*., 2008). Lillesand *et al*. (2008) outlined the 10 main criteria for the classification system developed by the USGS. These criteria were developed before the proliferation of computer-aided RS image classification. Consequently, computer-aided image classification has brought in its wake several complexities. These therefore make the practical application of some of the criteria, for example criteria 1 and 2 (minimum acceptable classification accuracy of 85% spelt out in the criteria) impossible (Lillesand *et al*., 2008).

Other applications of RS in forestry include tree species identification, timber volume estimation, survey and assessment of disease and pest damage to trees. The next sections briefly discuss the two main types of remote sensing and their applications in Forest management, particularly landuse/landcover mapping.

2.1.1 Passive Remote Sensing (Optical Sensors)

The principal remote sensing techniques used in Natural Resources Management (NRM), including forest management and landcover mapping, use passive sensors. Passive optical sensors record reflected radiation from the visible and near infrared portions of the electromagnetic spectrum. Optical remote sensing offers large area coverage and frequent revisit capabilities which makes its use in forest mapping at various scales viable (Toan *et al*., 2001). However, passive remote sensing can only take place when the sun illuminates the earth. This can be a major disadvantage in areas with frequent cloud cover. As a result, there are many regions in the tropics where passive remote sensing can rarely be effectively used. Thus, for such regions, active remote sensing by means of radar is a useful alternative.

Optical sensors are categorised based on their spatial resolution. They may be low/course, medium and high resolution depending on the pixel size (spatial resolution) of the image under consideration. The sections below are devoted to brief discussion of the different spatial resolutions mentioned above.

2.1.1.1 High Resolution

Tropical forest mapping using high resolution satellite images have been reported by several studies (Foody *et al*., 2003; Rahman *et al*., 2005). Such images provide a lot of spatial information that aid in the classification process. In some cases, data from high resolution sensors are used as ground truth data for classification accuracy assessment (Foody, 2002). However, as stated earlier, their application is often hampered by the frequent cloud cover issues in the tropics. Low temporal resolution makes their usage challenging since one has to wait for a relatively longer time to acquire the next expected cloud free image (Toan *et al*., 2001) (which may not be the case). Some examples of high resolution satellite images that have been used for landcover classification and their properties are summarized in table 1 below:

Table 1: Summary of high resolution satellite images and their properties

IMAGE DATA	PROPERTIES
Geoeye-1	It has one panchromatic and four multispectral bands with spatial resolutions of 0.41m and 1.65m respectively.
Quickbird	Have one panchromatic (0.45 – 0.90µm) and four multispectral bands (Blue = 0.45 – 0.52 µm, Green = 0.52 – 0.60 µm, Red = 0.63 – 0.69 µm and NIR = 0.76 – 0.90 µm). Spatial resolutions are 0.61m and 2.44m for the panchromatic and multispectral bands respectively.
IKONOS	Have one panchromatic and four multispectral bands ranging from 0.45 – 0.90µm. Spatial resolutions are 1m and 4m for the panchromatic and multispectral bands respectively.

2.1.1.2 Medium Resolution

Medium resolution satellite data have spatial resolution ranging between 4 – 30m (Satellite Image Corporation, 2011). They have been used extensively for landcover classification because their range of spatial resolution permits classification of landcover at local scales which is the focus of many landcover classification and change detection research. Examples of medium resolution images include Landsat (30m), SPOT (10m - panchromatic) and ASTER (15m - VNIR and 30m - SWIR). Medium resolution images also have similar disadvantages as mentioned for high resolution images in the previous section.

ASTER is one of the five state-of-the art instruments which consist of three main subsystems, the visible near-infrared (VNIR), shortwave infrared (SWIR) and thermal infrared (TIR). It is on-board the Terra satellite launched in December, 1999 (Satellite Image Corporation, 2011). ASTER has 14 bands (1 – 3 = VNIR, 4 – 9 = SWIR and 10 – 14 = TIR) and is suited for applications including landcover change monitoring, vegetation and ecosystem dynamics, geology, hydrology and digital elevation model (DEM) generation (Satellite Image Corporation, 2011).

2.1.1.3 Low Resolution

Low resolution images are mainly suitable for landcover classification on regional to global scales (Foody, 2002; Wulder *et al*., 2004). This type of image lack spatial details and is rarely used for local scale mapping due to the coarse resolution, ranging between 30 – >1000m (Satellite Image Corporation, 2011). MODIS and NOAA AVHRR are examples of low resolution images (Foody, 2002). MODIS for example is very useful for monitoring global vegetation productivity (Wulder *et al*., 2004).

2.1.2 Active Microwave Remote Sensing

Active remote sensing operates with sensors that produce their own energy to form an image. These sensors transmit energy beam towards a surface feature and analyses the energy reflected back (backscatter). One such sensor is the Radio Detection And Ranging (RADAR) system. The advantages and disadvantages of radar are briefly discussed in section 2.1.2.1 below.

2.1.2.1 Radar Remote Sensing

SAR data has been used in many researches in recent years due to the advantages it has over optical data. However, using SAR data alone for landcover mapping comes with many limitations (Hoan *et al*., 2011). SAR therefore has been used to complement the information extraction in several landcover classification studies (Hoan *et al.*, 2011; Pohl & Van Genderen, 1998; Youshi *et al.*, 2009).

Speckle noise inherent in SAR data makes its interpretation complicated compared to visible or optical data (Ling *et al*., 2008). This makes its usage challenging for many analysts and researchers. To get the best information out of SAR data, it is important to carefully consider the processing techniques to apply prior to information extraction (Ling *et al*., 2008). Among these techniques is filtering, which is normally done in the spatial domain. Over the years, the most common filters used in this respect include Frost, Lee and Gamma-MAP filters. In their research, Youshi *et al*. (2009) found that image fusion reduces the effect of speckle noise to a maximum extent.

According to Pohl & van Genderen (1998), SAR provides a valuable data source for regular monitoring purposes since data can be obtained at anytime under any weather condition. Another advantage of SAR is its cloud, smoke and haze penetration capabilities (Fransson *et al.*; Hoan *et al.*, 2011; Ling *et al.*, 2008; Toan *et al.*, 2001). Furthermore, depending on the signal transmission wavelength, some SAR, for example PALSAR (Phased Array L-band Synthetic Aperture Radar), can penetrate tree canopies and other above ground biomass (Rosenqvist *et al.*, 2007).

2.2 Image Classification

Image classification is basically the process of sorting different pixels in an image to extract information on the various features from the spectral classes (Lillesand *et al.*, 2008). Spectral responses for similar features are similar and unique in a scene. Two main methods of classification exist. They are supervised and unsupervised classification.

2.2.1 Supervised Classification

Supervised classification deals with the training of a computer by specifying the numerical descriptors of different landcover types based on a prior knowledge of the features (Foody, 2002) or scene under investigation by the analyst. Representative sample locations of different known landcover types are selected across the entire scene and used to develop training areas upon which the categorization of pixels will be based. In this form of classification the image analyst has full control over the classification process. According to Lillesand *et al.* (2008), supervised classification consists of three main stages namely, (i) training stage (ii) classification stage and (iii) output stage. The first stage has already been discussed briefly above. The second stage is the actual categorization or pixel grouping phase to compose a theme that finally comes out as an output thematic map (stage iii) which can serve as an input into a GIS (Lillesand *et al.*, 2008). The quality of any supervised classification depends on the training process of the classification and requires a substantially well distributed samples within each cover class (Lillesand *et al.*, 2008; Riggan Jr. & Weih Jr., 2009). A good knowledge of the geographical location of the data is critical to the success of the classification.

Some of the most commonly used supervised classification algorithms include the parallelepiped, minimum-distance-to-means and maximum likelihood classifiers (Navulur, 2007). The parallelepiped classifier is a very fast and computationally efficient technique but its inability to distinguish and classify similar spectral signatures (overlapping classes) is its major disadvantage. Similarly, the minimum-distance-to-means classifier is also simple and computationally efficient but is insensitive to different degrees of variance in the spectral response data (Lillesand *et al.*, 2008).

The Gaussian Maximum Likelihood Classifier (MLC) is a simple and robust classifier noted to produce accurate classification results, since pixels are classified and grouped based on their highest probability of belonging to a particular group or class (Foody, 2002). This classifier classifies unknown pixels by quantitatively evaluating the variance and covariance of the spectral response pattern of the class to be separated. Its main assumption is normality of the data (Lillesand *et al*., 2008). This makes it reasonable for the computation of the statistical probability of a pixel belonging to a given category. In this respect, the computer evaluates the posterior probability of an unknown pixel to belong to a particular class and assigns it to that class (Lillesand *et al*., 2008). If the probability values fall below a given threshold then the pixel is not assigned to any particular class but named "unknown". The large number of computations required to classify individual pixels, is a major drawback of the MLC, especially when many spectral bands or spectral classes are to be differentiated. A Principal Component Analysis (PCA) transformation (i.e. reducing data dimensionality) is one way of optimizing the implementation of an MLC (Pohl & Van Genderen, 1998).

2.2.2 Unsupervised Classification

In this type of classification, information extraction is based mainly on the spectral domain and the assigning of classes to image features is done automatically, solely by the computer (Jong-Sen *et al*., 1999). Unsupervised classification is an effective way of partitioning remotely sensed data to extract landcover information from them by pixel clustering (Foody, 2002). Human influence is limited. After the clustering which is based on statistical criteria, the clusters are assigned names on the basis of the thematic information classes of interest. The analyst therefore needs to understand the spectral characteristics of the terrain under investigation in order to correctly label the clusters into their respective information class.

2.3 Object Based Image Analyses (OBIA)

The OBIA is an image analyses technique similar to the human visual interpretation that uses both spectral and spatial domains for image classification (Lillesand *et al.*, 2008; Seetha *et al.*, 2010). Simultaneously, OBIA works at multiple scales integrating texture, shape, colour, pattern and context to categorize pixels into meaningful objects (Benz *et al.*, 2004; Lillesand *et al.*, 2008; Seetha *et al.*, 2010). Several names have been used to describe this area of satellite image analyses, including Geospatial Based Image Analysis (GEOBIA) and Object Oriented Analysis (OOA) (Blaschke, 2010). There is therefore an ongoing debate as to which terminology is appropriate for this rapidly developing research field. However, these terminologies are used interchangeably due to author preference (Blaschke, 2010). This paradigm of image analyses has been made possible in recent times due to the advent of high resolution satellite images and the advancement in the production of fast computers coupled with the availability of appropriate software. OBIA is also generally accepted (Benz *et al*., 2004; Blaschke, 2010; Blaschke *et al*., 2000; Castilla *et al*., 2008) as a concept that builds on old segmentation (generation of objects or regions based on one or several homogeneity criteria of a feature space) methods for image classification.

Two main steps are involved in OBIA classification. The first stage is the segmentation of the satellite image (e.g. ASTER, SAR or combined ASTER+SAR data) into discrete objects or regions. Secondly, a hierarchical analyses approach based on a "trial-and-error" combination of different spectral, contextual and textural parameters in any relevant software such as the Trimble eCognition (formally, Definiens eCognition). Lillesand *et al*. (2008) described the scale of the image object to be classified as one of the most important factors that affect the image segmentation process. The scale could be fine (e.g. tree crowns), medium (e.g. tree stands of similar species and size) or coarse (e.g. aggregation of large forest areas as objects).

OBIA has been noted as a method that overcomes the "salt-and-pepper" effects in image analyses (Blaschke *et al*., 2000; Duveiller *et al*., 2008; Xie *et al*., 2008; Yu *et al*., 2006). This is made possible due to the grouping of pixels to form an object (Blaschke, 2010) and there are claims that the method is becoming more popular compared to the traditional pixel based ones (Gamanya *et al*., 2009). An attempt to compare pixel based approach (Maximum Likelihood Classifier) and OBIA by some researchers including Shackelford and Davis (2003), Platt and Rapoza (2008), Ehlers *et al*. (2006) and Flanders *et al*. (2003) has shown that the introduction of texture and contextual analyses improved classification accuracy by 8 – 11%. Other advantages of OBIA over the pixel based approach include:

- Its ability to utilize the spectral, spatial, temporal, morphological and contextual domains in remote sensing.
- Its ability to integrate GIS functionalities in thematic classification.
- Extraction of information from a particular image/scene at different scale and resolutions (i.e. multi-scale approach).
- Incorporation of many and well tested algorithms including those implemented in supervised classification, fuzzy logic and knowledge based classification applications.

The many advantages associated with the OBIA technique are very promising for future image analyses projects.

2.4 Classification Accuracy Assessment

Classification accuracy assessment generally refers to the comparison of classification data to geographic or ground truth data (reference data) that are known or assumed to be correct. This assessment thus enables one to see how successful the classification process was (Congalton, 1991). Foody (2002) emphasised the need to conduct an accuracy assessment since it gives an indication of map quality and fitness as well as providing insight into classification errors and their implications. He summarised the reasons for accuracy assessment into three: (1) to give an indication of a map's overall quality (2) to form the basis for comparing different classification algorithms and (3) to help one to understand errors associated with classification. Congalton (1991) observed that some studies have used the same data for training classifiers in assessing accuracy of the classification result. This was noted to overestimate classification accuracy. To avoid bias, it is proper to avoid using the training datasets for validation (Congalton, 1991). According to Lillesand (2008), the completeness of a classified digital image lies in its validation.

Both qualitative and quantitative assessment of classified images (landcover maps) is possible on a category - by - category basis (IPCC, 2003; Podest & Saatchi, 1999) through the use of the confusion matrix as supported by many projects, for instance the Kyoto protocol under its "good practices guidance for LULCF" document (IPCC, 2003). The confusion matrix (Figure 3) measures producer's accuracy and user's accuracy for each landcover category as well as the overall accuracy of the classification (Riggan Jr. & Weih Jr., 2009). Though there is no
standardized accuracy assessment method, the error matrix and its associated kappa statistics have been accepted as the conventional measure of accuracy by the RS community (Foody, 2002).

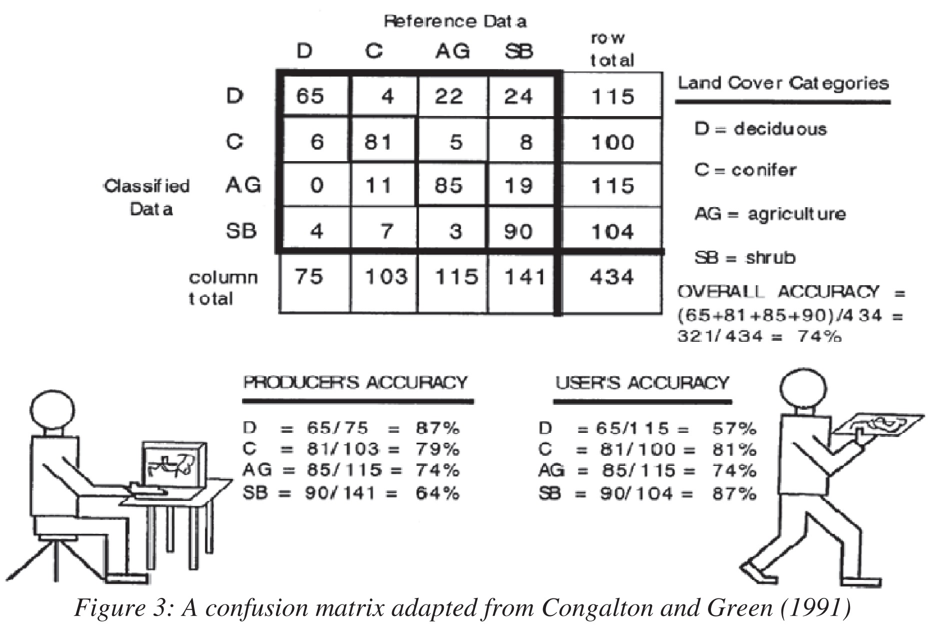

Figure 3: A confusion matrix adapted from Congalton and Green (1991)

The kappa statistic (Equation 1) simplified in equation 2 below is another useful indicator of classification accuracy and has been used very often to statistically determine the difference between two or more classified maps or the methods used in obtaining them (Congalton, 1991). Cohen's kappa is a discrete multivariate technique that has an advantage over the overall accuracy measure since kappa takes chance agreement into consideration and corrects for it (Jensen, 2005). The kappa coefficient normally ranges from 0 – 1. However, negative kappa can result, which is an indication of extremely poor agreement of the classification with the reference data. Furthermore, a negative kappa does not normally have a meaningful interpretation. A kappa of zero (0) and one (1) indicate an occurrence or agreement due to chance and perfect agreement respectively. Table 2 adapted from Munoz & Bangdiwala (1997), shows a detailed description of the range of kappa values and their interpretation:

Table 2: Interpretation of the kappa statistics

Kappa value	**Meaning/Interpretation**
Less than 0.00	Poor agreement
0.00 – 0.20	Slight agreement
0.21 – 0.40	Fair agreement
0.41 – 0.60	Moderate agreement
0.61 – 0.80	Substantial agreement
0.81 – 1.00	Almost perfect agreement

A pair-wise Z-test at significance level (α) = 5% (i.e. 95% Confidence Level) can be performed to test the significance of the difference between the two kappa values after Equation 3 below (Riggan Jr. & Weih Jr., 2009).

$$\widehat{K} = \frac{N\sum_{i=1}^{r} X_{ii} - \sum_{i=1}^{r}(X_{i+} * X_{+i})}{N^2 - \sum_{i=1}^{r}(X_{i+} * X_{+i})} \qquad \text{[Equation 1]}$$

Where,

X_{ii} is the number of observations in row i and column i (i.e. diagonals), X_{i+} is the marginal total of the row i, X_{+i} is the marginal total of column i and N is the total number of observations.

$$\widehat{K} = \frac{Po - Pc}{1 - Pc} \qquad \text{[Equation 2]}$$

$$Z = \frac{|\widehat{K}_1 - \widehat{K}_2|}{\sqrt{\widehat{Var}(\widehat{K}_1) + \widehat{Var}(\widehat{K}_2)}} \qquad \text{[Equation 3]}$$

Where,
$\widehat{K}$ is the estimate of kappa, Po is the actual agreement, Pc is the agreement by chance, Z is the calculated Z-test statistic, $\widehat{K}_1$ and $\widehat{K}_2$ are the kappa coefficients for the methods or datasets (e.g. OBIA and MLC or SAR alone and combined ASTER+SAR respectively) and $\widehat{var}$ is the variance of kappa (Congalton, 2009; Skidmore, 2002).

Although the kappa coefficient has been widely used for accuracy assessment, many researchers have criticized and argued that it overestimates chance agreement which culminates in the underestimation of classification accuracy.

2.5 Landcover And Landuse

The terms landuse and landcover have often been confused or used interchangeably but in actual sense they are different (CARA, 2006). A simple definition of landcover deals with the description of the natural features on the earth's surface without human interference. For example, a deciduous forest, coniferous forest, water bodies, grasslands, agricultural fields etc. Landuse on the other hand, refers to the activities currently being undertaken on the land and is driven by man. In other words, it refers to the economic use of the landscape by people, be it commercial or industrial (CARA, 2006). A landuse example can be a reservoir, tree nursery, backyard garden, recreation park etc. These two concepts describe a classification scheme that represents land information in space and time. One major difference however is that, landcover can be monitored and interpreted from satellite and other remotely sensed data through image analyses but landuse cannot, because it is difficult to interpret use from imagery. Changes in landcover and landuse are of great importance due to their impact on habitat, air and water quality as well as human well being.

2.6 Plantation Development In Ghana

All degraded forest reserves in Ghana have been put under plantation development to help restore the lost vegetation cover. Several plantation development programmes have been embarked upon since the 1970s under different names and projects. These programmes include the National Forest Plantation Development Programme (NFPDP), Government Plantation Development Programme (GPDP), Community Forest Management Project (CFMP) and Commercial Private Plantation (CPP) Development by individuals and organisations, both local and international. The objectives of these plantations include employment generation to reduce rural poverty, restoration of the degraded forest cover, improvement of environmental quality and enhancement of food production to ensure food security.

The NFPDP started in the year 2001. Before its inception several projects geared towards the restoration of degraded forests had been in place. For example collaborative resource management projects that aim at involving local communities in the management of the forest reserves were in place. The taungya system (discussed in section 2.6.1 below) before, was the main strategy for plantation development. The NFPDP was started with a modification of the old taungya system, named Modified Taungya System (MTS), to make it more appealing to local communities through the benefit sharing agreement (BSA) introduced by the Forestry Commission.

2.6.1 Taungya System (TS) *vis-à-vis* Modified Taungya System (MTS)

The taungya system (TS) is an agroforestry system usually practised in areas with land scarcity. Under this system, farmers are allocated portions of degraded forest reserves to grow their food crops and help replant the deforested areas. The system has been practised in Ghana since the early 1920s (FORIG, 2011). The implementation of the taungya system was at its peak in the 1970s, which is evident through the nationwide plantations established in most degraded forest reserves. However, due to policy and legislative failures on benefit sharing, system's abuse by farmers, insecurities in tenure and use rights as well as weak institutional monitoring and supervision by the Forestry Department (now Forest Services Division – Forestry Commission), the taungya system was suspended in 1984 (FORIG, 2011).

With the paradigm shift in forestry in Ghana towards collaborative forest resources management, forest fringe communities saw the taungya system as the most effective forest tenure and requested for its revitalization with possible modification by the government. In response, the MTS was introduced to involve various stakeholders (the Forestry Commission, farmers, traditional authorities and local communities) in the establishment and maintenance of the plantations (FORIG, 2011). Hence, the MTS unlike the TS confers a stronger ownership and tenure rights on farmers. Benefits from the plantations are shared based on the proportion of contribution from each party under the benefit sharing agreement (BSA) (Forestry Commisson Ghana, 2009b). Under the BSA, FC receives 40% of the proceeds, farmer(s) are entitled to 40%, stool land owners together with traditional authorities will receive 15% (8% and 7% respectively) and finally, the fringe community receives 5% (Forestry Commisson Ghana, 2009b).

The other plantation programmes including the CFMP, GPDP and CPP had their different sources of funding and BSA. The CFMP, GPDP and CPP are funded by the African Development Bank (AfDB), the Government of Ghana through the Highly Indebted Poor Countries (HIPC) funds and private investors respectively.

2.7 Invasive Species In The Afram Headwaters Forest Reserve

Two main invasive plant species (*Broussonetia papyrifera* and *Chromolaena odorata*) colonizing the AHFR are discussed in this section due to the influence they have on the forest reserve and the challenge they pose to landcover classification using RS data. In the AHFR where this research was conducted, *B. papyrifera* poses a major challenge in visual interpretation as some areas seen to be natural forest on the satellite image in reality is covered by York (*B. papyrifera).* The phenology of the species is similar to that of the natural forest trees in terms of the colour, size and shape of leaves; and the vertical structure of the vegetation. *C. odorata* on the other hand invades forest gaps and other open areas and poses a challenge with misclassification.

2.7.1 Paper Mulberry (*Broussonetia papyrifera*)

The paper mulberry (*Broussonetia papyrifera*), commonly known as York in Ghana, is a prolific woody perennial from the *Moraceae* family. Originating from South-East Asia, the humid tropics, subtropical and temperate environments are the most suitable habitat for the species (Bosu *et al*., 2009). According to Ali and Malik (2010), hillsides, roadsides, ditch banks, agricultural fields, valleys, forested areas and open spaces in urban areas with elevations lower than 1500m above m.s.l are the niches of *B. papyrifera.* The plant is grown mainly for its economic and aesthetic importance. It provides shade in home gardens, useful in soil stabilization and improvement, controls soil erosion, sap from the plant is used for glue production, pulp and paper production and the inner bark is also used for tapa cloth (Bosu *et al*., 2009).

Under conducive environments, paper mulberry, reaches a total height range of 10 – 20m and a diameter at breast height of 70cm. *B. papyrifera* bares a simple but alternate opposite, mulberry-like and papery leaves with serrate margins ranging from 8 – 25cm long (Bosu *et al*., 2009). It is a dioecious plant, with male and female inflorescence occurring on separate individuals.

When introduced to a non-native environment, the paper mulberry with its fast growing ability distorts the functioning of the natural habitat and ecosystem as a whole. *B. papyrifera* outcompetes native flora due to its very high water consumption ability which makes less water available for the sustenance of the native vegetation. Due to its adverse effects on the native vegetation, *B. papyrifera* has been listed among the six worst invasive plant species in the World (Malik & Husain, 2006).

The introduction of *B. papyrifera* into Ghana was in 1969 when the need for the industrial production of pulp and paper arose (Anonymous, 1970). It has now become the major invasive species in the country today and its control has become a very big challenge to farmers in the surrounding communities and plantation developers (both private and government) inside forest reserves. The Afram Headwaters Forest Reserve in the dry semi-deciduous forest zone and the Pra Anum Forest Reserve in the moist semi-deciduous Forest zone were the points of first introduction (Apetorgbor & Bosu, 2011) and due to its prolific nature have spread throughout the southern part of Ghana as shown in Figure 4, adapted from Apetorgbor and Bosu, (2011).

Rapid colonization and spread of *B. papyrifera* has been facilitated by the alarming rate of deforestation and the dispersal of the seeds by bats and other wildlife for which the fruit serves as food. *B. papyrifera* can be found mostly in large forest gaps, fallowed croplands and roadsides of the two points of introduction and surroundings (Apetorgbor & Bosu, 2011).

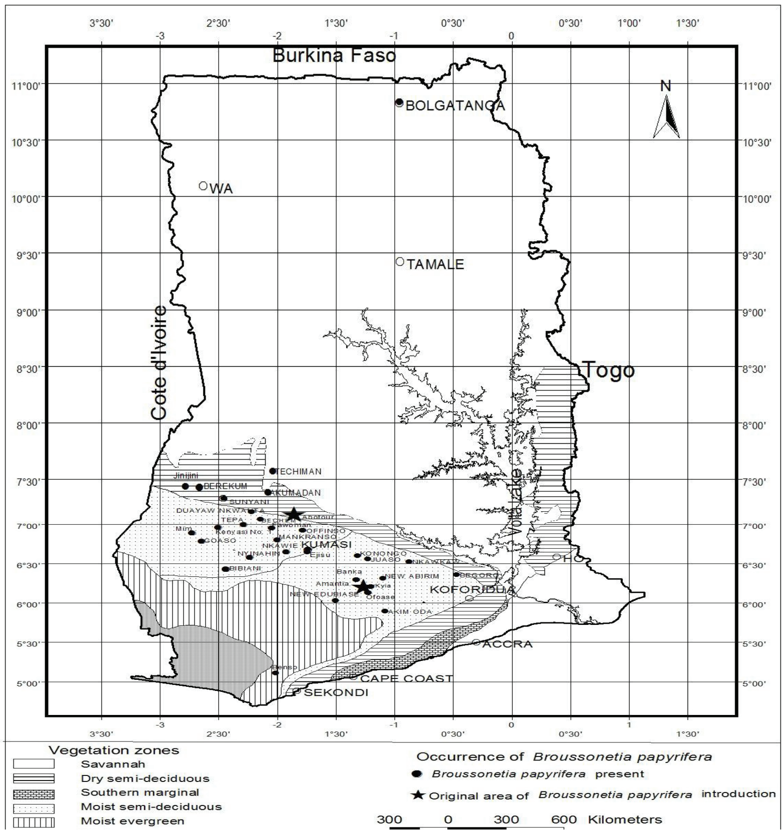

Figure 4: Areas of first introduction and occurrence of B. papyrifera

2.7.2 *Chromolaena odorata* (L. King & Robinson)

From the *Asteracea* family*, C. odorata,* Siam as it is popularly known (also known commonly in as Ghana Acheampong weed) is ranked as one of the most invasive plants species colonizing Southern Asia and tropical African forests, including the AHFR. It is also listed among the world's top hundred (100) invasive species (Bosu *et al*., 2009). *C. odorata* is a tropical herbaceous perennial weed originating from Tropical America. In tropical, subtropical and temperate ecosystems the plant grows in dense stands and attains a maximum height of 2.5m. Moreover, under favourable environments *C. odorata* can attain a height of 6 – 10m by climbing nearby vegetation with its long-winded branches (Vanderwoude *et al*., 2005). The plant produces many seeds from very small fruits of length and breadth 3 – 5mm and 1mm respectively. This therefore makes its dispersal by wind and animals easy, culminating in its aggressive colonisation of open areas in forests (Vanderwoude *et al*., 2005). The dispersal of *C. odorata* seeds by animals is further boosted by a small hook on the fruit that makes its attachment to the animal easy. Bosu *et al*. (2009) indicated that though reproduction by vegetative means is impossible, *C. odorata* has the ability to readily coppice from root crowns or stems after an event of fire or death of old stumps (probably through clearing). Though highly flammable and fire tolerant, *C. odorata* thrives very much on fire, as it promotes the multiplication of new shoots (McWilliam, 2000). It has been speculated that *C. odorata* facilitated the massive and devastating wildfires experienced in Ghana in 1983 due to its significant contribution of fuel or combustible material especially during the dry seasons.

The AHFR offers a congenial environmental and climatic condition for the survival of *C. odorata*. The weed thrives mostly in open areas (forest gaps) with a temperature of 30°C and relative humidity of 60 – 70% as well as an annual rainfall exceeding 1200mm. Conversely, the plant's growth as well as seed production is impeded under closed canopy conditions (Vanderwoude *et al*., 2005) explaining why *C. odorata* is found mainly in degraded forest areas, abandoned farmlands, roadsides and forest canopy gaps.

C. odorata has significant negative impacts on the regeneration and establishment of native species through the exhibition of allelopathic properties. The sustainable livelihoods of local farming communities is affected (McWilliam, 2000) since the weed outcompetes crops on farmlands. Apart from its adverse impact on the availability of livestock feed, through its competition with local pasture and fodder, its eradication is a big challenge to farmers. This is because its presence on the land increases the cost of land preparation for farming. Moreover, *C. odorata* is an unpalatable and toxic weed which makes it unsuitable for livestock feeding (McWilliam, 2000).

Furthermore, in spite of its negative impacts several benefits have been associated with its invasion of tropical African ecosystems. According to a research in West Timor (McWilliam, 2000), *C. odorata* is very effective in the eradication of the blade-like grass species (*Imperata cylindrica*) whose elimination on farmlands is always a big challenge to farmers. *C. odorata* quickly shades the grass and suppresses its growth. *C.*

odorata has been associated with yield increments of some crops such as maize, groundnut and cassava in West Africa. This is however a claim by farmers which needs research. Another benefit which is also a claim is its contribution to the reduction of fallow periods from the previous 10years to 3years currently. Again, the medicinal potential of *C. odorata* cannot be overemphasised. *C. odorata* has been successfully used to treat fresh wounds due to its ability to stop excessive bleeding. It is also used to cure eye and stomach conditions (Bosu *et al*., 2009).

Finally, several strategies (mechanical, chemical and biological) have been applied to control the spread of *C. odorata.* Among the above management strategies, mechanical control has been mostly applied in West Africa. However, a single strategy has not been as effective as their combination. For instance, local farmers under the modified taungya system plantation programme interviewed indicated that they slash the weed with cutlasses (mechanical) and burn after a few days (when the debris are dried) and then spray with herbicides (chemical). This they said eradicates the weed and favours the planting of their crops. However, this does not result in a total eradication of *C. odorata* as the very large seed bank germinates after a short while replacing the removed matured stand and the farmers have to weed again (Bosu *et al*., 2009)

3.0 MATERIALS AND METHODS

3.1 Study Area Description And Purpose of Selection

The study was carried out in the Afram Headwaters Forest Reserve (AHFR) in the Ashanti Region of Ghana. Historically, the reserve, which is the largest of the Afram Headwaters group of reserves, comprising Afrensu-Brohuma, Aboma, Gianima, Abrimasu and Mankrang was named after the Afram River which runs through the eastern part of the area. The AHFR was chosen for this research because of three main reasons. First, the Forestry Commission's plans to use the area as one of the pilot sites for the REDD+ programme. Second, the area is located on a relatively flat ground which will reduce the effect of topography on the satellite data. Third, there is both primary and secondary data (field and satellite data from previous research) available for the area as well as the presence of different landcover types such as natural forest, plantations, agroforestry and degraded lands which makes this area particularly suitable for the research.

3.1.1 Location details

The AHFR is approximately 20,100ha (77.657sq ml) in size and geographically located between Longitude 1° 32' W and 1° 48' W and between Latitude 6° 45' N - 7° 25' N in the Offinso Forest District of the Ashanti Region, Ghana (Figure 5). It is bordered on the west by the Kumasi – Techiman main road which also forms the main boundary between the AHFR and the Opro Forest Reserve.

For management purposes, the reserve has been partitioned into two parts – Afram East and West. The Kwapanin – Asuboe road shown in Figure 6 forms the main dividing line between the Eastern and Western parts of the reserve. Furthermore, the reserve is demarcated into smaller management units called compartments, found in both parts (Figure 7 below). A standard compartment size in Ghana is 128ha. However, some may be larger or smaller than the standard size as a result of blockages by natural features like rivers. Compartments numbered zero (0) in Figure 7 represent research plots, portions containing the so called "admitted farms" and legal settlements on-reserve. Admitted farms are farms that existed prior to the legal State reservation of an area as a forest reserve. Farmers owning those farms before reservation are registered by the relevant authorities and still maintain their ownership of the farm land.

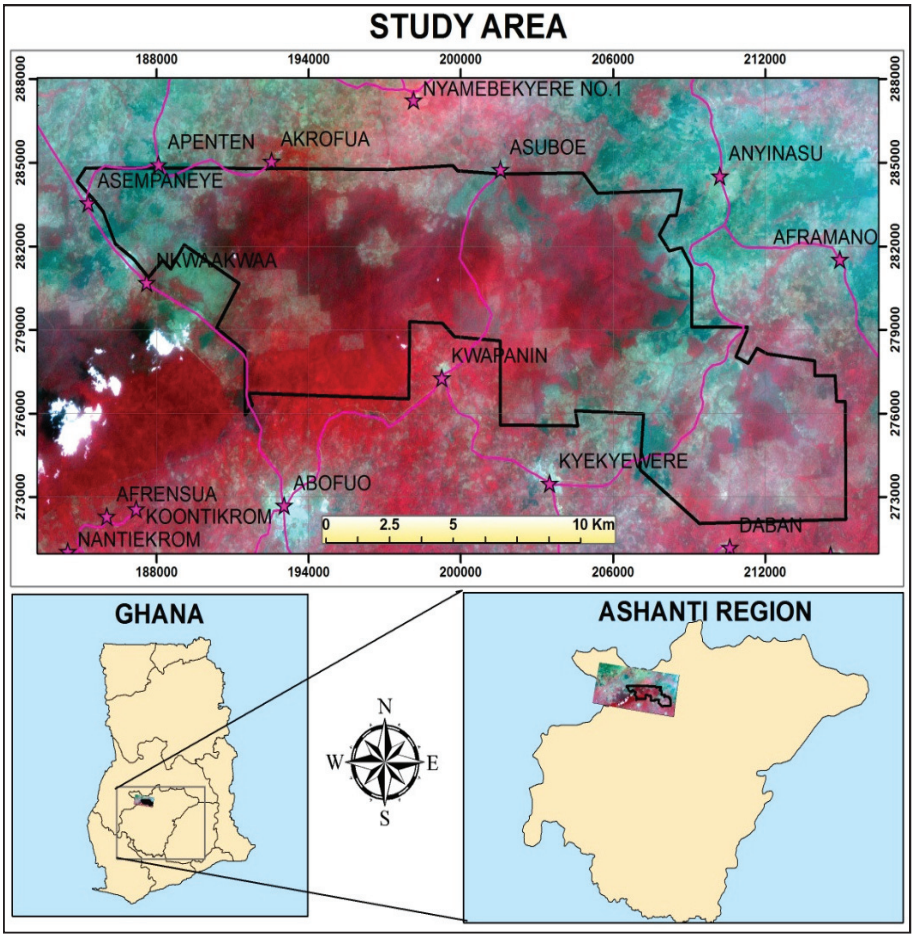

Figure 5: Study area map showing the Country, Region and the AHFR (thick black boundary) with surrounding towns.

ROADS AND TOWNS MAP SHOWING THE DEMARCATION BETWEEN THE EAST AND WEST PORTIONS OF THE AFRAM HEADWATERS FOREST RESERVE

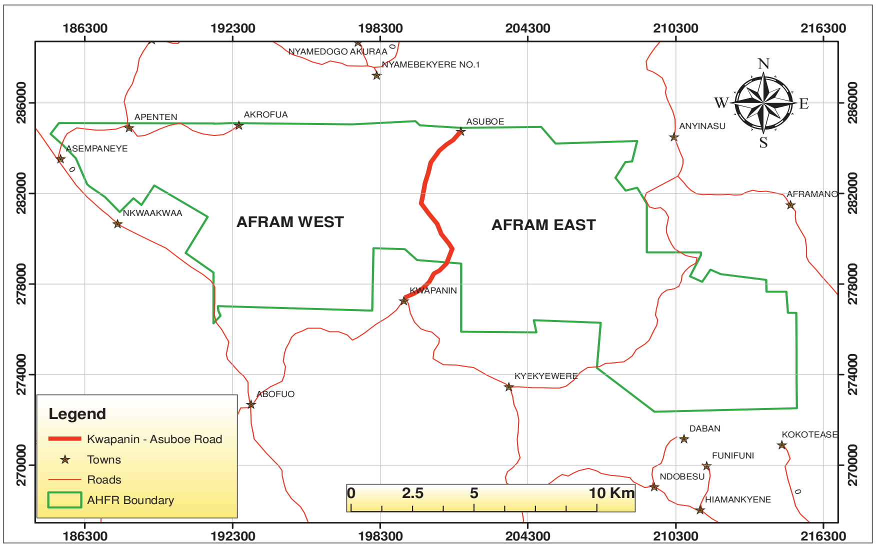

Figure 6: Map showing the main demarcation line between AHFR East and West

COMPARTMENT MAP OF THE AFRAM HEADWATERS FOREST RESERVE SHOWING ROADS AND SURROUNDING TOWNS

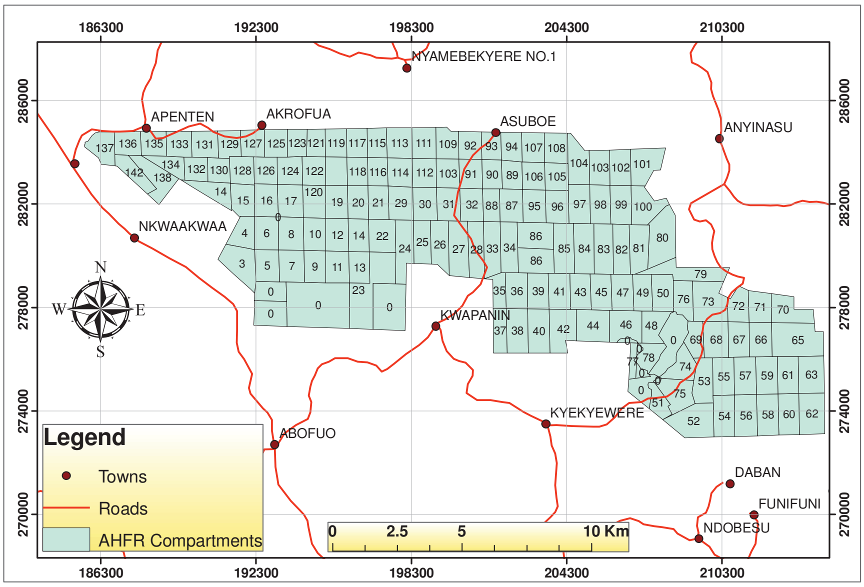

Figure 7: Compartment map of the Afram Headwaters Forest Reserve (Source: RMSC – FC, Kumasi).

3.1.2 Vegetation Characteristics

Under the ecological/vegetation zones classification of Ghana, the AHFR is found in the dry semi-deciduous forest zone subtype (DSFZ). Found within the forest – savanna transition zone of Ghana (Figure 8), the study area is characterised by sparse woody understory with well illuminated forest floor being a result of the extensive forest fires in 1983. This has given rise to the colonisation of the area by dense weedy undergrowth species from *Marantaceae* (prayer plant or arrowroot) and *Zingiberaceae* (ginger) families and other non-native invasive species such as *Chromolaena odorata* (also called "Acheampong" or other names as in Appendix A) and *Broussonetia papyrifera* (Paper Mulberry or York). The AHFR is mostly degraded due to its fire prone nature and is currently left with patches of remnant natural vegetation, forest plantations - mainly *Tectona grandis* (Teak) and agroforestry areas established through the Taungya system (now Modified Taungya System - MTS). The sections below (3.1.2.1 – 3.1.2.4) briefly describe the four main vegetation cover types in the AHFR.

3.1.2.1 Natural Forest vegetation

A natural forest is a forest that has spontaneously generated itself with naturally occurring tree species in a particular location without any human intervention through planting. The natural forest vegetation in the AHFR is the relics of natural mixed tree species that were originally found in the area. The natural forest which was the dominant landcover with class I – III species (Appendix B) at the time of reservation now forms a small proportion in relation to agroforestry and plantation stands. This is a result of deforestation. Due to the degradation of the forest, non-native invasive species, mainly York (referring to the name of the technical officer at the time of introduction of the paper mulberry (*B. papyrifera*) in the early 1970s) have colonised the entire forest reserve.

3.1.2.2 Plantations

Deforestation of the AHFR has given rise to the establishment of plantations to restore the integrity of the forest. In the reserve, monocultures of exotic trees species that are fast growing including *Cedrella odorata* (Cedrella) and *Tectona grandis* (Teak) have been planted. Figure 9A shows a teak plantation stand photographed during fieldwork (more fieldwork photos in Appendix G) in the AHFR. In a few cases, these exotic species are mixed with indigenous ones including *Terminalia spp*. (Ofram and Emire), *Ceiba pentandra* (Onyina or Ceiba), *Entandrophragma spp*. (Mahogany) to avoid the establishment of single species (Figure 9B) thereby enhancing biological diversity of the AHFR.

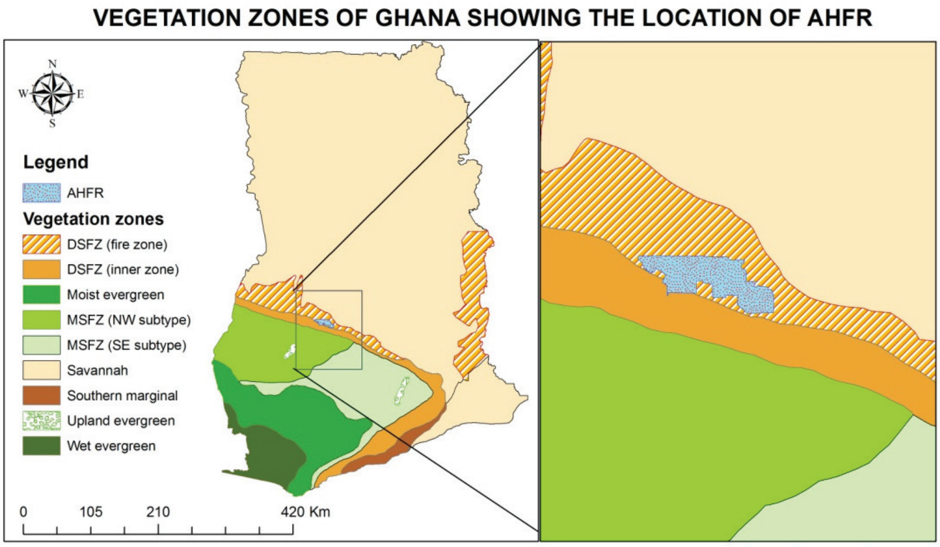

Figure 8: Vegetation zones of Ghana showing the location of the AHFR in the transition zone between the Forest and Savannah zones.

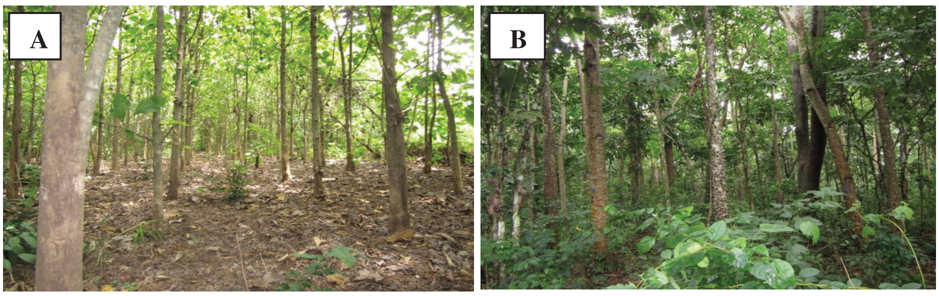

Figure 9: (A) Pure teak monoculture and (B) Mixed exotic – indigenous species plantation.

3.1.2.3 Agroforestry

The agroforestry areas in the AHFR shown in Figures 10A and 10B are young plantation stands (1-year old teak and cedrella trees) established through the Modified Taungya System (MTS – discussed in Section 2.6.1) in which farmers are allocated portions of degraded forest lands to grow their crops alongside the maintenance of newly established plantations. Normally, farmers are allowed in these stands for a maximum of four (4) years when the canopy closes and food crops productivity drops due to competition for light and allelopathy of the trees species planted. The main food crops grown in the agroforestry areas are plantain, maize, cassava, yam, pepper, okro and cocoyam.

3.1.2.4 Fallow / Grasslands

Fallow and grassland cover types are normally abandoned farmlands with mainly grass vegetation including elephant grass. Farmers leave the land to regain its fertility (fallow) after farming for several years. Due to the open nature of the AHFR, the area is colonized by *Chromolaena odorata* whose growth is supported by open forest gaps. The presence of this invasive species makes the cover type highly susceptible to frequent bushfires.

Figure 10: (A) A 1-year old teak agroforestry stand (B) A 1-year old cedrella agroforestry stand

3.2 Settlements within and around the AHFR

There are communities and admitted farms that have been demarcated and mapped within the AHFR. The Bimi Community found on the eastern part of the reserve is one of such communities. Other communities close to the reserve include Abofour, Kwapanin, Anyinasu, Asuboe, Nkwankwaa and Asempanaye. The main occupation of the people is farming, hunting and palm wine tapping. One of the major maize and yam producing districts in the country, Afigya Sekyere Dumasi political district (capital in Ejura), borders the AHFR on the north. Produce from these areas are transported to Accra, Kumasi and some even exported outside Ghana. Most of these foodstuffs are grown in the forest reserves under the MTS plantation development introduced by the Forestry Commission.

3.3 Local drainage and topographic conditions

The AHFR is drained on the East and West by the Afram and Birimu rivers respectively. The reserve serves as a protection for the major water bodies that drain through it and provides water for domestic and commercial use for local communities as well as surrounding towns such as Abofour and Offinso. The study area has a relatively flat topography with a gently undulating terrain (Offinso South Municipal Assembly, 2006). Apart from a few areas in the eastern part that have steeper slopes between 10 – 15%, most parts of the reserve are flat with slopes less than 5% (Figure 11). The altitude of the reserve varies between 270 – 400m above mean sea level.

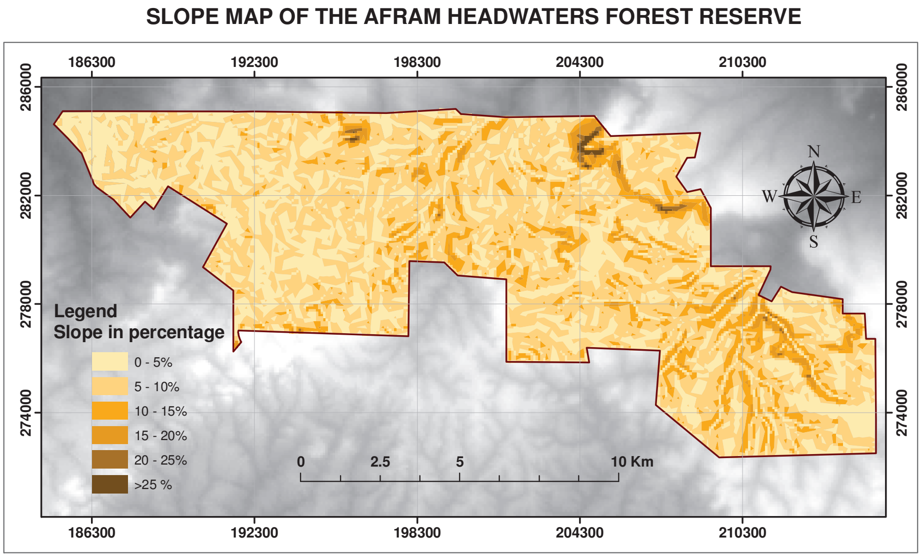

Figure 11: Slope map of the Afram Headwaters Forest Reserve.

3.4 Climate

The closest meteorological stations to the AHFR are located in Offinso and Bechem respectively, approximately 35Km away from the reserve. The forest reserve lies within the tropical humid climate zone. The AHFR is characterised by its uniform high temperatures and two peak rainfall seasons, major and minor rainy seasons, occurring in June and October respectively. The major rainfall season starts from April and ends in July and the minor one between September and November. The mean annual rainfall in the study area ranges between 1250 – 1500mm.

The dry season spans from December to March. Thus, maximum temperature is usually around 30°C and is recorded in March and April with an average monthly temperature of 27°C. During the dry season, the North-Eastern trade winds (Harmattan) blow into the entire country with dry and fine dust particles. This dry condition facilitates the drying of litter and other combustible materials that result in severe forest fires which have been one of the major contributing factors to the degradation of the AHFR.

The relative humidity is normally high during the rainy season, between 75 - 90% (Offinso South Municipal Assembly, 2006) but drops considerably for a short period, especially at the peak of the dry season due to the harmattan.

3.5 Rocks and Soils

The AHFR overlies rocks of the upper and lower Birrimian series on the western end and the rest of the reserve overlies rocks of upper Voltain sandstones accounting for over 70% of the area. Thus, the latter forms the main geological formation in the study area. The north-western part is made up of Granites (Dahomeyan) accounting for 20% of the study area.

Most of the AHFR is covered by sandy loam soils varying from reddish to reddish brown in colour. A few patches of clay also exist. Except for areas with rocky outcrops, soil depth generally is over 30cm. Gravelly soils in the reserve have very low water holding capacity and experiences drought conditions during the latter parts of the long dry season.

3.6 Description of the Forest and its management

Prior to its demarcation as a forest reserve, the area around the AHFR had a very small population; hence farming in the area was on a very small scale and subsistence. Also, knowledge of the history of the area was very little. The reserve was demarcated and its boundaries surveyed in 1927. Farms in existence before the selection of the reserve area (admitted farms) were demarcated from 1928 – 1930 and a re-survey and re-demarcation was carried out in 1951. The area at the time was well stocked with class I – III species (see description and list in Appendix B). There was less demand by local communities for non-timber forest products (NTFPs) though a few timber trees were exploited. This was because timber and firewood was relatively abundant outside the forest reserve. Furthermore, the reserve originally was under a protective and restrictive management with few prescribed administrative plans including:

i. Restricted felling subject to the exercise of communal rights

ii. Fire protection through early burning

iii. Boundary maintenance (both internal and external) and

iv. Provision of land for taungya.

Due to over-exploitation and frequent bushfires in the AHFR, most parts of the reserve are degraded and hence listed among the degraded forest reserves in Ghana. The location of the reserve in the DSFZ (fire zone subtype) (Figure 8) exposes it to frequent annual fires that cause considerable damage to the forest. The degraded condition has favoured the invasion and colonisation of the area by non-native weeds, whose eradication has become a big management and research issue (Bosu *et al.*, 2009). In order to restore the AHFR to its near original state, various plantation establishment programmes have been undertaken by the government and other private individuals and organisations. Species planted in these plantations include indigenous and exotic ones. However, the exotic species are planted more due to their fast growth and disease and pest resistance abilities.

The external boundaries of the forest reserve as well as farm boundaries within reserves are regularly maintained by forest guards to avoid encroachments and illegal farming inside the reserve. These boundaries have been line-planted with Teak, Gmelina, Cassia and Mango which make their identification easy. Numbered concrete boundary pillars have been placed at intervals of approximately 800m and at all changes of direction along the external boundary.

3.7 Field Data Collection

The field data collection campaign was carried out between 13th September and 12th October, 2011 in the study area. The aim of the campaign was to obtain ground truth information about the different major landcover classes in the study area and their spatial extent to aid in the classification and validation of classified maps.

3.7.1 Fieldwork Map

An unsupervised classification was run on the ASTER data and compared with the outcome (landcover map) of a previous study (Nguyen, 2010). The result of the unsupervised classification revealed a close visual relationship with the map from the previous study; hence the latter was adopted as a basis for identifying the different landcover classes in the field. A total of 82 random points were generated in ArcGIS. These points were distributed over the different landcover classes in varying proportions depending on the area covered by each class (i.e. sampling by probability proportional to size).

3.7.2 Sampling Design

In order to minimize variability in each cover class (stratum) and improve precision of the population estimate (Husch *et al*., 2003), a stratified random sampling approach was used. The study area was stratified based on landcover class and sample plots were selected randomly within each stratum. Out of the four landcover classes (identified in the previous study) in the AHFR; agroforestry, plantation and natural forest classes contributed the largest areas in terms of hectares. For that reason, greater number of the random sample points (plots) was allocated to those classes as summarised in Table 3 below:

Table 3: Number of sample points per each landcover class before fieldwork.

No.	Landcover Class	Number of Points
1	Natural Forest	25
2	Agroforestry	30
3	Plantation	22
4	Fallow/Grassland	5
Total		**82**

3.7.3 Fieldwork Expectations

Since the datasets (both optical and SAR) used for this research were acquired three (3) years before the field data collection it was expected that there would be a slight change in landcover especially the graduation from agroforestry class to plantations, based on the classification scheme (Appendix C). This was anticipated because the agroforestry areas were mainly young plantations planted with exotic tree species that have the tendency to grow very fast at the early stages of development and their canopy closes usually after three years. Another expectation was the conversion of degraded areas into plantations. Furthermore, it was anticipated that there could also be a very slight change in the Natural forest cover class. This was expected due to the alarming rate of deforestation and forest degradation in Ghana. However, it was observed that most of the areas classified as Natural Forest from the previous study are now colonised by York (*Broussonetia papyrifera*), as popularly known by the local people. Consequently, parts of these stands have been cleared for plantation development by both government and commercial private plantation (CPP) developers.

The largest CPP developer in the study area is an international company registered in the UK called Mere Plantations Limited (MPL), with a land allocation of 4,000ha. The company is committed to an initial investment of fifty million pounds sterling (£50M) and a total of three hundred million (£300M) over the 25 years lifespan of reforestation project in the AHFR. MPL commenced the project in the first quarter of 2011 and now employs over 700 Ghanaians, majority of them from the surrounding communities. The benefit sharing agreement (BSA) for the CPP development is different from the MTS. Under the BSA of the CPP development, the investor takes 90% of the proceeds from the plantation and the remaining 10% is shared amongst the stool land owners (6%), the Forestry Commission (2%) and the local community (2%). Stool land owners here, refer to the traditional authorities legally owning the forest reserve land, which is managed in trust by the Forestry Commission on their behalf.

3.7.4 Field Equipments and Materials

Before the field trip, the field equipments and materials in Table 4 were ordered from ITC and tested. They were found to be in good condition for the intended use.

Table 4: Fieldwork instruments / materials and their purpose in the field

No.	Material/Instrument	Purpose	Units
1	GPS and iPAQ	Navigation/plot location	DD*, DMS
2	Prismatic Compass	Determine Bearing	DMS**
3	Diameter tape	DBH measurement	cm
4	Haga Hypsometer	Height measurement	m
5	Measuring tape (50m)	Length measurement	m
6	Densiometer (Spherical)	Crown cover measurement	%
7	Clip board	Data entry	-
8	Data entry sheet	Data entry	-
9	Pencils/erasers etc	Data entry	-

** Decimal degrees **Degrees/Minutes/Seconds*

3.7.5 Field data collection

A reconnaissance survey was conducted on the first day in the field with the assistance of a forest guard to get familiar with the terrain and, since the time available was limited, to devise a strategy for an effective data collection process. For the subsequent days, actual data collection (recording of GPS points and measurement of stand parameters) was done. An iPAQ was used to navigate to the plot centre and the coordinates recorded in WGS 84, decimal degrees (DD) with the Garmin GPS as well as in Degrees Minutes and Seconds (DMS) from the iPAQ. The coordinates of the plot centres were measured again in the field due to possible positional inaccuracies and inaccessibility to some of the random points generated before data collection. Spatial attributes of the plots such as slope, aspect and elevation were recorded. All trees with DBH ≥10cm in stands occupied by trees (mainly agroforestry, plantation and natural forest) were identified and measured within circular plots of radius 12.62m and recorded on a field data collection sheet (Appendix D). Apart from being the standard radius (12.62m) used in most biomass and carbon stock estimations the circular plot is preferred because of the ease of usage and also the perimeter for the entire plot can be defined by only the radius (Husch *et al.*, 2003). That radius also satisfies the minimum sample unit requirement of the Kyoto protocol (IPCC, 2003). However, on slopes greater than 5%, a slope correction table (Appendix E) was used to determine the appropriate radius.

The heights of two tall and two short selected trees in the plots were measured with the aid of a Haga hypsometer. In dense forests, such as those in AHFR, tree height is one of the most challenging tree parameters to measure in the field. Measurement errors may arise from the wrong identification of the actual tip of the crown and lack of experience in the use of the instrument. Crown diameters and canopy cover within the plots were also measured with the aid of a measuring tape and spherical densiometer respectively and recorded. In estimating the crown diameter, two people on the ground measure the longest (A) and shortest (B) diagonals of the crown from leaf tip to leaf tip through the canopy mass and averaged as shown in Figure 12 below:

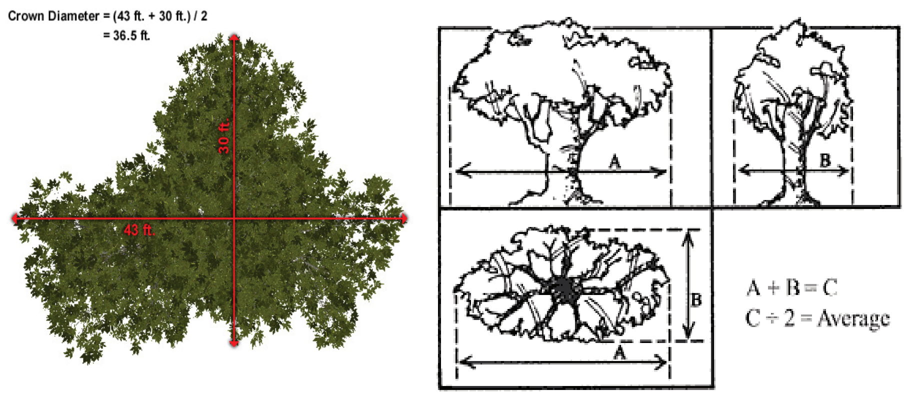

Figure 12: Measurement of tree crown diameter in the field
(Source: Google images)

Within each plot canopy cover percentage was estimated. To reduce bias, readings were taken in five different locations (centre, east, west, north and south directions) within the plots with the spherical densiometer and the readings averaged for each plot.

Although the tree height, DBH and crown cover data collected in the field was not used directly in the classification process, they were used in the analyses and interpretation of the classification results. For example, because the available SAR data (ALOS PALSAR) for the research was obtained from a longer wavelength (L-band) that interacts strongly with the canopy, branches, tree trunk (stem diameter) and the ground, the data gave the basis for the definition of the relationship between radar backscatter and the tree parameters measured in the field (Figure 13). Unlike the X and C bands that are of shorter wavelength and thus only interact with the top of the canopy and the tree crown respectively, the L - band is able to penetrate the canopy.

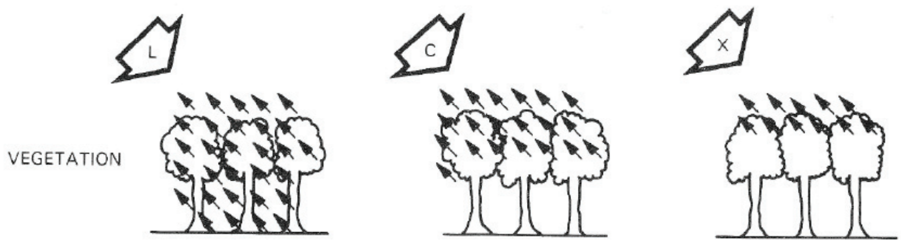

Figure 13: Penetration of different SAR signals (L-band, C-band and X-band) through vegetation adapted from Carver et al., (1988).

In all, 79 sample plots were assessed and information on tree parameters and general plot condition was recorded. Three (3) of the original 82 plots were not measured because they were inaccessible due to the flooding of a river on the way to the plots. Table 5 shows the number of points actually recorded per each cover class. The three (3) points recorded in fallow/grassland cover type were found to be homogenous yet were small (mostly less than 1 hectare) in size except for the Bimi community (Settlement) which is located in the forest reserve.

Table 5: Number of sample plots assessed in each landcover classes in the field

No.	**Landcover Class**	**Number of Points**
1	Natural Forest	16
2	Agroforestry	29
3	Plantation	27
4	Fallow/Grassland	3
5	Settlement/Bareground	4
Total		**79**

3.8 Satellite Data

Available is a 12.5m spatial resolution Advance Land Observing Satellite (ALOS) carrying a phased array L band SAR (PALSAR) data covering the extent of the study area. This image was acquired in January, 2009 and has a fine beam dual polarization of Horizontal-Horizontal and Horizontal Vertical (HH and HV). In HH polarization, the radar pulse is transmitted horizontally and the backscatter received horizontally. On the other hand, the radar pulse is transmitted horizontally and received vertically which is referred to as HV polarization. The data supplied by ITC was already geometrically corrected. Also available for use in this study is a level 1-B ASTER scene acquired in February, 2008 with a spatial resolution of 15m (VNIR) and 30m (SWIR). These datasets were chosen on the basis of suitability and availability. They were used for the MLC and OBIA landcover classification separately and in combination.

3.8.1 ASTER Data Processing

No atmospheric correction was done on the 1% cloud covered ASTER data. This was because the data supplied by ITC had already been atmospherically corrected and geometrically corrected to the UTM zone 30 coordinate system of Ghana. Due to positional inaccuracies the spatial reference of the image was updated by relating tie points on the image to 15 ground control points (GCPs) identified in topographic maps (road and river crossings) of the area and re-projected to the Ghana meter grid (GMG) projection system. The Ghana meter grid projection was used because it is the current projection system used for Ghana. Furthermore, efforts are being made to pool all data related to climate change / Carbon stock changes research in support of REDD+. One of the requirements of this programme which has already started is data consistency (including projection information in a common system - GMG). The use of the GMG projection is therefore in line with current efforts in making REDD+ a reality in Ghana.

A second order polynomial transformation was implemented in ArcGIS on the ASTER data and yielded a root mean square error (RMSE) of 0.387 (≈6m) the pixel size. This positional error is acceptable since it is less than half (<0.5) the pixel size (Jensen, 1996). However, other researchers have identified an RMSE range between 0.1 – 0.2 pixel size as being acceptable depending on the application (Townshend *et al*., 1992).

A subset of the ASTER data (RGB false colour composite (FCC)) covering the extent of AHFR (Figure 14A) was created in ERDAS IMAGINE 2011 to improve computational efficiency during classification. The RGB FCC was made on the ASTER data because the main cover types in the area were vegetation and the display of vegetation in red makes identification and interpretation by the analyst relatively easy. Vegetation appeared red because of its sensitivity to the near infrared channel (chlorophyll absorption channel) of the ASTER data that was assigned the colour red in the colour composite.

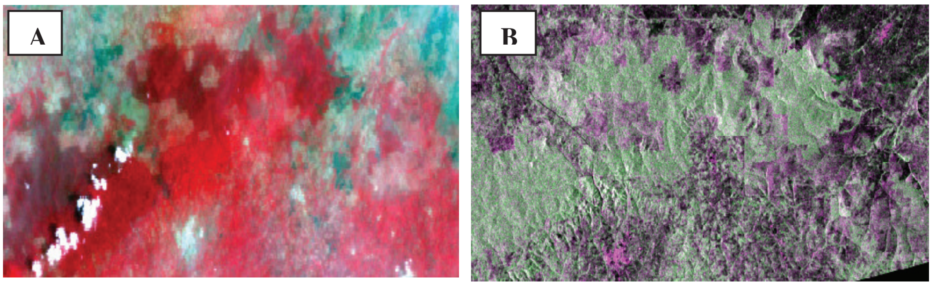

Figure 14: Available and suitable ASTER (A) and ALOS PALSAR (B) datasets for the research.

3.8.2 ALOS PALSAR Data Processing

The ALOS PALSAR data obtained from ITC was already geometrically corrected. It was re-projected to Ghana meter grid projection system to be consistent with the ASTER data. This was done to enable the combination of the two different datasets from different sensors.

An important step in the processing of SAR data for further analyses is de-speckling. Due to the inherent nature of speckle noise in SAR data, a 7 x 7 gamma- MAP filter was applied to the ALOS PALSAR data to reduce the speckle noise. This filter was applied since it produces a smoothened image with less degradation of textural information. The gamma-MAP filter (an adaptive filter) and frost filter have been supported by literature as the most promising and suitable filters for landcover classification projects

(Nyoungui *et al*., 2002). As shown in Figure 15, a significant amount of speckle was removed whilst some still remained after using a 7x7 window.

A subset of the SAR dataset was also created and converted from 16bit to 8bit as shown in Figure 14B above, to enhance processing speed.

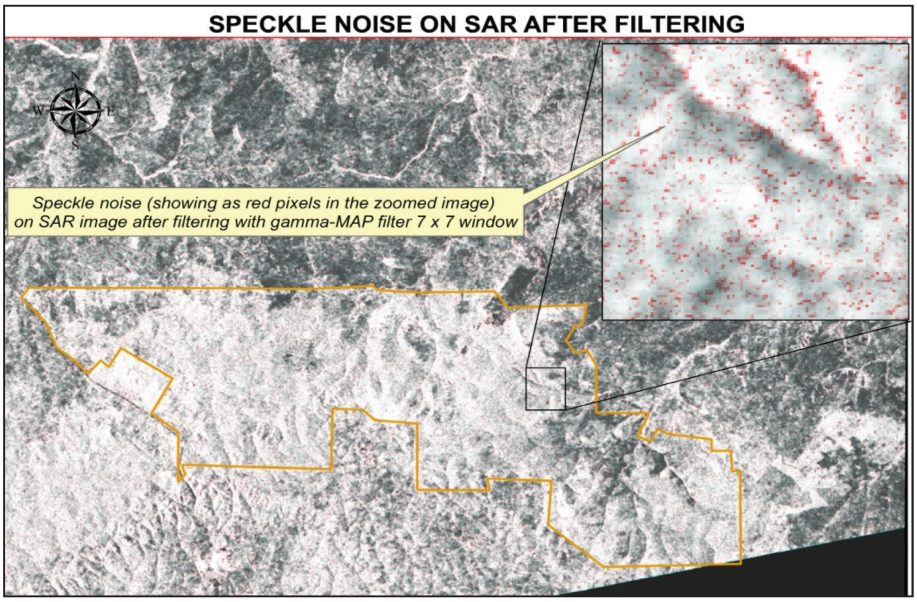

Figure 15: Speckle noise on SAR after 7x7 Gamma-MAP filtering.

3.9 Classification

A supervised classification using a Maximum Likelihood algorithm was implemented in ERDAS IMAGINE 2011. Training samples (Table 6) collected from the field were used to create the training areas (spectral signature) for the different landcover classes in the area. Post classification filtering was applied to the final images in each process to remove speckles resulting from the inherent spectral variability encountered by classifiers (Lillesand *et al*., 2008).

The OBIA technique was also implemented in Trimble eCognition v8.64. The results from the two methods and the different datasets (ASTER alone, SAR alone and combined ASTER+ SAR) were compared statistically to test any significant differences (Skidmore, 2002). Figure 16 shows the detailed flowchart of the methods.

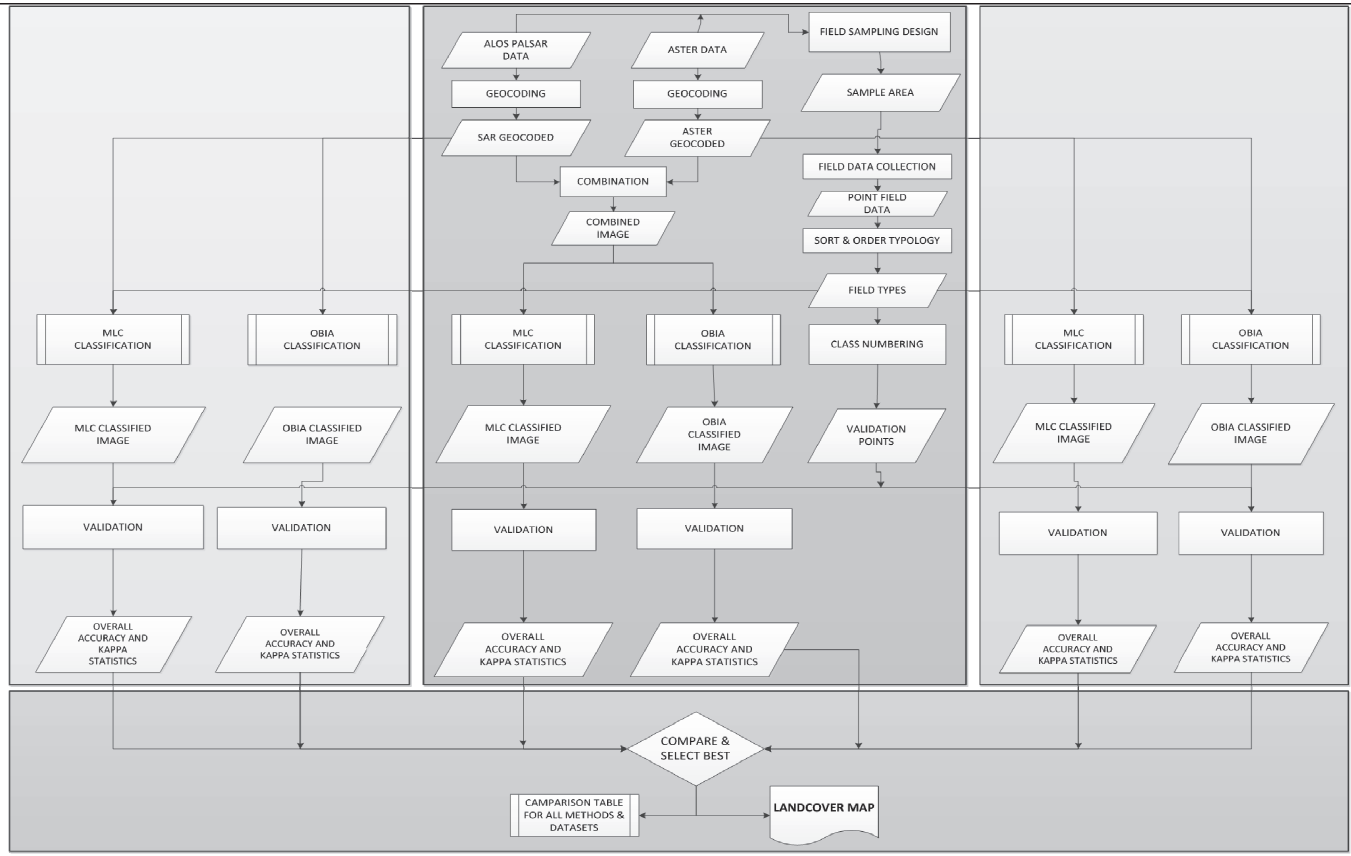

Figure 16: Detailed flowchart of MLC and OBIA Classification of AHFR

Table 6: Training and validation dataset distribution

Class Code	Class Name (Abbreviation)	No. Of samples	Training samples	Validation samples
1	Natural Forest (NF)	16	3	13
2	Plantation (P)	27	4	23
3	Agroforestry (AF)	29	3	26
4	Settlement/Bareground (S)	4	1	3
5	Fallow/Grassland (FG)	3	1	2
TOTAL		***79***	***12***	***67***

3.9.1 Maximum Likelihood Classification (MLC) Implementation

MLC on ASTER

The ASTER image alone in an RGB false colour composite (comprising bands 1, 2 and 3N) was classified using the MLC after digitizing polygons covering homogenous areas of the different cover classes (developing training areas) around 12 field collected points (Van Niel *et al*., 2005). The distribution of the points for the identified landcover classes is shown in Table 6 above. A post classification majority filtering using 3x3, 5x5 and 7x7 windows (Figure 17(*left*)) was done on the resulting image to remove noise and also investigate the effect of these filter windows on the classification results. Accuracy assessment was done on the classified image before and after filtering.

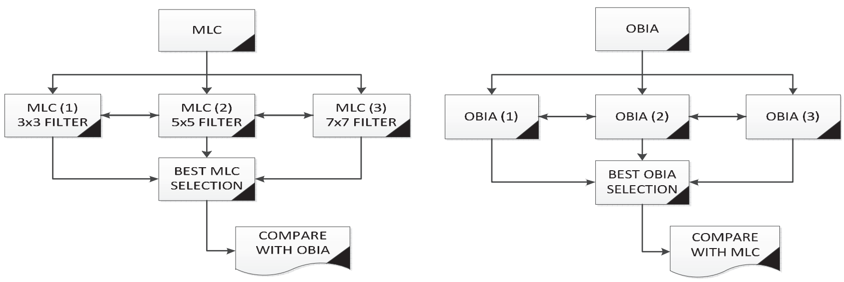

Figure 17: Post classification filtering and texture combination flowcharts for MLC (left) and OBIA (right)

MLC on ALOS PALSAR

The same procedure used for the ASTER data was repeated for the ALOS PALSAR data. Specifically, the classification was implemented on the HV, HH and HH/HV polarizations forming three bands that could show reasonable distinction between different landcover types. The Natural Forest and Plantation classes were merged before validation since the two could not be clearly differentiated from the ALOS PALSAR data.

MLC on combined ASTER and ALOS PALSAR

After the separate dataset classification, a combination (layer stacking in ERDAS 2011) was done using all the three ASTER bands and the three ALOS PALSAR bands for another classification to investigate the effect of image combination on the classification. Finally, filtering and accuracy assessment was done on the output (classified image).

3.9.2 Object Based Image Analyses (OBIA) Implementation

OBIA on ASTER

A multi-resolution segmentation algorithm was implemented in Trimble eCognition v6.84 on the 3 band ASTER data to form meaningful objects representing different landcover in the study area. After several trials, a scale parameter of 25, shape factor of 0.1 and compactness of 0.5 were found to be appropriate for this dataset. Screenshots of the process is shown in Appendix F. Training samples were selected and the area was classified (standard nearest neighbour) into the five main landcover classes identified in the previous method (MLC). Accuracy assessment was done on all the trial results and the one with the best accuracy in terms of overall accuracy and kappa coefficient was selected to be compared with the results from the same dataset using the MLC method (Figure 17(*Right*)).

OBIA on ALOS PALSAR

For the ALOS PALSAR data a multi-resolution segmentation was used to create image object primitives upon which the classification would be based. A scale parameter of 25, shape of 0.2 and compactness of 0.5 were found to be the best result. The standard deviation (a texture measure) from the grey level co-occurrence matrix (GLCM) in eCognition v6.84 was used on the three bands (HH, HV and HH/HV) for classification. The standard nearest neighbour classification algorithm was chosen. Finally, accuracy assessment was done on the different texture combination and the best was selected for comparison purposes.

OBIA on combined ASTER and ALOS PALSAR

The standard nearest neighbour classification algorithm was implemented after segmentation (multi-resolution in eCognition) of the combined ASTER+SAR data. The best parameters for the combined data were similarly to those of the ALOS PALSAR data alone. After several texture combination trials for the classification, accuracy assessment was conducted on the outputs and the best was selected for comparison.

3.10 Statistical And Spatial Comparison /Analyses

3.10.1 Statistical comparison of MLC and OBIA results

Error matrices for all the six selected classifications results (Appendix J) from the two methods and three datasets were compared and their significance tested statistically using equation 3. Significance testing is conducted by researchers to determine whether the null hypothesis is rejected in favour of the alternative hypothesis or otherwise. A code was written in MATLAB to calculate the variance of kappa (Congalton, 2009; Skidmore, 2002) from which the significance was tested at 5% significance level (i.e. $\alpha = 0.05$ and $\alpha/2 = 0.025$ for a two way test as done in this research). Figure 18 below illustrates the critical values (+/- 1.96) and the rejection regions for a two-way Z test. The 5% significance level was chosen because it is conventional (Stigler, 2008) and has been used by many researchers.

3.10.2 Spatial comparison of MLC and OBIA classification results (Maps)

Spatial comparison of the classification results were made to assess the agreement and disagreement areas in the maps produced (Figures 29 - 31). The comparison was made for both MLC and OBIA methods on the ASTER, SAR and combine SAR+ASTER datasets by overlaying the resulting maps and reclassifying them into agreement (Green) and disagreement (Red) areas.

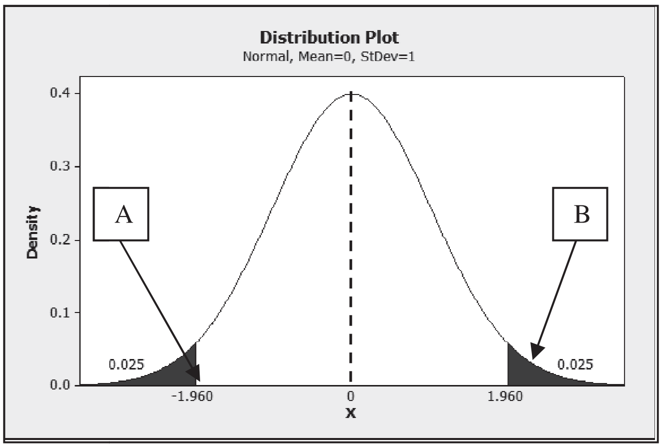

Figure 18: A normal distribution curve showing the critical value (A) and rejection region in black (B) of a 2-way 5% significance level (Source: Google Images).

Results of all these are presented in the next Chapter.

4.0 RESULTS

This chapter provides the answers to the questions posed by this study. It is therefore structured in a way to follow the questions as outlined in section 1.5 of the Introduction chapter. Issues like the relevant landcover types that can be identified in the study area, the effects of different filter windows on classification accuracy, overall best classification result and the statistical as well as spatial difference between the MLC and OBIA methods are well addressed in this chapter.

1. **What relevant landcover can be identified on SAR and ASTER data?**

Four (4) main classes namely Natural Forest/Plantation, Agroforestry, Fallow/Grassland and Settlement/Bareground (made up of rocky areas, exposed soil surface and settlements within the AHFR) were identified on SAR. The Natural Forest and Plantation classes were combined because they could not be well separated. Five (5) classes were identified on ASTER alone (and the combined ASTER+SAR datasets) namely Natural Forest, Plantation, Agroforestry, Fallow/Grassland and Settlement/Bareground. The relevant landcover classes identified on SAR and ASTER are shown in Figures 19 and 20 respectively.

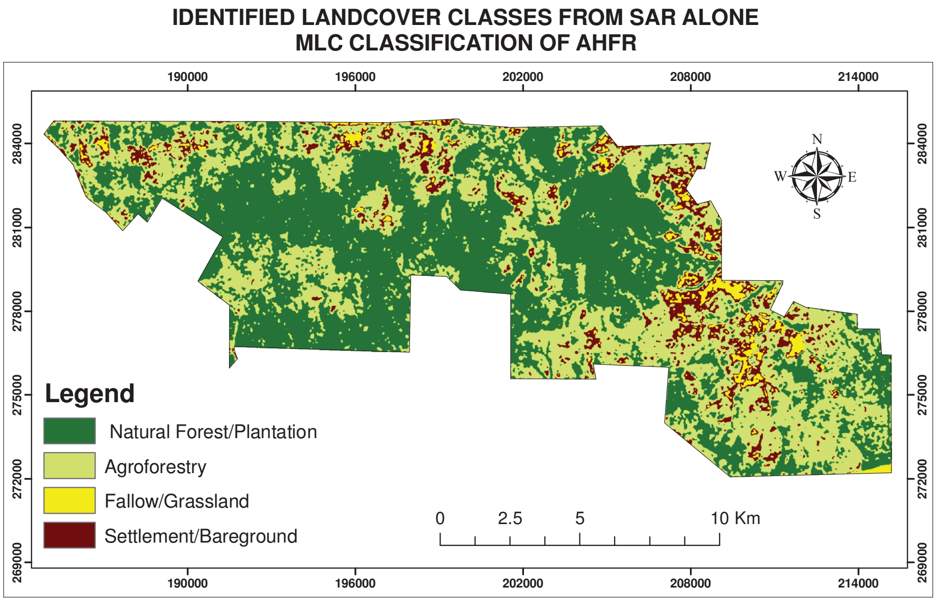

Figure 19: SAR MLC map of AHFR showing the four identified landcover classes.

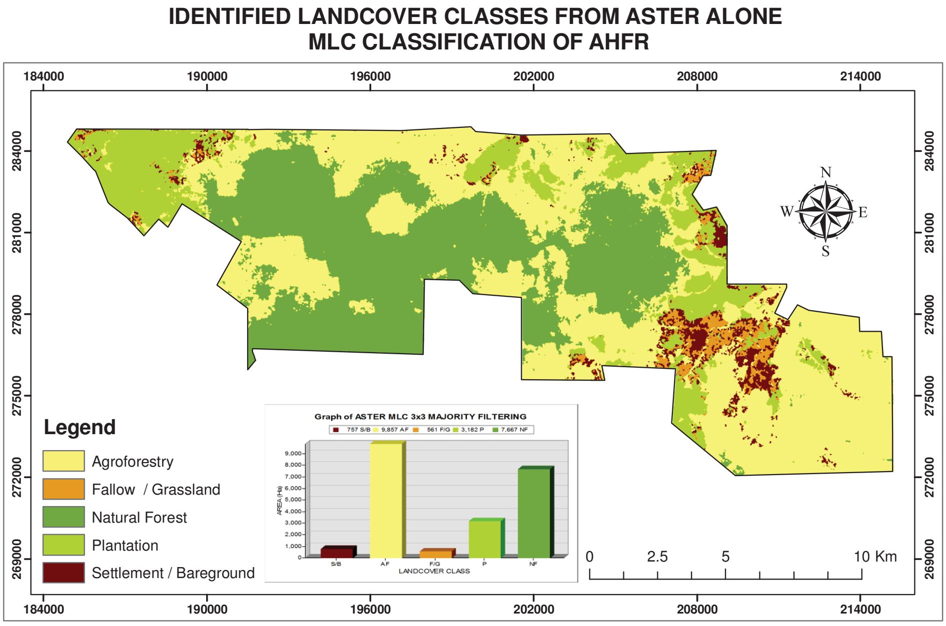

Figure 20: ASTER MLC map of AHFR showing the five identified landcover classes.

2. **Are there significant differences in the quality of landcover type classification obtained from MLC and OBIA on ASTER, SAR and combined ASTER+SAR data?**

The statistical test conducted showed that the difference between OBIA and MLC classification accuracy results (kappa) for the same datasets was not statistically significant. Comparison between methods, MLC ($\widehat{K}_1$) and OBIA ($\widehat{K}_2$) yielded Z_{test} values of 0.64, 1.82 and 1.18 for ASTER alone, SAR alone and combined ASTER+SAR respectively.

However, comparing maps from different datasets using the same method showed there was a significant difference between SAR and ASTER; as well as SAR and combined ASTER+SAR maps for both MLC and OBIA. There was no significant difference between the kappa coefficients for ASTER alone and combined ASTER+SAR maps produced from OBIA and MLC. Table 7 shows the Z_{test} values for the comparison within methods.

These results will be interpreted and discussed in Chapter 5.

Table 7: Calculated Z (Z_{test}) values for comparing MLC and OBIA maps

	METHODS	
MAPS	MLC (Z_{test} value)	OBIA (Z_{test} value)
SAR/ASTER	2.33*	3.60*
ASTER/combined ASTER+SAR	0.43	0.09
SAR/combined ASTER+SAR	2.70*	3.58*

** Significant*

3. Which kind of texture combination (in OBIA) gives the best results in ASTER, SAR and combined ASTER+SAR data classification?

The standard deviation (measure of texture) based on the Haralick *et al* (1973) Grey Level Co-occurrence Matrix (GLCM) on combined ASTER+SAR data produced the second best result after ASTER alone (difference however not significant) in the OBIA classification. Figure 21 – 23 show the resulting maps for the three different datasets. OBIA classification accuracies for the selected best texture combination per each dataset is summarised in Table 8 below:

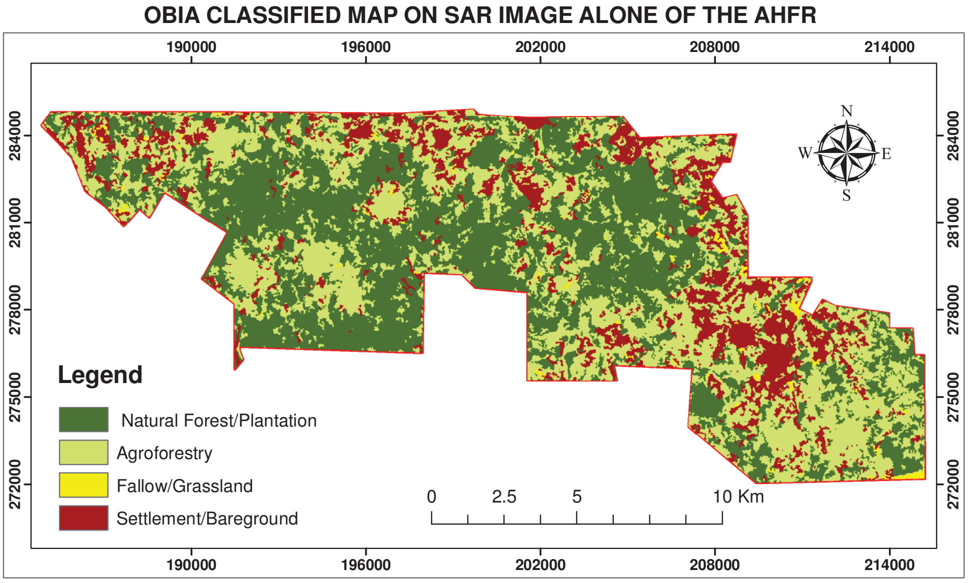

Figure 21: Best OBIA texture combination result on SAR data alone

Table 8: Summary of OBIA classification accuracy results for SAR, ASTER and combined ASTER+SAR

	ASTER ALONE			COMBINED ASTER+SAR			SAR ALONE		
LANDCOVER CLASS	PRODUCER ACCURACY	USER ACCURACY	KAPPA	PRODUCER ACCURACY	USER ACCURACY	KAPPA	PRODUCER ACCURACY	USER ACCURACY	KAPPA
NF	92.31%	70.59%	0.6351	100.00%	65.00%	0.5657	69.44%	60.98%	0.1566
P	65.22%	88.24%	0.8209	73.91%	80.95%	0.7100			
AF	76.92%	71.43%	0.5331	61.54%	84.21%	0.7420	30.77%	40.00%	0.0195
S	100.00%	100.00%	1.0000	100.00%	50.00%	0.4766	66.67%	33.33%	0.3021
FG	0.00%	0.00%	-0.0308	0.00%	0.00%	-0.0308	---	---	0.0000
TOTALS	**74.63%**		**0.6368**	**73.13%**		**0.6269**	**52.24%**		**0.1337**

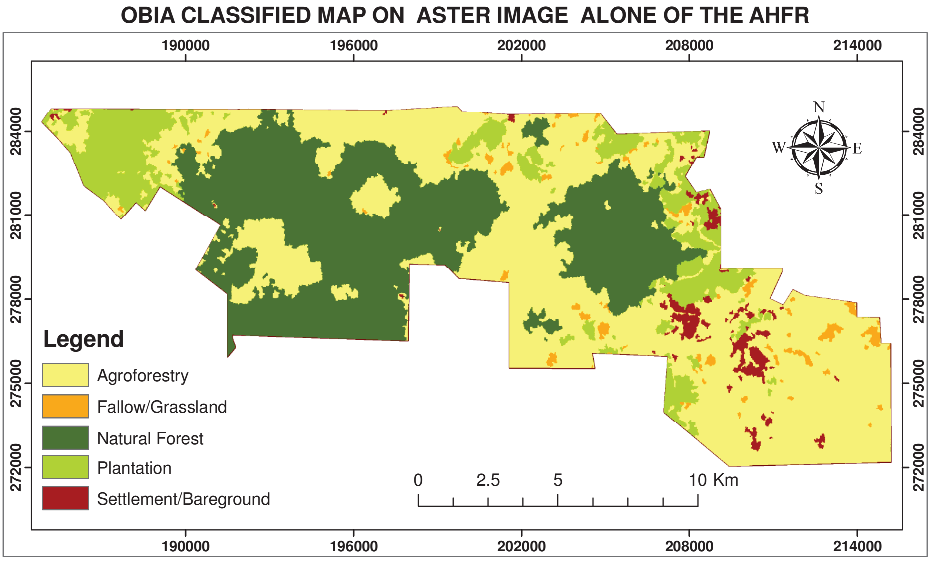

Figure 22: Best OBIA combination result on ASTER data alone

An interesting intermediate results in the OBIA classification that is worth mentioning is the complete elimination of speckle noise (Appendix F) from the SAR and combined ASTER+SAR data during the segmentation stage (even before the actual classification) of the analyses.

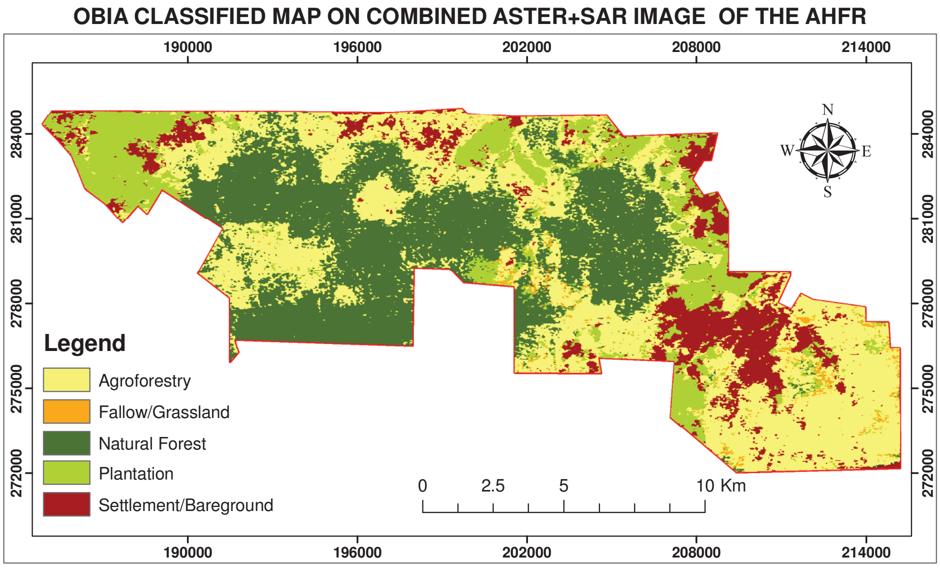

Figure 23: Best OBIA texture combination result on combined ASTER+SAR data

4. **Which filter window (in MLC) gives the best result in ASTER, SAR and combined ASTER+SAR data classification?**

Apart from the ASTER alone MLC classification in which the accuracy was improved from 77% to 79% after 3x3 filtering (Figure 24), none of the results from the other datasets (SAR and combined ASTER+SAR) was improved. Table 9 gives a summary of the best results from the three datasets after filtering. The 3x3 majority filter was found to be the most suitable.

Table 9: Summary of MLC classification accuracy for SAR, ASTER and Combined ASTER+SAR after 3x3 majority filtering

	ASTER ALONE			COMBINED ASTER+SAR			SAR ALONE		
LANDCOVER CLASS	PRODUCER ACCURACY	USER ACCURACY	KAPPA	PRODUCER ACCURACY	USER ACCURACY	KAPPA	PRODUCER ACCURACY	USER ACCURACY	KAPPA
NF	100.00%	65.00%	0.5657	100.00%	72.22%	0.6553	83.33%	73.17%	0.4201
P	69.57%	88.89%	0.8308	73.91%	85.00%	0.7716			
AF	80.77%	84.00%	0.7385	84.62%	88.00%	0.8039	61.54%	69.57%	0.5027
S	100.00%	75.00%	0.7383	100.00%	100.00%	1.0000	0.00%	0.00%	-0.0308
FG	---	---	0.0000	0.00%	0.00%	-0.0308	---	---	0
TOTALS	**79.10%**		**0.7025**	**82.09%**		**0.7435**	**68.66%**		**0.4159**

General visual assessment of the outcome of the various majority filtering windows showed that the 7x7 window produced a smoother map. However, a lot of details were removed from the classified map without any quantitative improvement in the classification accuracy. Figure 24 shows MLC classified map of the study area with no filtering, 3x3, 5x5 and 7x7 majority filtering, as small inserts below the main map. Summary of the classification accuracy of the three datasets with different filtering windows can be found in Appendix H. The effect of the three different majority filtering windows on the entire study area mapped can be found in Appendix I.

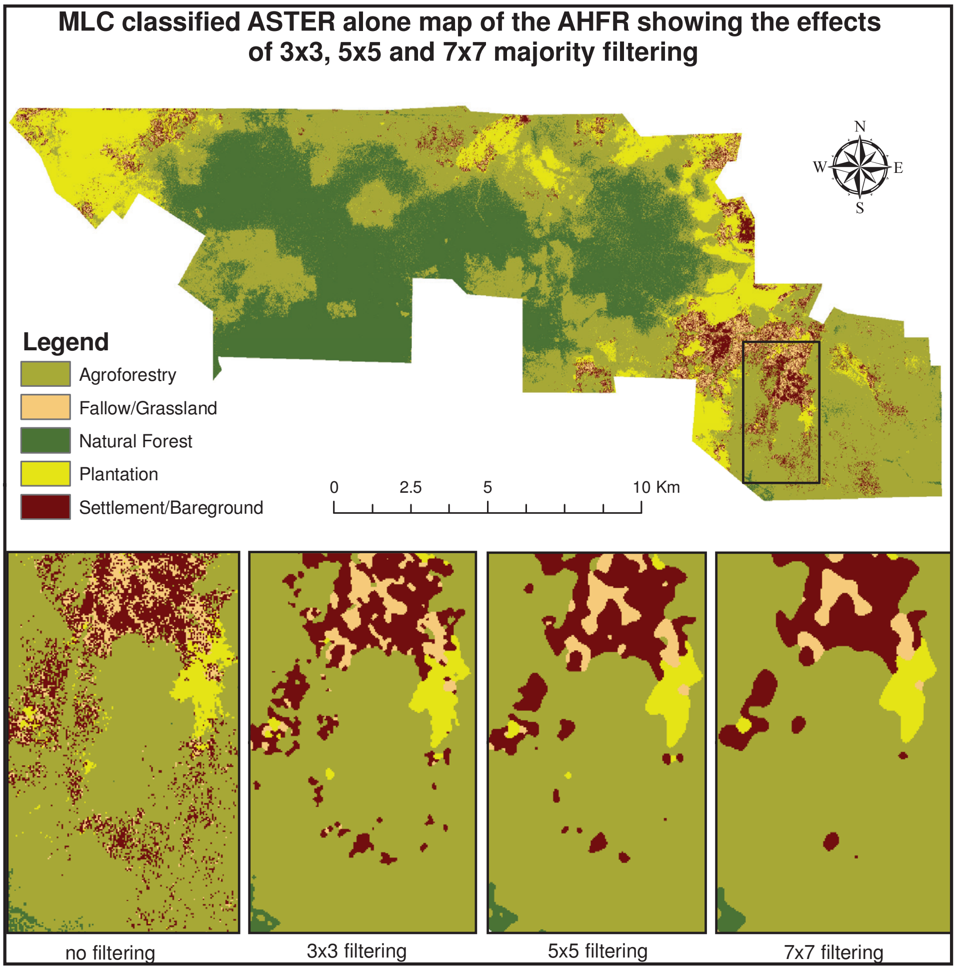

Figure 24: MLC classified ASTER Landcover map of AHFR showing the effect of different majority filtering windows (Inserts)

Figure 25 shows the effect of filtering on the SAR MLC classified image. A small portion of the study area was zoomed into to show the removal of post classification noise using the different filtering windows (3x3, 5x5 and 7x7).

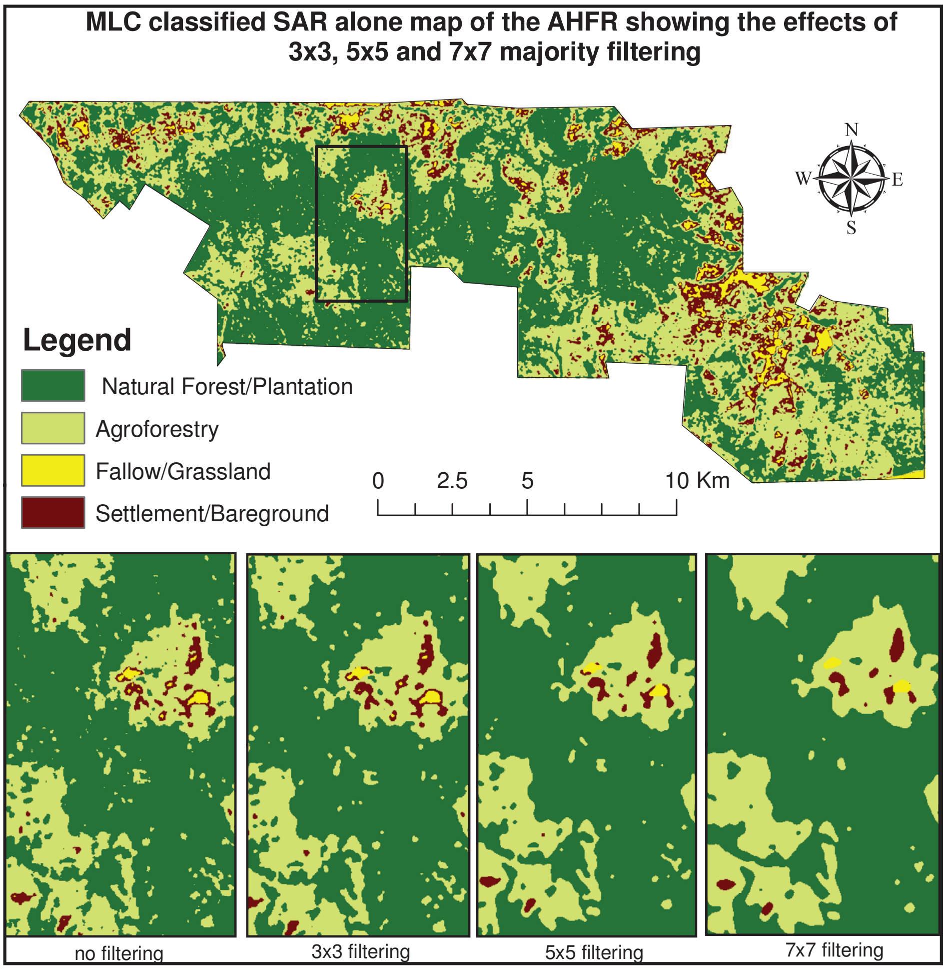

Figure 25: MLC classified SAR Landcover map of AHFR showing the effect of different majority filtering windows (Insert).

Another portion was selected on the combined ASTER+SAR MLC classified landcover map of the AHFR to show how different filtering widows affect the classification result. As indicated already in the case of the ASTER alone map, there was no quantitative improvement in the accuracy of the combined ASTER+SAR map. Figure 26 below shows the visual (qualitative) effect the 3x3, 5x5 and 7x7 filters have on the classified map.

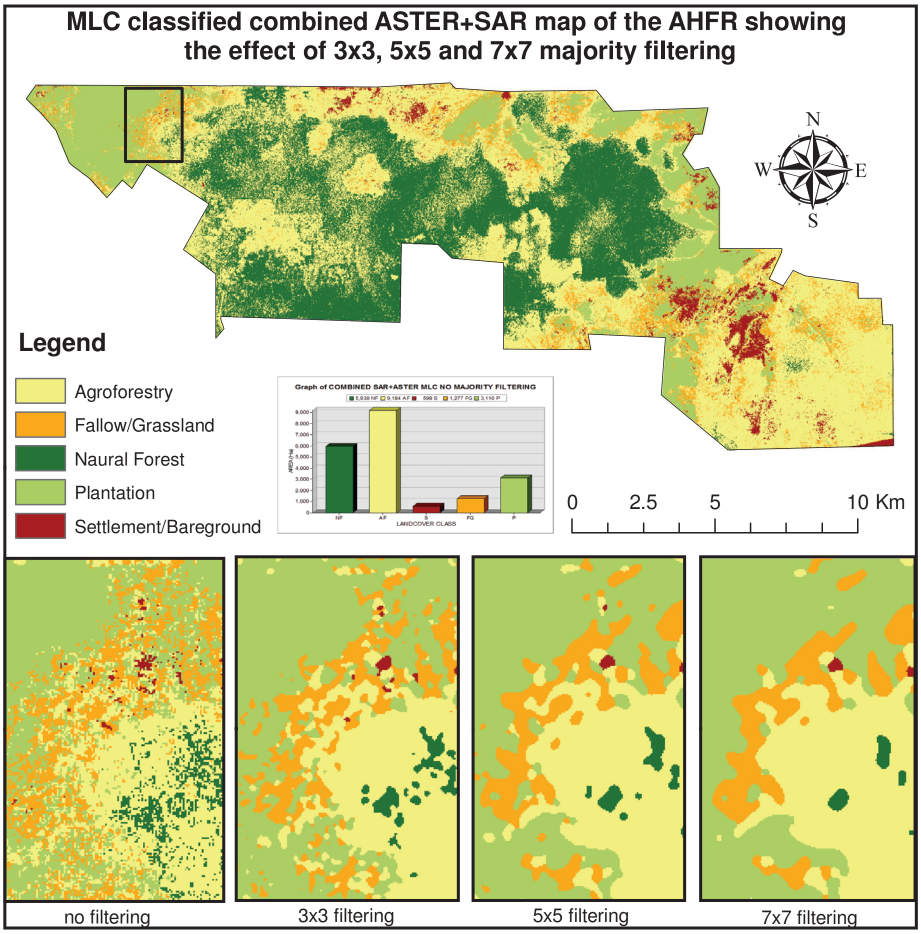

Figure 26: MLC classified combined ASTER+SAR Landcover map of AHFR showing the effect of different majority filtering windows (Insert).

5. **What is the overall best classification accuracy (in terms of kappa) obtained from ASTER, SAR and combined ASTER+SAR data classification?**

The MLC classified combined ASTER+SAR data gave the overall best result in terms of kappa (and overall accuracy). The overall best kappa coefficient was 0.7435. This was followed by MLC on ASTER alone (0.7025), OBIA on ASTER alone (0.6368), OBIA on combined ASTER+SAR (0.6269), MLC on SAR alone (0.4159) and finally OBIA on SAR alone (0.1337). Appendix J shows the respective error matrices for the above.

6. What is the quality of the landcover map produced from the overall best classification of ASTER, SAR and combined ASTER+SAR data?

The overall best landcover map of the AHFR produced from this study is 82.09% accurate (Figure 27). It was obtained from the MLC classification (after 3x3 post classification majority filtering) of the combined ASTER+SAR data. Out of the total area of 20,108ha, the Agroforestry cover type was the largest, contributing 47% followed by Natural forest (30%), Plantation (16%), Fallow/grassland (4%) and finally Settlement/Bareground (3%). Figure 28 shows the distribution of the landcover types in the study area in hectares. Furthermore, Table 10 shows the category-by-category user's and producer's accuracies as well as their respective conditional kappa coefficients. Except for the Fallow/Grassland class, all the classes have user's and producer's accuracies above 70%, with the Settlement class being the highest (100%).

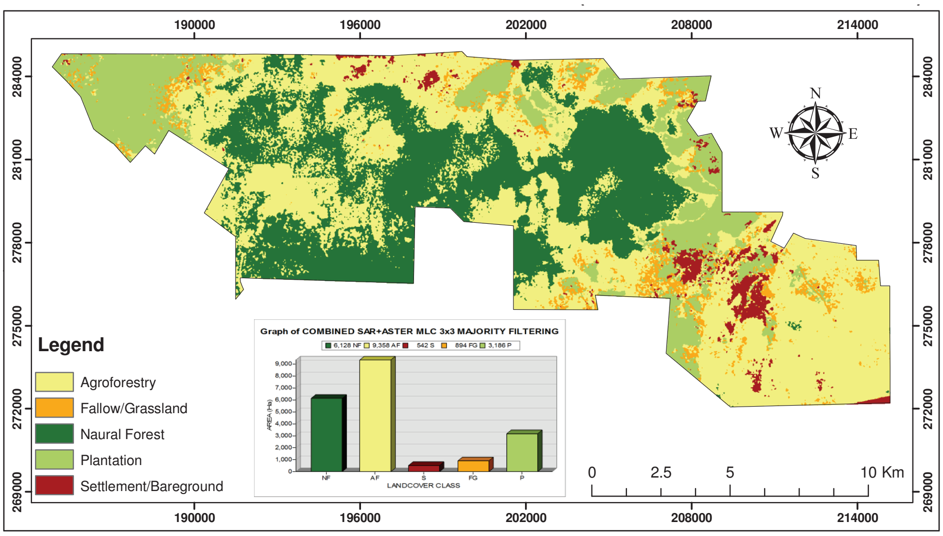

Figure 27: Overall best classified landcover map of the AHFR

Table 10: Accuracy totals and respective conditional kappa coefficients for the five (5) landcover classes of the overall best landcover map of the AHFR.

COMBINED ASTER+SAR RESULTS AFTER 3x3 MAJORITY FILTERING						
ACCURACY TOTALS						
Landcover Class	**Reference Totals**	**Classified Totals**	**Number Correct**	**Producers Accuracy**	**Users Accuracy**	**Conditional Kappa**
NF	13	18	13	100%	72.22%	0.66
P	23	20	17	73.91%	85.00%	0.77
AF	26	25	22	84.62%	88.00%	0.80
S	3	3	3	100%	100%	1.00
FG	2	1	0	0.00%	0.00%	-0.03
	67	**67**	**55**			
OVERALL ACCURACY = 82.09%						
OVERALL KAPPA = 0.74						

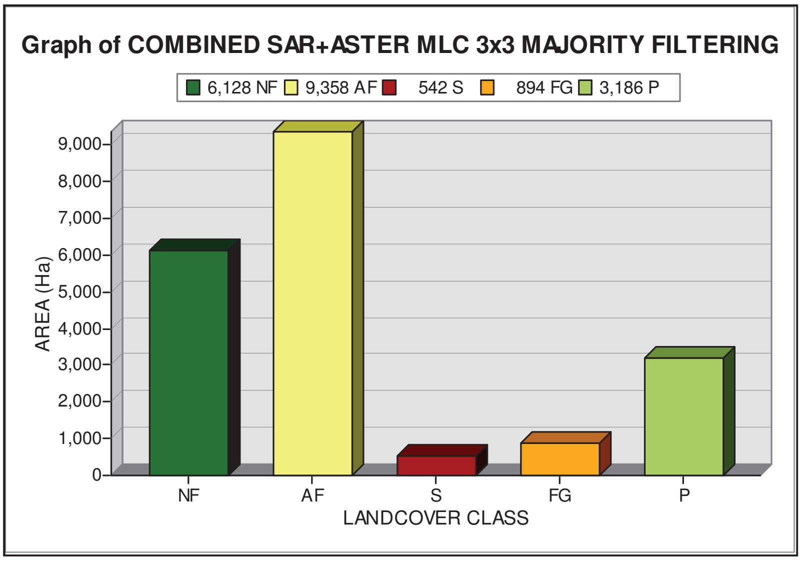

Figure 28: Distribution of the identified landcover types in the AHFR

SPATIAL COMPARISON OF OBIA AND MLC CLASSIFIED MAPS

Spatial comparisons between the OBIA and MLC Classification are shown in Figures 29 – 31. The black dashed boxes show areas of major disagreement. The disagreement areas are mostly in the Settlement (south-eastern portion), Natural Forest and Agroforestry classes. The level of agreement between MLC and OBIA for ASTER alone was the highest (80%) followed by the combined ASTER+SAR (72%) and the SAR alone (64%).

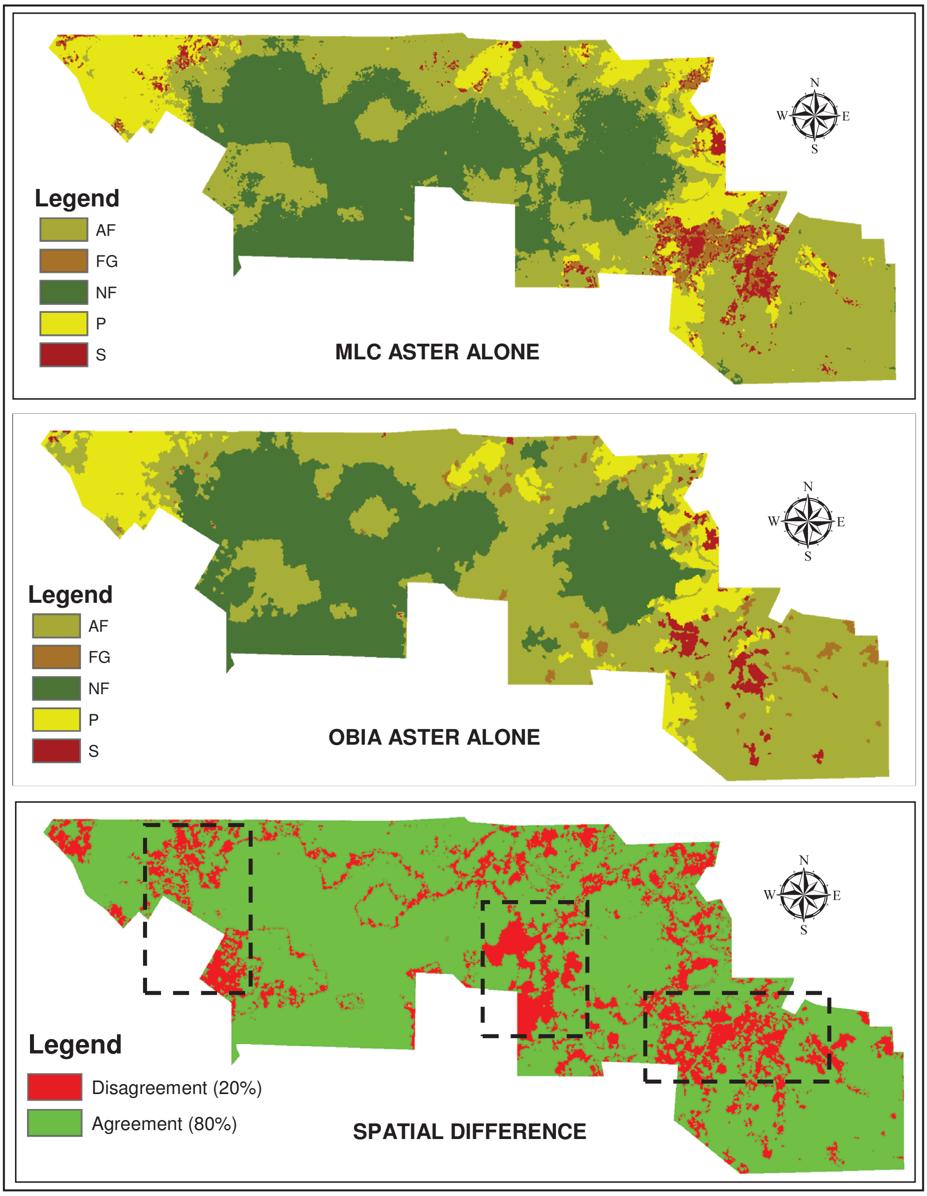

Figure 29: Spatial comparison between OBIA and MLC classification on ASTER alone

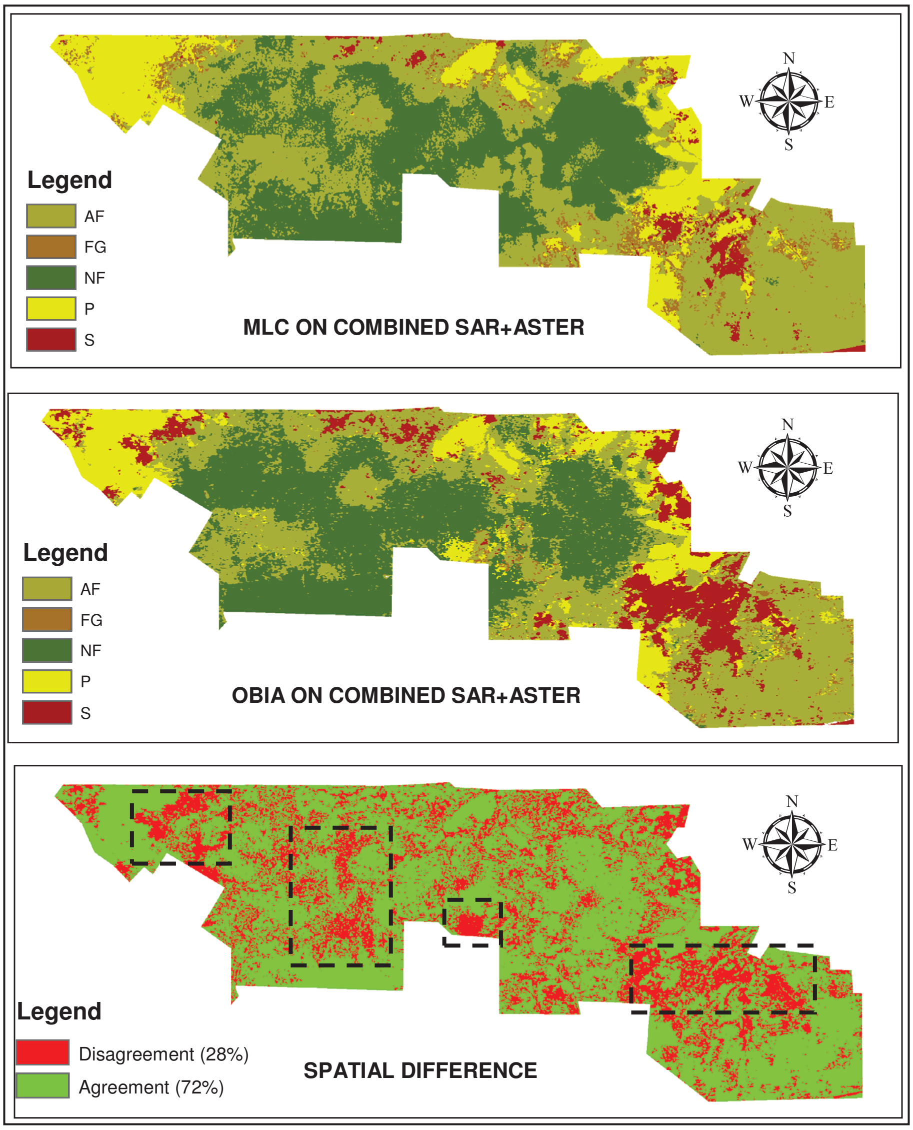

Figure 30: Spatial comparison between OBIA and MLC classification on combined ASTER+SAR

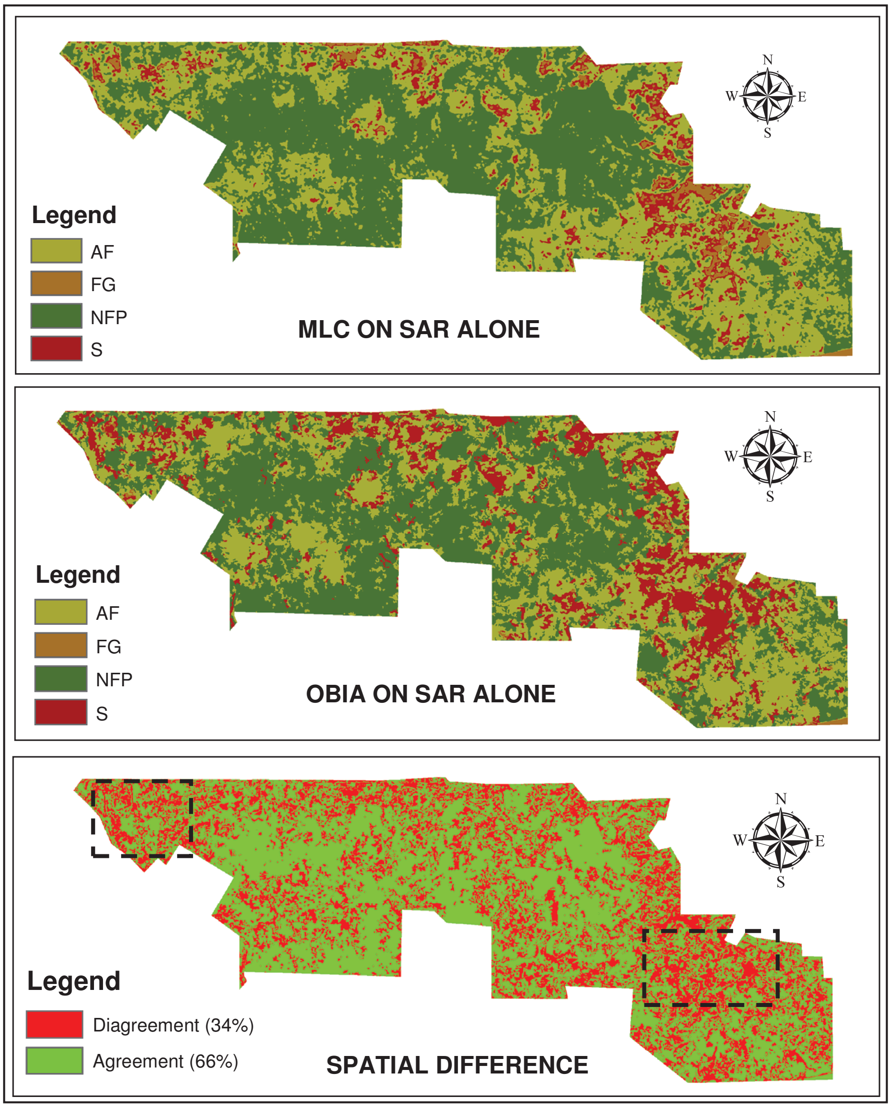

Figure 31: Spatial comparison between OBIA and MLC classification on SAR alone

5.0 DISCUSSION

This chapter discusses the results of this study and provides possible reasons for the observations made. As described in chapter 4, two (2) different classification approaches were tested on two (2) different images separately and on the combination of these images. This resulted in a total of six (6) products to compare in the context of the research objectives.

5.1 Identified Landcover Classes In The Afram Headwater Forest Reserve

The study identified five (5) main landcover types in the AHFR on the ASTER multispectral data alone and the combined ASTER+SAR data. In the case of these datasets, each of the different landcover types showed a unique reflectance. Therefore the Natural Forest (NF) and Plantation (P) classes could be distinguished.

For the ALOS PALSAR, on the other hand, the NF and P classes could not be properly separated because of the similarity (nature of the vegetation structure) in the cover types in terms of their vertical structure (texture) and backscatter. Podest and Saatchi (2002) in a similar study using JERS-1 data were able to separate forests from non-forests (and not separation within similar vegetation classes like NF and P) with a high accuracy (i.e. over 90%). This was because of the sensitivity of the radar backscatter to biomass levels in the landcover types. An exploratory data analyses conducted on the tree parameters measured in the field showed a marginal difference in the mean tree height and crown diameter of the NF and P classes. Most of the NF plots inventoried in the field were remnants of natural forest vegetation with very few tall trees. Majority of the trees are regenerated ones with an average height similar to those in plantations. Moreover, the colonisation of the reserve by York (*Broussonetia papyrifera*) has made the species an inseparable component of the NF class. This could be a result of deforestation (through unsustainable legal and illegal logging) which creates forest gaps that favour the colonisation of York. Consequently, York showed a reflectance akin to the NF cover type. For instance, in the study of Nguyen (2010), areas that were classified as NF and formed the basis for the landcover stratification for this study were found to be York stands. Most of these stands adjoin remnant NFs and some were cleared by the time of the fieldwork in 2011.

The problem of spectral mixing occurred in the classification of both the SAR and multispectral data resulting in low accuracies. This may be due to the fact that the major cover types in the area (NF, P and AF) forming over 90% of the AHFR are vegetation and have some structural and spectral similarities. This problem has been usually reduced in studies that used reasonably large and distinct landcover/landuse types (e.g. urban/built-up, vegetation, water etc.) thereby resulting in higher accuracies.

5.2 Significance test for OBIA and MLC maps of AHFR

The tabulated Z (critical value) at 5% significance level was compared with the calculated Z (Z_{test}) to test the null hypotheses put forward for this study as stated in section 1.6 of chapter 1. The null hypothesis that the kappa coefficients of two maps being compared is the same is rejected if the calculated or Z_{test} is greater than the tabulated Z (i.e. $Z_{test} > Z$ (1.96)).

Comparison **between methods**, MLC ($\widehat{K}_1$) and OBIA ($\widehat{K}_2$) yielded Z_{test} values of 0.64, 1.82 and 1.18 for ASTER alone, SAR alone and combined ASTER+SAR respectively. The null hypothesis that there is no significant difference between the kappa of MLC and OBIA ($H_O : \widehat{K}_1 = \widehat{K}_2$) was therefore not rejected because all the Z_{test} statistics for the three datasets were less than the critical value (meaning they fell outside the rejection region) (Figure 18). The results of this statistical test revealed that there was no significant difference between the accuracy results (kappa) obtained from the two **different methods** for the **same datasets**.

However, comparison **within methods** (i.e. comparing maps from **different datasets** using the **same method**) showed there was a significant difference between SAR and ASTER; as well as SAR and combined ASTER+SAR maps for both MLC and OBIA (Table 7). This was because their Z_{test} statistics fell within the rejection region (Figure 18). The null hypothesis in this case was therefore rejected and concluded that there is a significant difference (Congalton, 2009; Skidmore, 2002). There was no significant difference between the kappa coefficients for ASTER and combined ASTER+SAR maps produced from the two methods (Table 7). Consequently, the null hypothesis was not rejected and the conclusion is that there is no significant difference between the two maps. This is an important result because it contradicts to some extent the IPCC's expectation, for image combination to improve classification accuracy. The result, however, agrees with the IPCC's expectation when looking at SAR classification, in which the combination of ASTER and SAR gave a significant improvement.

5.3 Effect of filtering and texture combination on classification.

Trial of the three (3) majority filters (3x3, 5x5 and 7x7 windows) revealed the superiority of the 3x3 majority filter window over the 5x5 and 7x7 in this study. The 3x3 window was chosen as the best in the MLC because classification accuracy improvement stopped after applying the 3x3 filter. Any further filtering (e.g. 5x5, 7x7 etc) removed details from the map, making it smooth and visually appealing, without necessarily adding anything in terms of accuracy improvement.

Although the standard deviation measure in this study produced the best results in the OBIA classification it was evident in the Trimble eCognition software however, that many options and combinations are still available that could be tried in order to bring out a better result. This requires some amount of time to explore through "trial-and-error".

Speckle noise was reduced in the combination of ASTER and SAR data and was completely eliminated during segmentation in the OBIA as shown in Appendix F. This is the result of grouping pixels into objects by automatically assigning every pixel to a group to form an object. The main idea behind OBIA stems from this and the technique is promising for SAR classification and speckle noise removal. It would be very important for studies in the tropics to focus on SAR and the OBIA technique in view of the advantages the data offers as well as the promise shown by the technique.

5.4 The overall best classification accuracy in terms of kappa.

The combination of ASTER and SAR data brought about improvement in the classification accuracies over what could be obtained by each dataset when classified separately. Although in the case of the ASTER alone the improvement is very slight. This observation was supported by (Hoan *et al*., 2011) in a similar study. In their study, the overall classification accuracy was improved from 77% (kappa coefficient of 0.73) to 88% (kappa coefficient of 0.86) after the combination of ALOS PALSAR (microwave) and ALOS/AVNIR-2 (multi-spectral) data. The main forest classes in that study were mapped with accuracies higher than 90%.

The overall best classification accuracy in terms of kappa of 0.7435 for this study indicates that the final map selected from the six chosen, agrees with reality by 74%. This means that the accuracy was 0.74 out of 1, not by chance. The kappa is a good statistic recommended by most researchers including Skidmore (2002) since it takes into consideration all the cells in the error matrix. As interpreted by Munoz & Bangdiwala (1997) and Navulur (2007) (Table 2), there is a substantial agreement between the classified map and the reference data. Conditional kappa coefficients for individual classes from the classification accuracy assessment revealed that except for the FG class, all the major landcover classes had a substantial agreement with the least being the NF class ($\widehat{K}$=0.66). Table 10 shows the various conditional kappa coefficients for the 5 identified landcover classes in the AHFR. There was an extremely poor agreement between the classified and reference data for the FG class which eventually affected the magnitude of the overall kappa. This could be because the few areas identified in the field were small (barely a hectare in size) and areas selected as FG before fieldwork had been converted into Agroforestry as part of the on-going NFPDP by the Government. It was therefore a challenge to get large homogenous areas to represent the FG landcover.

5.5 Quality of the landcover map produced

The quality of the overall best landcover map of the area (obtained from the combined ASTER+SAR data) was marginally less (82.09%) but not significantly different from the expected accuracy (of ≥85%) indicated by the USGS landcover classification systems criteria (Lillesand *et al*., 2008). The accuracy of the map is therefore acceptable and can be used for forest management purposes to support the REDD+ programme in Ghana. From the accuracy totals summaries by categories it can be interpreted that if a user takes the map to the field the likelihood of correctly identifying a Natural Forest landcover is 72%. For a Plantation, Agroforestry and Settlement it is 85%, 88% and 100% respectively, which is actually very good and reliable. The reliability of the Fallow/grassland landcover type could not be guaranteed by this research though it forms a vital part of the existing landcover in the area. This is because both producer's and user's accuracies for the Fallow/Grassland class were all 0%.

From the error matrix of the overall best map, some confusion between the NF, AF and P classes was observed. The confusion between the P and AF was expected and could be because the P class is basically a graduation from the AF class and there might be some similarities in their reflectance. For instance young plantation stands do not have a completely closed canopy just as in old AF stands and therefore grass and *C. odorata* undergrowth are common to both classes. These may therefore show up in the image.

Another point worth noting from the results of this study is that the dominant landcover type is AF forming almost 3 times that of Plantation and approximately one and half times Natural Forest (Figure 28) in the area. This is an indication that the major activity in the reserve now is plantation development aimed at restoring the degraded forest cover. As mentioned earlier in this document, the main strategy for the establishment of these plantations is through the modified taungya system (MTS) which is an Agroforestry concept (section 2.6.1).

5.6 Comparison with previous research

The results of this study agree very well with previous research in the same study area using the same datasets. Nguyen (2010) estimated aboveground biomass and produced a carbon map of the study area. In that study, an 81.25% accurate landcover map of the area was produced by applying the MLC on a fused (or combined) ASTER and ALOS PALSAR data. In another study, Dwomoh (2009) developed a fire model to estimate the area of burnt tropical forest after an instance of fire. A landcover map of the study area created using ASTER data alone for the classification was found to be 78.10 % accurate. The method used for that study too was the MLC.

However, the two studies mentioned above did not classify ALOS PALSAR data alone because that was not the focus of the research. This study thus filled this gap by classifying the three datasets separately and comparing the quality of the resulting maps. Also, a different technique (OBIA) apart from the MLC was tested to provide a basis for the comparison of methods. For MLC, the classification accuracy of SAR improved by 14% (from 68 – 82%) through the combination of SAR and ASTER. Moreover, applying OBIA resulted in the classification accuracy increasing by 21% (from 52 – 73%), after combining ASTER and SAR. This was because the two separate datasets complemented each other with their unique advantages (spectral and textural information) when combined to bring about the improvement.

Furthermore, this study agrees with that of Walker *et al* (2010) who explored the potential of SAR to complement optical remote sensing in designing a robust forest monitoring systems to support REDD+. Their study also showed that as the number of class aggregation levels increased (e.g. from 15 to 2 classes) classification accuracy improves. In their case SAR was improved from 58% to 92% (i.e. by 34%) which was higher than that obtained in this study (21%). This was expected because only two classes, merely forest and non-forest, which are easy to discriminate due to reduced inter-class confusion, were assessed.

5.7 Possible sources of errors

There was approximately an 18% (i.e. 82% accurate) error associated with the overall best classified map of the Afram Headwaters Forest Reserve. This error could be due to one or more of the following factors since a map is simply a model (Foody, 2002). Foody (2002) hinted that because maps generalise reality they will always have errors and uncertainties associated with them. It is therefore always important to give an indication of the error and uncertainties associated with models.

- **Errors in input data**

The presence of speckle noise in the ALOS PALSAR data is an obvious source of input data error for this study. For instance, in Figure 15, the data used for the classification after 7x7 Gamma-MAP filtering is shown. Although a significant amount of the speckle noise was removed, some still remained which may cause spectral confusion during classification. This error could be propagated especially when combining the ALOS PALSAR data with the ASTER data. Furthermore, the difference in spatial resolution and acquisition times of ASTER (February, 2008) and ALOS PALSAR (January, 2009) may reduce classification accuracy.

- **Errors from the image processing techniques**

Some amount of data quality was degraded especially when converting the 16bits ALOS PALSAR data into 8bits for easy processing. Another processing technique error could arise from the frequent switching between ArcGIS, ERDAS imagine and eCognition software. During the data processing stage it was observed that though the images were already corrected to the UTM Zone 30N system, there was a spatial mismatch with the shapefiles in the same coordinate system. The resultant RMSE (0.387, ≈39%) after georeferencing clearly shows that there could be potential positional inaccuracies (Delafontaine *et al.*, 2009) which could eventually influence the results of this study.

- **Expertise of the analyst**

Although care was taken in entering the data it is worth mentioning that it is one area in any RS/GIS project that can introduce errors (Congalton, 2009). Furthermore, classification in the field (e.g. in this study area with the main cover types being vegetation) is not 100% clear as one would do for classes like “land” and “water”. In the field, fuzzy classes are usually encountered and the expertise or discretion of the analyst is used. This is normally very subjective and has its associated errors.

5.8 Spatial comparison between OBIA and MLC maps

Spatial comparison done on the MLC and OBIA maps shows some disagreements. Interestingly, the areas of agreement especially for the ASTER alone and combined ASTER+SAR far outweighed the disagreement areas. Such a result was expected because the study dealt with two different methods and datasets which may have their own errors associated with them. For instance, using ASTER alone may have fewer errors compared to combining it with SAR. This is because there would be a propagation of errors from one dataset to the other. This can be further explained by the reduction in MLC/OBIA map agreement areas for ASTER alone and combined ASTER+SAR map from 80% to 72% respectively shown in Figures 29 and 30. Moreover, the difference in the time of acquisition of this satellite images could contribute to these disagreements between the maps. These disagreement areas are portrayed as sliver polygons which are said to be the result of classification errors (Delafontaine *et al.*, 2009). According to Delafontaine (2009), slivers cannot be avoided because of the errors (including positional inaccuracies) and uncertainties associated with geographical data.

From the spatial comparison results, it can be observed especially in the case of ASTER alone and the combined ASTER+SAR maps that the disagreement areas were mostly along class boundaries, Settlement/Bareground class and also between the NF and AF classes. However, on the SAR data alone there was no regular pattern to the disagreement of the two maps produced from MLC and OBIA. It was more of a random distribution over the entire study area. Most of the disagreement areas in SAR were found in the north western and south eastern portions of the AHFR with main cover types being AF, NFP and Settlement. This may be due to the effect of speckle noise on the SAR data or the inability of the classifiers to accurately separate different classes. This result on SAR re-emphasizes the difficulty in its usage to produce landcover maps through image classification, though it is a useful alternative to landcover mapping in the tropics with the cloud cover problem.

5.9 Number of training samples for classification

This study dealt with a reasonably large and homogenous landcover types (especially the main cover types) that are distinct in reflectance and therefore did not require too many samples in training the classifiers (Van Niel *et al.*, 2005). Moreover, for the minority cover types (Settlement/Bareground and Fallow/grassland (FG)) especially the FG, only three (3) points were collected in the field. This was because those areas had been converted into agroforestry stands and was no longer FG.

One of the major problems in image classification projects is the cost of acquiring training data. Random sampling has been observed as the most robust method for obtaining samples for training classifiers (Richards & Xiuping, 2008). However, due to the cost involved in data acquisition training is usually done by identifying pixels that are assumed to be homogenous independent fields or contiguous blocks.

Richards and Xiuping (2008) introduced a technique that works on the principle that the near neighbours of a user-defined training pixels are likely to belong to the same class. In this regard therefore, emphases on training a classifier is not based on number of location points collected in the field but on the number of pixels used for training the classifier. The method thus, deals with selection of larger regions (region growing) around available labelled training samples. Their study concluded that the optimal number of training pixels for training a classifier is about 1000, beyond which the resulting accuracy stabilizes.

Van Niel *et al.* (2005) also argued that the generally accepted rule in remote sensing application which defines the number of training samples (n) to be 10 – 30 times the number of bands (p) has been enforced universally without questioning its relevance to the particular project in hand (complexity of the discrimination problem). In their study, it was observed that 95% of the accuracy obtained using the number of samples equals 30 times the number of bands (i.e. $n = 30p$) could be achieved by using approximately $n = 2p$ *to* $4p$. This therefore implies that the number of samples required for training a classifier depends on the complexicity of the problem. A simple discrimination problem requires few training samples and a complex one requires more training samples. This may therefore provide a justification for the use of only 12 points in training (Table 6) the classifiers in this research.

6.0 CONCLUSION

The aim of this study was to develop a suitable method to improve the classification of different land and forest cover types for use in tropical environments where cloud cover is a major impediment to the use of multispectral data. Two main classification algorithms (MLC and OBIA) were applied on two different datasets – ALOS PALSAR and ASTER, and their combination. The results were compared and statistically tested. The Afram Headwaters Forest Reserve was chosen for this study for the reasons mentioned in Section 3.1. This chapter presents conclusions based on the research questions (set out in Section 1.5) and hypothesis (Section 1.6) tested in this study.

1. What relevant landcover information (classes) can be identified from the classification of SAR and ASTER data?

Four (4) landcover types can be identified from SAR data classification. The classes Natural Forest/Plantation, Agroforestry and Settlement can be reliably identified (Figure 19, Tables 8 and 9). However, Fallow/Grassland, which is also a relevant cover type in the area, could not be reliably identified (Tables 8 and 9). The Natural Forest and Plantation cover types could not be separated on the SAR data alone.

It is possible to separate Natural Forest and Plantation on the ASTER data alone. As a result, five (5) different landcover types can be identified on ASTER imagery which is a slight improvement compared to the SAR data alone.

2. Are there significant differences in the quality of landcover type classification obtained from MLC and OBIA on ASTER, SAR and ASTER+SAR data?

There was no significant difference in the classification results obtained for each dataset using MLC and OBIA. That is to say, using MLC and OBIA on the same data gave statistically the same results and therefore it is prudent to use the simpler method among the two. Statistically significant differences were, however, observed when maps from different datasets (e.g. SAR alone and ASTER alone) obtained by applying the same method (e.g. MLC) were compared / tested. When classifying ASTER, adding SAR gives very little (<4%) improvement. On the other hand, when classifying SAR, adding ASTER gives a significant improvement. It is therefore concluded that combining ASTER and SAR improves the classification of SAR in both MLC and OBIA by 14% and 21% respectively.

Classifying ASTER alone gives similar result as combining SAR and ASTER. Therefore in situations where cloud free ASTER is available it would make more sense to simply use ASTER alone rather than combining the two, which is time consuming and expensive. In areas where cloud cover is a problem, SAR gives good results, and if the cloud cover is total, or almost total, the use of SAR alone is the most feasible approach even though the accuracy is lower than ASTER. However, if the area is only partly covered by clouds, the addition of SAR to the cloud-free portions of ASTER will result in an improvement. The threshold for acceptable cloud cover (i.e. the % of cloud) on ASTER to merit a combination with SAR is a subject for further research.

3. Which kind of texture (in OBIA) combination gives the best results in ASTER, SAR and combined ASTER+SAR data classification?

The Standard deviation texture measure (Texture after Haralick) using the GLCM stddev in eCognition gave the best result in OBIA. However, it is anticipated that with the many texture combinations available in eCognition (for which, due to time constraints, not all could be explored in this research) better results could be obtained in future and the result of this study is a promising beginning.

4. Which filter window (in MLC) gives the best result in ASTER, SAR and combined ASTER+SAR data classification?

A better MLC classification accuracy of ASTER, SAR and combined ASTER+SAR data was obtained by using a 3x3 window and not 5x5 as hypothesised. Increasing the window size beyond 3x3 does not further improve classification accuracy but rather removes useful details from the classified image.

5. What is the quality of the landcover map produced from the overall best classification of ASTER, SAR and combined ASTER+SAR data?

The overall best classification result (82.09% and $\widehat{K} = 0.7435$) was obtained from the MLC classification of combined ASTER+SAR data. This is better in terms of magnitude than the result obtained from the OBIA for the same dataset but it is not significantly different statistically. If the aim of the project is to get rid of speckle noise then one can consider using OBIA. With the current gradual paradigm shift from “pixel based” towards “object based” image analysis, the study provides a useful contribution to this area of research.

7.0 RECOMMENDATIONS

Due to the want of time and limited resources, this study could not address all the aspects of improving the classification of different land and forest cover types using MLC and OBIA in the AHFR. And as is normal with scientific research, one can only do a little at a time to contribute to the realization and understanding of the complex world around us. The following recommendations are therefore made to provoke further research:

1. Further analyses on different textural combination available in Trimble eCognition or any other object based software (e.g. Imagine Objective) could be done to further study the improvement of SAR classification using OBIA.

2. The confusion matrix and kappa coefficient which have been a conventional accuracy assessment measure with varying criticisms from different researchers were used in this study. More emphases could be laid on accuracy assessment by comparing different accuracy assessment methods since there is no standard methodology so far in the remote sensing community.

3. To study the change in the landcover of the study area, a change detection research could be conducted using old and recently acquired time series SAR data of the AHFR.

4. Combination of ASTER and SAR resulted in the improvement of SAR by 14% - 21% as concluded by this study. It was also observed that the classification accuracy for ASTER alone without cloud cover was similar to that of the combined data, so it would make economic sense to work with ASTER alone when it is available. A possible further research need from the above conclusion is to find out at what threshold (percentage) of cloud cover on ASTER data is it not worth combining with SAR data for classification.

8.0 REFERENCES

Ainsworth, T. L., Kelly, J. P., & Lee, J. S. (2009). Classification comparisons between dual-pol, compact polarimetric and quad-pol SAR imagery. *ISPRS Journal of Photogrammetry and Remote Sensing, 64*(5), 464-471.

Ali, S. M., & Malik, R. N. (2010). Vegetation communities of urban open spaces: Green belts and parks in Islamabad city. *Pakistan Journal of Botany., 42(2)*, 1031-1039.

Anonymous. (1970). *Local production of industrial cellulose, Special Trials.*: Forest Products Research Institute, CSIR.

Apetorgbor, M. M., & Bosu, P. P. (2011). *Occurence and control of paper mulberry (Broussonetia papyrifera) in southern Ghana.* Kumasi: Forestry Research Institute of Ghana, Kumasi.

Benz, U., Baatz, M., & Schreier, G. (2001). *OSCAR-object oriented segmentation and classification of advanced radar allow automated information extraction.* Paper presented at the Geoscience and Remote Sensing Symposium, 2001. IGARSS '01. IEEE 2001 International.

Benz, U., & Pottier, E. (2001). *Object based analysis of polarimetric SAR data in alpha-entropy-anisotropy decomposition using fuzzy classification by eCognition.* Paper presented at the Geoscience and Remote Sensing Symposium, 2001. IGARSS '01. IEEE 2001 International.

Benz, U. C., Hofmann, P., Willhauck, G., Lingenfelder, I., & Heynen, M. (2004). Multiresolution, object-oriented fuzzy analysis of remote sensing data for GIS-ready information. *ISPRS Journal of Photogrammetry and Remote Sensing, 58(3 - 4) pp 239-258*

Birikorang, G., Okai, R., Asanso-Okyere, K., Afrane, S., & Robinson, G. (2001). *Ghana wood industry and log export ban study: Final report*. Accra: Forestry Commission.

Blaschke, T. (2010). Object based image analysis for remote sensing. *ISPRS Journal of Photogrammetry and Remote Sensing, 65*(1), 2-16.

Blaschke, T., Lang, S., Lorup, E., Strobl, J., & Zeil, P. (2000). Object-oriented image processing in an integrated GIS/remote sensing environment and perspectives for environmental applications. In A. Cremers & K. Greve (Eds.), *Environmental Information for Planning, Politics and the Public* (Vol. 2, pp. 555 - 570). Metropolis Verlag, Marburg,.

Bosu, P. P., Apetorgbor, M. M., & Refera, A. (2009). Ecology and management of tropical Africa's forest invaders. In: Invasive plants and forest ecosystems. (Ed. Kohli, R. K., Jose, S., Singh, H. P., Batish, D. R.): Taylor and Francis Group, USA. pp 355 - 376.

CARA. (2006). Land Use Primer. *What is the difference between Land use and Land Cover* Retrieved 15th December, 2011, from http://www.cara.psu.edu/land/lu-primer/luprimer01.asp

Carver, K. R., Cimino, J. B., Elaschi, C., Syvertson, M., Beal, R., Engman, T., Schaber, G., Ulaby, F. T., Weeks, W., Campbell, W., Carsey, F., et al. (1988). *SAR: Synthetic Aperture RADAR – Earth Observing System* (Instrument Panel Report). Washington D.C.: NASA

Castilla, G., Hay, G. J., & Ruiz, J. R. (2008). Size-constrained region merging (SCRM): An automated delineation tool for assisted photointerpretation. *Photogrammetric Engineering & Remote Sensing*(74(4)), 409 - 419.

Chu, H., Guisong, X., & Hong, S. (2007). SAR images classification method based on Dempster-Shafer theory and kernel estimate. *Journal of Systems Engineering and Electronics, 18*(2), 210-216.

Congalton, R. G. (1991). A review of assessing the accuracy of classifications of remotely sensed data. *Remote Sensing of Environment, 37*(1), 35-46.

Congalton, R. G. (2009). Assessing the accuracy of remotely sensed data Principles and practices (2nd ed.). Boca Raton: FL: CRC/Taylor & Francis.

Cramer, W., Bondeau, A., Schaphoff, S., Lucht, W., Smith, B., & Sitch, S. (2004). Tropical forests and the global carbon cycle: impacts of atmospheric carbon dioxide, climate change and rate of deforestation. *Philosophical Transactions of the Royal Society of London. Series B: Biological Sciences, 359*(1443), 331-343.

de Groot, R. S., Wilson, M. A., & Boumans, R. M. J. (2002). A typology for the classification, description and valuation of ecosystem functions, goods and services. *Ecological Economics, 41*(3), 393-408.

Delafontaine, M., Nolf, G., van de Weghe, N., Antrop, M., & de Maeyer, P. (2009). Assessment of sliver polygons in geographical vector data. *International Journal of Geographical Information Science, 23*(6), 719-735.

Dostovalov, M. Y., Ermakov, R. V., Moussiniants, T. G., & Vnotchenko, S. L. (2010). Comparison of Polarimetric Classification Results Using ALOS PALSAR Data. *Synthetic Aperture Radar (EUSAR), 2010 8th European Conference on*, 1-4.

Duveiller, G., Defourny, P., Desclée, B., & Mayaux, P. (2008). Deforestation in Central Africa: Estimates at regional, national and landscape levels by advanced processing of systematically-distributed Landsat extracts. *Remote Sensing of Environment, 112*(5), 1969-1981.

Dwomoh, F. K. (2009). *Forest fire and carbon emission from burnt tropical forest : the case study of Afram headwaters forest reserve, Ghana.* Unpublished MSc. Thesis, ITC, Enschede.

Ehlers, M., Gähler, M., & Janowsky, R. (2006). Automated techniques for environmental monitoring and change analyses for ultra high-resolution remote sensing data. *Photogrammetric Engineering & Remote Sensing, 72 (7)* 835 - 844.

FAO. (2010). *Global forest resources assessment 2010, Country Report: Ghana.* Rome: Forestry Department, Food and Agriculture Organization of the United Nations

Fernandez, M. Q. (2002). Polarimetric data for tropical forest monitoring studies at the Colombian Amazon. The Netherlands, Wageningen University. p. 160.

Flanders, D., Hall-Beyer, M., & Pereverzoff, J. (2003). Preliminary evaluation of eCognition object-based software for cut block delineation and feature extraction. *Canadian Journal of Remote Sensing, 29*(4), 441-452.

Foody, G. M. (2002). Status of land cover classification accuracy assessment. *Remote Sensing of Environment, 80*(1), 185-201.

Foody, G. M., Boyd, D. S., & Cutler, M. E. J. (2003). Predictive relations of tropical forest biomass from Landsat TM data and their transferability between regions. *Remote Sensing of Environment, 85*(4), 463-474.

Forestry Commisson Ghana. (2009a). International mechanisms on REDD. *Reduced Emissions from Deforestation and Degradation* Retrieved 12th June, 2011, from http://www.fcghana.com/page.php?page=290&section=28&typ=1&subs=314

Forestry Commisson Ghana. (2009b). National Forest Plantation Development Progamme Annual Reports. *2008 Annual report* Retrieved 15th December, 2011, from http://76.12.220.51/assets/file/Publications/Forestry_Issues/National%20Forest%20Plantation%20Development%20Programme/Annual%20Reports/nfpdp_annual%20report_2008(1).pdf

Forestry Commisson Ghana. (2009c). National Forest Plantation Development Programme. Retrieved 23rd June, 2011, from http://www.fcghana.com/page.php?page=291&section=28&typ=1

FORIG. (2011). Equitable forest reserve plantation revenue sharing in Ghana. Retrieved 15th December, 2011, from http://csir-forig.org.gh/Useful-Links/new-publications.html

Fransson, J. E. S., Magnusson, M., Olsson, H., Eriksson, L. E. B., Sandberg, G., Smith-Jonforsen, G., & Ulander, L. M. H. (23-28 July 2007). *Detection of forest changes using ALOS PALSAR satellite images.* Paper presented at the Geoscience and Remote Sensing Symposium, 2007. IGARSS 2007. IEEE International.

Gamanya, R., De Maeyer, P., & De Dapper, M. (2009). Object-oriented change detection for the city of Harare, Zimbabwe. *Expert Systems with Applications, 36*(1), 571-588.

Gaston, G., Brown, S., Lorenzini, M., & Singh, K. D. (1998). State and change in carbon pools in the forests of tropical Africa. *Global Change Biology, 4*(1), 97-114.

Haralick, R. M., Shanmugam, K., & Dinstein, I. H. (1973). Textural features for image classification. *Systems, Man and Cybernetics, IEEE Transactions on, 3*(6), 610-621.

Hay, G. J., & Castilla, G. (2008). Geographic Object-Based Image Analysis (GEOBIA): A new name for a new discipline Object-Based Image Analysis. In T. Blaschke, S. Lang & G. J. Hay (Eds.), (pp. 75-89): Springer Berlin Heidelberg.

Hoan, N. T., Tateishi, R., Bayan, A., Ngigi, T. G., & Lan, M. (2011, 24-29 July 2011). *Improving tropical forest mapping using combination of optical and microwave data of ALOS.* Paper presented at the Geoscience and Remote Sensing Symposium (IGARSS), 2011 IEEE International.

Husch, B., Beers, T. W., & Kershaw Jr., J. A. (Eds.). (2003). *Forest Mensuration* (4th ed.). New York: John Wiley & Sons, Inc.

IPCC (Ed.). (2003). *Good practice guidance for land use, land change and Forestry, IPCC National greenhouse gas inventories programme UNEP*: Institute for Global Environmental Strategies (IGES) for the IPCC, ISBN 4-88788-003-0.

Jarabo-Amores, P., Rosa-Zurera, M., Mata-Moya, D., & Vicen-Bueno, R. (2009, 5-7 May 2009). *Filtering to reduce speckle noise in SAR images.* Paper presented at the Instrumentation and Measurement Technology Conference, 2009. I2MTC '09. IEEE.

Jensen, J. R. (1996). .Introductory Digital Image Processing: a Remote Sensing Perspective, (Second ed., pp. 544 pp.). Saddle River, NJ: Prentice Hall.

Jensen, J. R. (2005). Introductory digital image processing, a remote sensing perspective, 3rd. Edition, (pp. 164-169; 322-328; 337-344; 372-378; 389-392; 393-398; 421-426; 468; 474-482; 506-509.). Upper Saddle River: Pearson Prentice Hall.

Jie, C., Jing, Z., Chunsheng, L., & Yinqing, Z. (2009). A novel speckle filter for SAR images based on information-theoretic heterogeneity measurements. *Chinese Journal of Aeronautics, 22*(5), 528-534.

Jong-Sen, L., Grunes, M. R., Ainsworth, T. L., Li-Jen, D., Schuler, D. L., & Cloude, S. R. (1999). Unsupervised classification using polarimetric decomposition and the complex Wishart classifier. *Geoscience and Remote Sensing, IEEE Transactions on, 37*(5), 2249-2258.

Lee, J. S., Wen, J. H., & Ainsworth, T. L. (2009). Improved Sigma filter for speckle filtering of SAR imagery. *IEEE Trans Geosci Remote Sensing, 47(1)* pp. 202-213.

Lefebvre, A., Corpetti, T., & Hubert-Moy, L. (2008). *Object-oriented approach and texture analysis for change detection in very high resolution images.* Paper presented at the Geoscience and Remote Sensing Symposium, 2008. IGARSS 2008. IEEE International.

Lillesand, T. M., Kieffer, R. W., & Chipman, J. W. (2008). *Remote sensing and image interpretation* (6th ed.). New York: John Wiley & Sons, Inc.

Ling, F., Li, Z., Chen, E., & Wang, Q. (2008). *Forest mapping with multi-temporal dual polarization ALOS PALSAR data*, Wuhan, China.

Lopez-Martinez, C., & Fabregas, X. (2003). Polarimetric SAR speckle noise model. *Ieee Transactions on Geoscience and Remote Sensing, 41*(10), 2232-2242.

Lu, D. S. (2006). The potential and challenge of remote sensing-based biomass estimation. *International Journal of Remote Sensing, 27*(7), 1297-1328.

Malik, R. N., & Husain, S. Z. (2006). Classification and ordination of vegetation communities of the Lohibehr reserve forest and its surrounding areas. Rawalpindi, Pakistan. *Pakistan Journal of Botany, 38*, 543-558.

Mallinis, G., Koutsias, N., Tsakiri-Strati, M., & Karteris, M. (2008). Object-based classification using Quickbird imagery for delineating forest vegetation polygons in a Mediterranean test site. *ISPRS Journal of Photogrammetry and Remote Sensing, 63*(2), 237-250.

McWilliam, A. (2000). A Plague on your house? Some impacts of Chromolaena odorata on Timorese livelihoods. *Human Ecology, 28*(3), 451-469.

Metz, J. J. (2009). Deforestation. In K. Rob & T. Nigel (Eds.), *International Encyclopedia of Human Geography* (pp. 39-50). Oxford: Elsevier.

Mitchell, A. L., Milne, A., Tapley, I., Lowell, K., Caccetta, P., Lehmann, E., & Zheng-Shu, Z. (2010). *Wall-to-wall mapping of forest extent and change in Tasmania using ALOS PALSAR data.* Paper presented at the Geoscience and Remote Sensing Symposium (IGARSS), 2010 IEEE International.

Munoz, S. R., & Bangdiwala, S. I. (1997). Interpretation of Kappa and B statistics measures of agreement. *Journal of Applied Statistics, 24*(1), 105-112.

Navulur, K. (2007). *Multispectral image analysis using the object-oriented paradigm*. Boca Raton, FL.: CRC Press.

Nguyen, N. T. (2010). *Estimation and mapping of above ground biomass for the assessment and mapping of carbon stocks in tropical forest using SAR data : A case study in Afram headwaters forest, Ghana.* Unpublished MSc. Thesis, University of Twente Faculty of Geo-Information and Earth Observation ITC, Enschede.

Nyoungui, A. N., Tonye, E., & Akono, A. (2002). Evaluation of speckle filtering and texture analysis methods for land cover classification from SAR images. *International Journal of Remote Sensing, 23*(9), 1895-1925.

Offinso South Municipal Assembly. (2006). District profile. Retrieved 29th October, 2011., from http://ghanadistricts.com/districts/?r=2&_=24&rlv=topology

Ouyang, Z.-T., Zhang, M.-Q., Xie, X., Shen, Q., Guo, H.-Q., & Zhao, B. (2011). A comparison of pixel-based and object-oriented approaches to VHR imagery for mapping saltmarsh plants. *Ecological Informatics, 6*(2), 136-146.

Platt, R. V., & Rapoza, L. (2008). An evaluation of an object-oriented paradigm for land use/land cover classification. *The Professional Geographer, 60*(1), 87-100.

Podest, E., & Saatchi, S. (1999). *Application of texture to JERS-1 SAR imagery for tropical forest land cover classification.* Paper presented at the Geoscience and Remote Sensing Symposium, 1999. IGARSS '99 Proceedings. IEEE 1999 International.

Podest, E., & Saatchi, S. (2002). Application of multiscale texture in classifying JERS-1 radar data over tropical vegetation. *International Journal of Remote Sensing, 23*(7), 1487-1506.

Pohl, C., & Van Genderen, J. L. (1998). Review article Multisensor image fusion in remote sensing: Concepts, methods and applications. *International Journal of Remote Sensing, 19*(5), 823-854.

Rahman, M. M., Csaplovics, E., & Koch, B. (2005). An efficient regression strategy for extracting forest biomass information from satellite sensor data. *International Journal of Remote Sensing, 26*(7), 1511-1519.

Richards, J. A., & Xiuping, J. (2008). Using Suitable Neighbors to Augment the Training Set in Hyperspectral Maximum Likelihood Classification. *Geoscience and Remote Sensing Letters, IEEE, 5*(4), 774-777.

Riggan Jr., N. D., & Weih Jr., R. C. (2009). A comparison of pixel-based versus object-based land use/land cover classification methodologies. *Journal of the Arkansas Academy of Science, 63*, pp 145 - 152.

Rosenqvist, A., Shimada, M., Ito, N., & Watanabe, M. (2007). ALOS PALSAR: A pathfinder mission for global-scale monitoring of the environment. *Geoscience and Remote Sensing, IEEE Transactions on, 45*(11), 3307-3316.

Satellite Image Corporation. (2011). Characterization of satellite remote sensing systems. *Spatial Resolution* Retrieved 15th December, 2011., from http://www.satimagingcorp.com/characterization-of-satellite-remote-sensing-systems.html

Seetha, M., Sunitha, K. V. N., Lalitha Parameswari, D. V., & Ravi, G. (2010). *Accuracy assessment of object oriented and knowledge base image classification using P-trees.* Paper presented at the Computer and Automation Engineering (ICCAE), 2010 The 2nd International Conference.

Shackelford, A. K., & Davis, C. H. (2003). A hierarchical fuzzy classification approach for high-resolution multispectral data over urban areas. *Geoscience and Remote Sensing, IEEE Transactions on, 41*(9), 1920-1932.

Skidmore, A. (2002). Accuracy assessment of spatial information : Spatial statistics for remote sensing. In A. Stein, F. Meer & B. Gorte (Eds.), (Vol. 1, pp. 197-209): Springer Netherlands.

Stigler, S. (2008). Fisher and the 5% level. *CHANCE, 21*(4), 12-12.
Sun, X. (2004). A comparison of object-oriented and pixel-based classification approachs using quickbird imagery. *ISPRS STM*(2005), pp. 281-284.
Thiel, C., Weise, C., Riedel, T., & Schmullius, C. (2006). *Object based classification of L-band SAR data for the delineation of forest cover maps and the detection of deforestation.* Paper presented at the Conference on OBIA - 2006.
Toan, L. T., Picard, G., Martinez, J. M., Melon, P., & Davidson, M. (2001). *On the relationships between radar measurements and forest structure and biomass.* Paper presented at the Proceedings of the third international symposium on retrieval of bio- and geophysical parameters from SAR data for land applications, Sheffield, UK.
Townshend, J. R. G., Justice, C. O., Gurney, C., & McManus, J. (1992). The effect of mis-registration on the detection of vegetation change. *IEEE Transactions on Geosciences and Remote Sensing, 30*, 1054–1060 pp.
Tupin, F. (2010). Fusion of optical and SAR images. In U. Soergel (Ed.), *Radar Remote Sensing of Urban Areas* (Vol. 15, pp. 133-159): Springer Netherlands.
UNEP. (2011). UN - REDD Programme. *The UN-REDD Programme Strategy 2011 - 2015* Retrieved 9th August, 2011, from http://www.unep.org/forests/Portals/142/docs/UN-REDD%20Programme%20Strategy.pdf
Van Niel, T. G., McVicar, T. R., & Datt, B. (2005). On the relationship between training sample size and data dimensionality: Monte Carlo analysis of broadband multi-temporal classification. *Remote Sensing of Environment, 98*(4), 468-480.
Vanderwoude, C., Scanlan, J. C., Davis, B., & Funkhouser, S. (2005). *Plan for national delimiting survey for Siam weed. Natural Resources and Mines Land Protection Services. Queensland Government, Queensland.*
Walessa, M., & Datcu, M. (2000). Model-based descpeckling and information extraction from SAR images. *IEEE TransGeosci Remote Sensing, 38(9)* pp. 2258-2269.
Walker, W. S., Stickler, C. M., Kellndorfer, J. M., Kirsch, K. M., & Nepstad, D. C. (2010). Large-Area Classification and Mapping of Forest and Land Cover in the Brazilian Amazon: A Comparative Analysis of ALOS/PALSAR and Landsat Data Sources. *Selected Topics in Applied Earth Observations and Remote Sensing, IEEE Journal of, 3*(4), 594-604.
Wulder, M. A., Hall, R. J., Coops, N. C., & Franklin, S. E. (2004). High spatial resolution remotely sensed data for ecosystem characterization. *BioScience, 54*(6), 511-521.
Xie, Z., Roberts, C., & Johnson, B. (2008). Object-based target search using remotely sensed data: A case study in detecting invasive exotic Australian Pine in south Florida. *ISPRS Journal of Photogrammetry and Remote Sensing, 63*(6), 647-660.
Youshi, Y., Baojun, Z., & Linbo, T. (2009). *SAR and visible image fusion based on local non-negative matrix factorization.* Paper presented at the Electronic Measurement & Instruments, 2009. ICEMI '09. 9th International Conference.
Yu, Q., Gong, P., Chinton, N., Biging, G., Kelly, M., & Schirokauer, D. (2006). Objectbased detailed vegetation classification with airborne high spatial

resolution remote sensing imagery. *Photogrammetric Engineering & Remote Sensing, 72 (7)*, 799 - 811.

9.0 APPENDICES

Appendix A – Local names of *C. odorata* in different parts of Ghana (Source: Timbilla and Braimah, 1994)

Name	Region	Meaning/Significance of Name
Acheampong	Central, Eastern, Greater Accra, Western, Ashanti, Brong Ahafo, Northern and Volta.	Name of Head of State
Topaye	Central/Western	Spreader
Krawuni	Western/Brong Ahafo	Send for your mother
Abaafo	Western	New entrant
Bompowder	Western/Central	Powder me up (reference to seed)
Sukusuku	Western	Unknown
Woafa me fuo	Brong Ahafo	You have taken my farm
Adiawuo	Brong Ahafo	Killer
Wo amma me gye	Brong Ahafo	I am taking over if you are not coming
Alisi	Western	Name of a church
Busia	Western/Central	Name of Head of State

Appendix B – List of class I, II & III natural forest tree species in Ghana

CLASS NAME / MEANING	SCIENTIFIC NAME	COMMON NAME
CLASS I SPECIES (These are species of major economic importance)	*Milicia excelsa*	Odum, Iroko
	Entandrophragma angolense	Edinam
	Entandrophragma cylindricum	Penkwa, Sapele
	Entandrophragma utile	Ashanti cedar, Utile
	Khaya anthotheca	White Mahogany
	Khaya grandifoliola	Mahogany
	Khaya ivorensis	Mahogany Dubini
	Tieghemella heckelli	Makore, Abacu, Baku
	Nauclea diderrichii	Kusia, Opepe
	Pericopsis elata	Afromosia, African Teak
	Lovoa trichilioides	African walnut, Dubini-biri
	Terminalia ivorensis	Emire
	Triplochiton scleroxylon	Wawa
	Tarrietia densiflora	Nyankom
CLASS II SPECIES (These are species of lesser economic importance)	*Entandrophragma candollei*	Penkwa-akowaa, Kosipo
	Guarea cedrata	Guarea, Light bosse, Kwabohoro
	Guarea thompsonii	Black guarea, Dark bosse
	Lophira alata	Kaku, Ekki
	Piptadeniastrum africanum	Dahoma
	Antiaris toxicaria	Kyenkyen
	Mansonia altissima	Mansonia
	Mitragyna ciliata	Subaha
	Mitragyna stipulosa	Subaha, Sofo
	Nesogordonia papaverifera	Danta
	Turraeanthus africanus	Avodire, Apapaya

CLASS III SPECIES (These are species of possible future economic importance)	*Albizia adianthifolia*	West African albizia
	Albizia ferruginea	Wiemfuosamina
	Albizia zygia	Okoro
	Afzelia africana	Papao
	Anopyxis klaineana	Kokoti
	Canariun schweinfurthii	Bediwunua, Eyere
	Celtis adolfi-friderici	Celtis / Esakosua
	Celtis zenkeri	Celtis / Esakokoo
	Combretodendron africanum	Essia
	Cylicodiscus gabunensis	Denya
	Cynometra ananta	Ananta
	Diospyros sanza-minika	Esono-afe, Ankyeyi, Esunseka
	Distemonanthus benthamianus	Bonsamdua, Ayan, Distemonanthus
	Erythrophleum guineense	Kassa, Sasswood, Ordeal tree
	Holoptelea grandis	Onakwa
	Mammea africana	Bompegya
	Pycnanthus angolensis	Otie
	Scottellia chevalierii	Koroko, Kruku
	Sterculia rhinopetala	Wawabima
	Strombosia glaucescens	Afina
	Terminalia superba	Ofram

Appendix C – Landcover Classification Scheme for AHFR

LANDCOVER CLASS (SET OF LABELS)	DESCRIPTION (SET OF RULES)
1. NATURAL FOREST	▪ Dense natural vegetation ▪ Less dense natural vegetation ▪ Riparian vegetation ▪ Admitted Cocoa farms
2. PLANTATION	▪ Young pure teak plantations >4yrs (Private and Government) ▪ Young teak, cedrella & indigenous mixed stands >4yrs (both private and government owned) ▪ Mature pure teak plantation ▪ Mature mixed species plantation
3. AGROFORESTRY	▪ Taungya plantations below 2/3 years ▪ Croplands within admitted farms
4. FALLOW / GRASSLAND	▪ Open vegetated areas (with basal area less than $5m^2$/ha) ▪ Grasslands and bushes ▪ Shrub vegetations
5. SETTLEMENT / BAREGROUND	▪ Unvegetated areas ▪ Settlements within the forest reserve ▪ Bareground or exposed soil surfaces ▪ Rocky areas

Appendix D – Field data collection sheet

FIELD DATA COLLECTION SHEET

Name of Recorder: .... Date: ..../......./2011 Previous Forest cover type:..

Plot No.			Slope			Stand Age					
X-Coordinate			Elevation			Current Forest cover type					
Y-Coordinate			Aspect			Crown cover (%)					
Tree No.	Species	DBH (cm)	Height (m)	Crown dia. (m)	Remarks	Tree No.	Species	DBH (cm)	Height (m)	Crown dia. (m)	Remarks
1						26					
2						27					
3						28					
4						29					
5						30					
6						31					
7						32					
8						33					
9						34					
10						35					
11						36					
12						37					
13						38					
14						39					
15						40					
16						41					
17						42					
18						43					
19						44					
20						45					
21						46					
22						47					
23						48					
24						49					
25						50					

Appendix E – Slope correction table

SLOPE CORRECTION TABLE

Plot size	$500m^2$

Slope%	Radius(m)	Slope%	Radius(m)	Slope%	Radius(m)
0	12.62				
1	12.62	36	13.01	71	13.97
2	12.62	37	13.03	72	14
3	12.62	38	13.05	73	14.04
4	12.62	39	13.07	74	14.07
5	12.62	40	13.09	75	14.1
6	12.63	41	13.12	76	14.14
7	12.63	42	13.14	77	14.17
8	12.64	43	13.16	78	14.21
9	12.64	44	13.19	79	14.24
10	12.65	45	13.21	80	14.28
11	12.65	46	13.24	81	14.31
12	12.66	47	13.26	82	14.35
13	12.67	48	13.29	83	14.38
14	12.68	49	13.31	84	14.42
15	12.69	50	13.34	85	14.45
16	12.7	51	13.37	86	14.49
17	12.71	52	13.39	87	14.52
18	12.72	53	13.42	88	14.56
19	12.73	54	13.45	89	14.6
20	12.74	55	13.48	90	14.63
21	12.75	56	13.51	91	14.67
22	12.77	57	13.53	92	14.71
23	12.78	58	13.56	93	14.74
24	12.79	59	13.59	94	14.78
25	12.81	60	13.62	95	14.82
26	12.82	61	13.65	96	14.85
27	12.84	62	13.68	97	14.89
28	12.86	63	13.72	98	14.93
29	12.87	64	13.75	99	14.97
30	12.89	65	13.78	100	15
31	12.91	66	13.81	101	15.04
32	12.93	67	13.84	102	15.08
33	12.95	68	13.87	103	15.12
34	12.97	69	13.91	104	15.15
35	12.99	70	13.94	105	15.19

A. de Gier - 2000

Appendix F – Screenshots of the OBIA segmentation process

(a) Segmented SAR data alone showing objects before classification

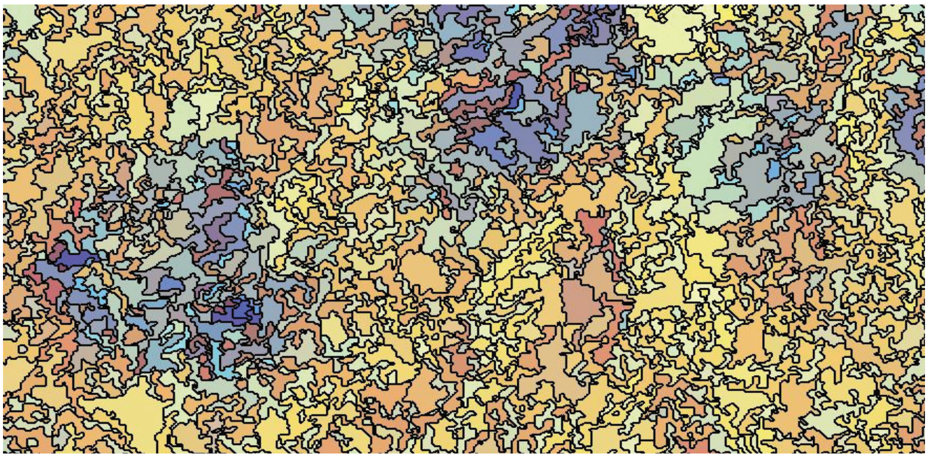

(b) Speckle noise elimination from SAR data alone after segmentation

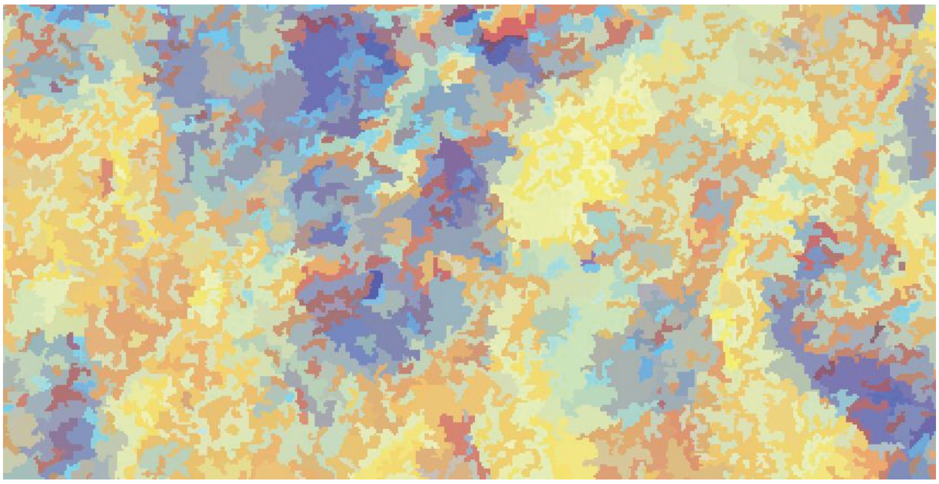

Appendix G – Photos from fieldwork

(a) Measurements of tree DBH and height in a teak plantation

(b) Rainy day in the field using plantain leaf as an "umbrella" and some illegal chain-sawing activities

Appendix H – Summary of classification accuracy of the three datasets using different filter windows

(a) Summary of classification accuracy of ASTER data alone using different filter windows

	BEFORE FILTERING			3X3 MAJORITY FILTER			5X5 MAJORITY FILTER			7X7 MAJORITY FILTER		
LANDCOVER	PRODUCER ACCURACY	USER ACCURACY	KAPPA	PRODUCER ACCURACY	USER ACCURACY	KAPPA	PRODUCER ACCURACY	USER ACCURACY	KAPPA	PRODUCER ACCURACY	USER ACCURACY	KAPPA
NF	100.00%	68.42%	0.6082	100.00%	65.00%	0.5657	100.00%	65.00%	0.5657	100.00%	65.00%	0.5657
P	69.57%	88.89%	0.8308	69.57%	88.89%	0.8308	69.57%	88.89%	0.8308	69.57%	88.89%	0.8308
AF	80.77%	80.77%	0.6857	80.77%	84.00%	0.7385	80.77%	84.00%	0.7385	80.77%	80.77%	0.6857
S	66.67%	66.67%	0.6510	100.00%	75.00%	0.7383	100.00%	75.00%	0.7383	100.00%	100.00%	1.0000
FG	0.00%	0.00%	-0.0308	---	---	0.0000	---	---	0.0000	---	---	0.0000
TOTALS	**77.61%**		**0.6800**	**79.10%**		**0.7025**	**79.10%**		**0.7025**	**79.10%**		**0.7003**

(b) Summary of classification accuracy of combined ASTER+SAR data using different filter windows

	BEFORE FILTERING			3X3 MAJORITY FILTER			5X5 MAJORITY FILTER			7X7 MAJORITY FILTER		
LANDCOVER	PRODUCER ACCURACY	USER ACCURACY	KAPPA	PRODUCER ACCURACY	USER ACCURACY	KAPPA	PRODUCER ACCURACY	USER ACCURACY	KAPPA	PRODUCER ACCURACY	USER ACCURACY	KAPPA
NF	100.00%	76.47%	0.7081	100.00%	72.22%	0.6553	92.31%	70.59%	0.6351	92.31%	66.67%	0.5864
P	73.91%	89.47%	0.8397	73.91%	85.00%	0.7716	73.91%	85.00%	0.7716	73.91%	89.47%	0.8397
AF	84.62%	84.62%	0.7486	84.62%	88.00%	0.8039	84.62%	84.62%	0.7486	84.62%	84.62%	0.7486
S	100.00%	100.00%	1.0000	100.00%	100.00%	1.0000	100.00%	100.00%	1.0000	100.00%	100.00%	1.0000
FG	0.00%	0.00%	-0.0308	0.00%	0.00%	-0.0308	0.00%	0.00%	-0.0308	0.00%	0.00%	-0.0308
TOTALS	**82.09%**		**0.7441**	**82.09%**		**0.7435**	**80.60%**		**0.7209**	**80.60%**		**0.7218**

(c) Summary of classification accuracy of SAR data alone using different filter windows

	BEFORE FILTERING			3X3 MAJORITY FILTER			5X5 MAJORITY FILTER			7X7 MAJORITY FILTER		
LANDCOVER	PRODUCER ACCURACY	USER ACCURACY	KAPPA	PRODUCER ACCURACY	USER ACCURACY	KAPPA	PRODUCER ACCURACY	USER ACCURACY	KAPPA	PRODUCER ACCURACY	USER ACCURACY	KAPPA
NF/P	83.33%	73.17%	0.4201	83.33%	73.17%	0.4201	83.33%	73.17%	0.4201	80.56%	72.50%	0.4056
AF	61.54%	69.57%	0.5027	61.54%	69.57%	0.5027	61.54%	69.57%	0.5027	61.54%	64.00%	0.4771
S	0.00%	0.00%	-0.0308	0.00%	0.00%	-0.0308	0.00%	0.00%	-0.0308	0.00%	0.00%	-0.0308
FG	---	---	0	---	---	0	---	---	0	---	---	0
TOTALS	**68.66%**		**0.4159**	**68.66%**		**0.4159**	**68.66%**		**0.4159**	**68.66%**		**0.4125**

Appendix I – Effect of post classification filtering on whole maps

Effect of post classification filtering on MLC classified ASTER image

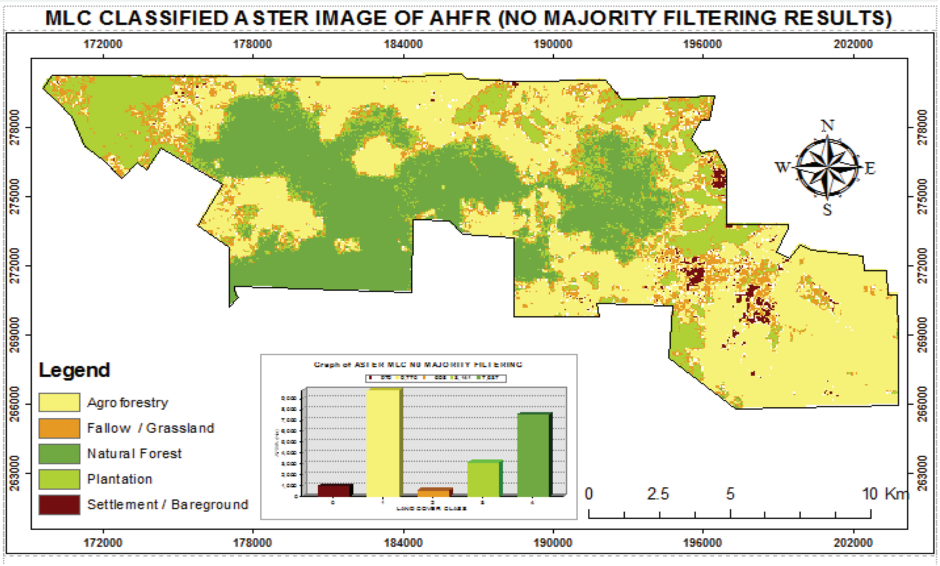

ASTER MLC classified Landcover map of AHFR without majority filtering.

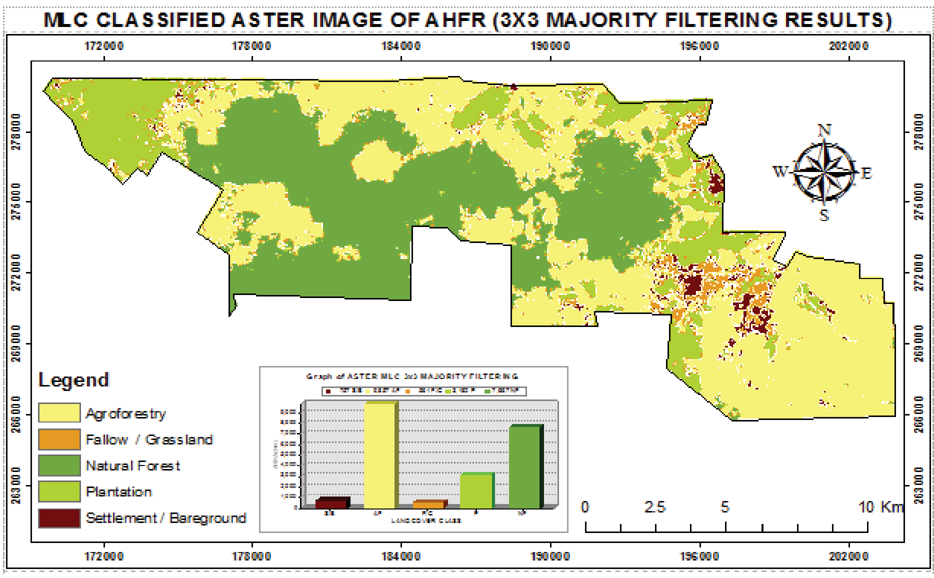

The effect of 3x3 majority filtering window on ASTER MLC map of AHFR.

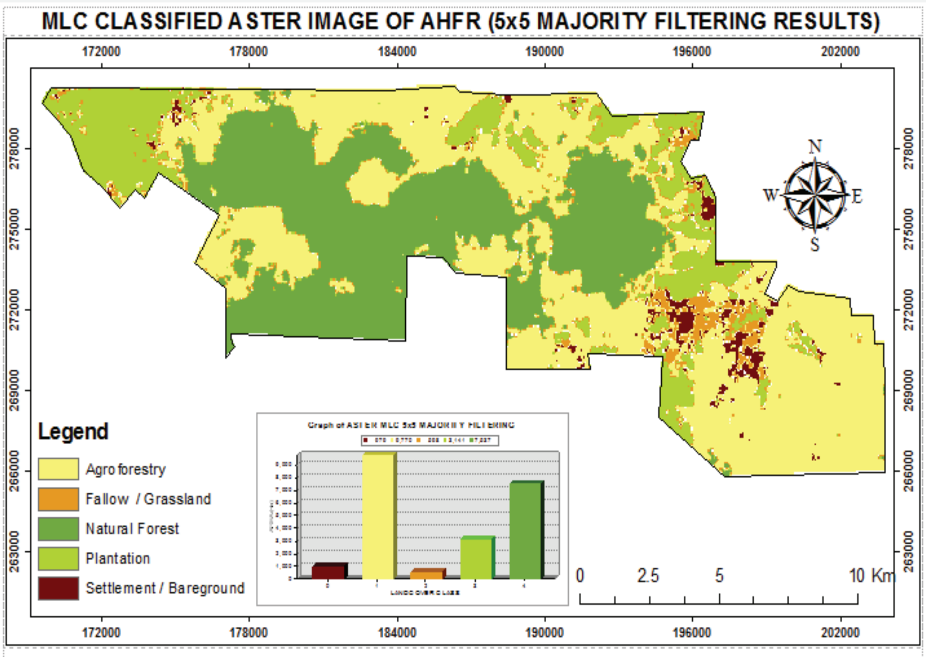

The effect of 5x5 majority filtering window on ASTER MLC map of AHFR.

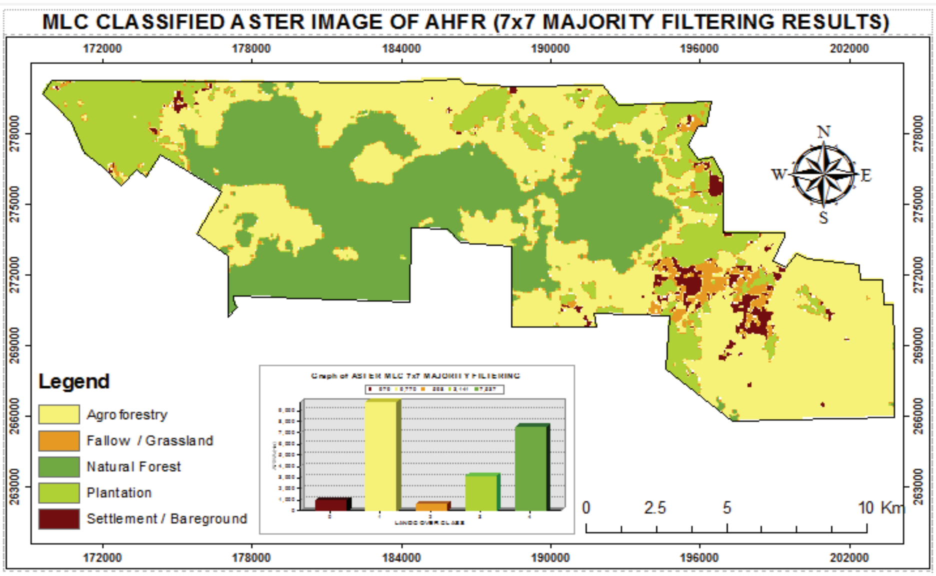

The effect of 7x7 majority filtering window on ASTER MLC map of AHFR.

Effect of post classification filtering on MLC classified SAR image

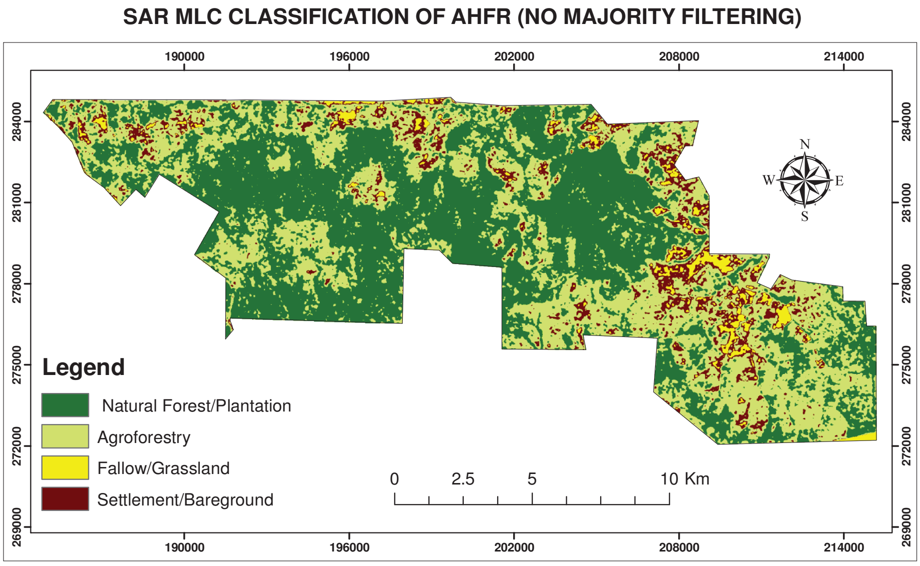

SAR MLC classified Landcover map of AHFR without majority filtering.

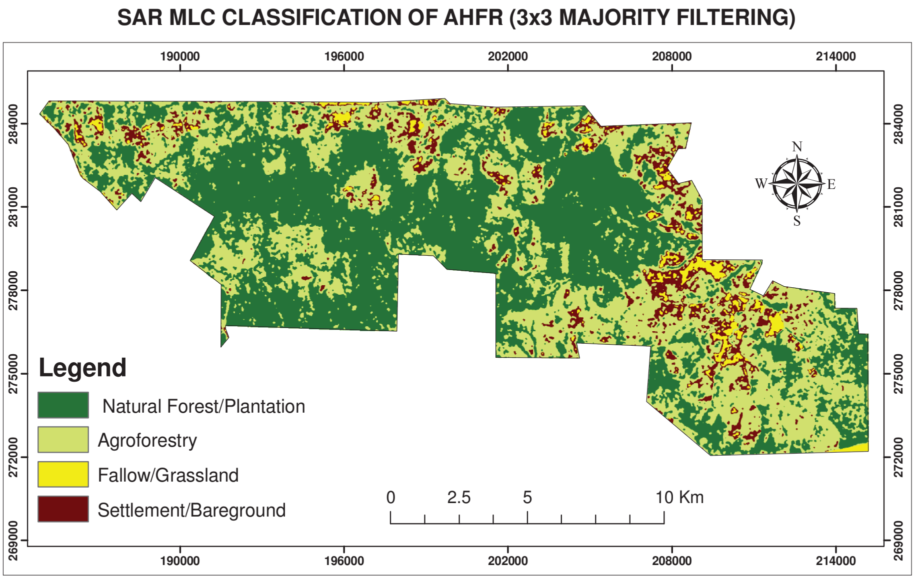

The effect of 3x3 majority filtering window on SAR MLC map of AHFR.

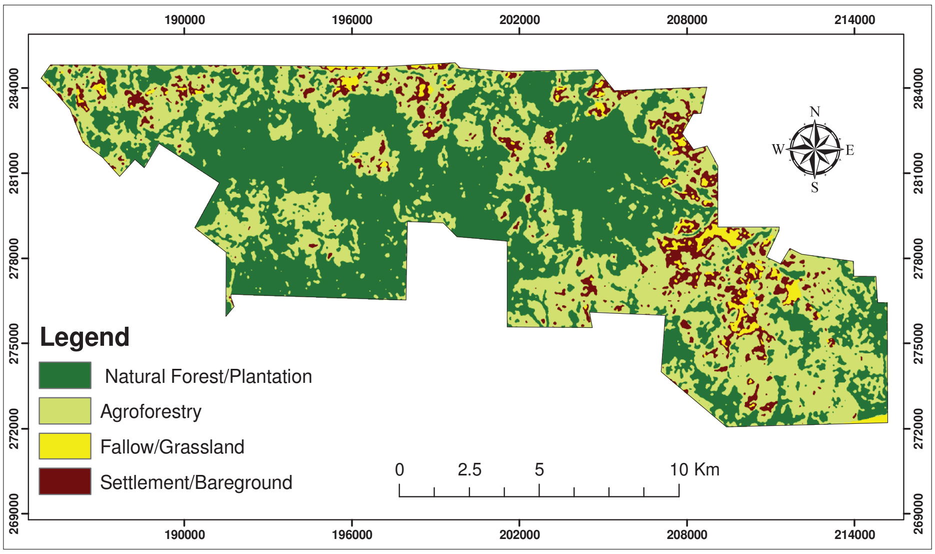

The effect of 5x5 majority filtering window on SAR MLC map of AHFR.

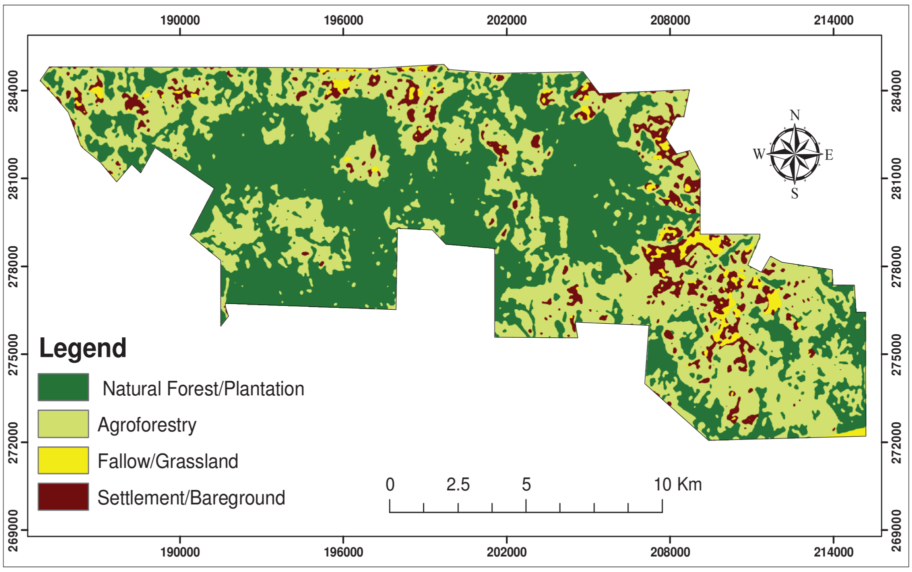

The effect of 7x7 majority filtering window on SAR MLC map of AHFR.

Effect of post classification filtering on MLC classified combined ASTER+SAR image

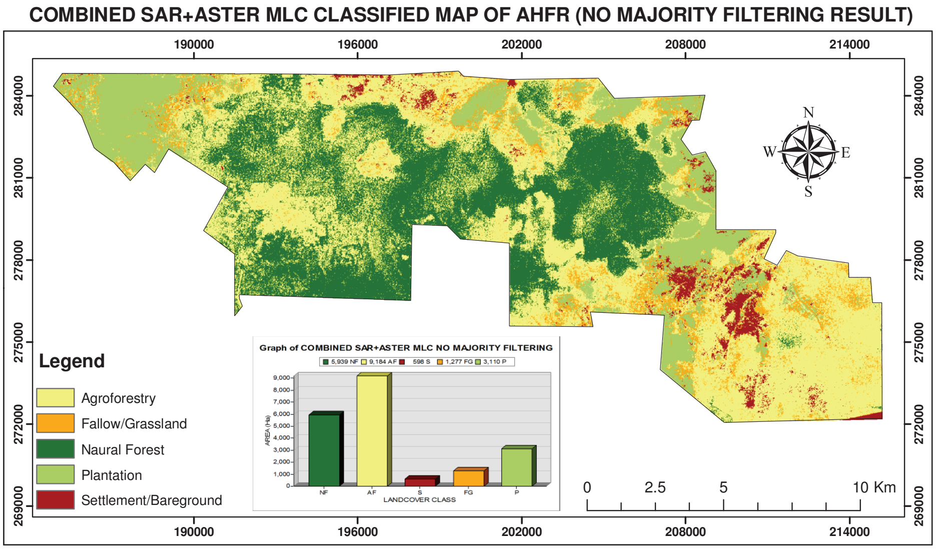

Combined ASTER+SAR MLC classified Landcover map of AHFR without majority filtering.

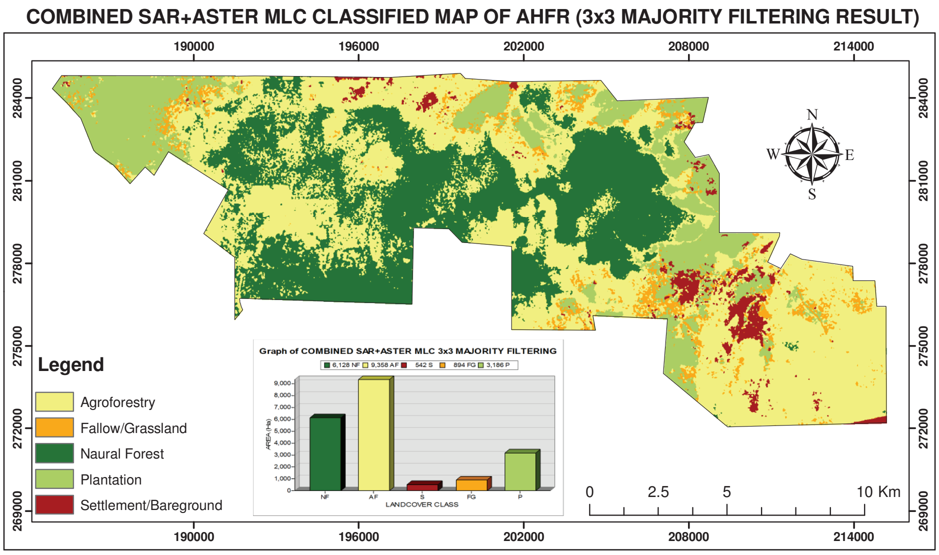

The effect of 3x3 majority filtering window on combined ASTER+SAR MLC map of AHFR.

COMBINED SAR+ASTER MLC CLASSIFIED MAP OF AHFR (5x5 MAJORITY FILTERING RESULT)

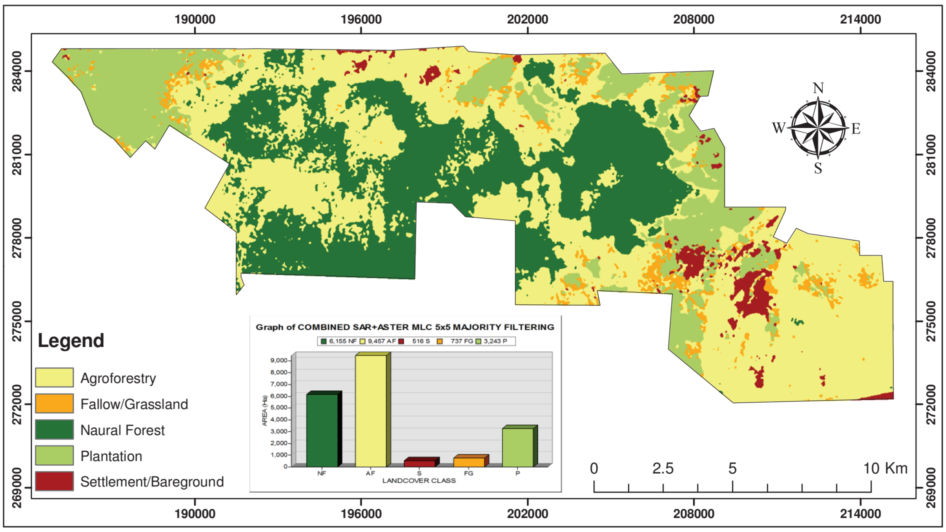

The effect of 5x5 majority filtering window on combined ASTER+SAR MLC map of AHFR.

COMBINED SAR+ASTER MLC CLASSIFIED MAP OF AHFR (7x7 MAJORITY FILTERING RESULT)

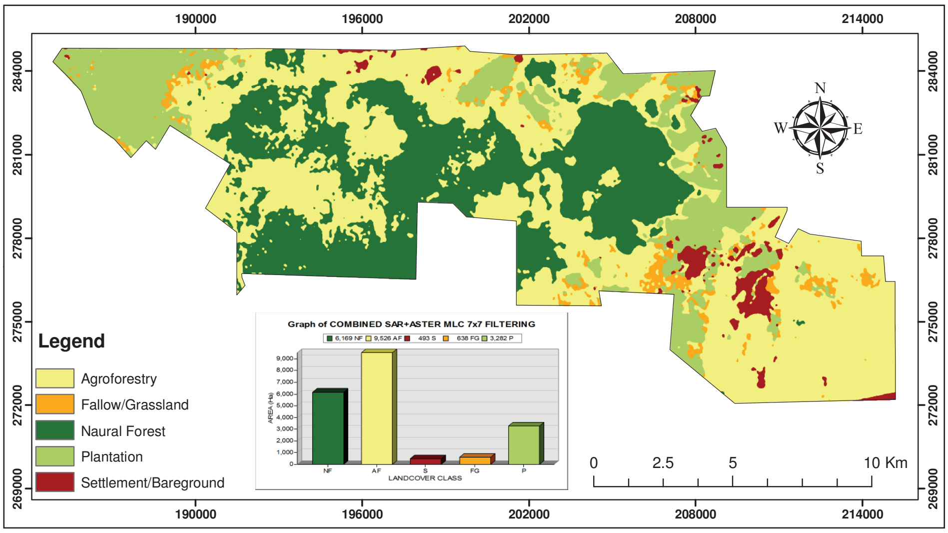

The effect of 7x7 majority filtering window on combined ASTER+SAR MLC map of AHFR.

Appendix J: Error matrices for the six (6) different classified maps

A1 and A2: Error matrices of MLC classified SAR data alone and OBIA classified SAR data alone

A1

		Reference Data				
		NFP	AF	S	FG	Row Total
Classified Data	NFP	30	9	0	2	41
	AF	5	16	2	0	23
	S	0	0	0	0	0
	FG	1	1	1	0	3
	Column Total	36	26	3	2	**67**

A2

		Reference Data				
		NFP	AF	S	FG	Row Total
Classified Data	NFP	25	15	0	1	41
	AF	10	8	1	1	20
	S	1	3	2	0	6
	FG	0	0	0	0	0
	TOTAL	36	26	3	2	**67**

A3 and A4: Error matrices of MLC classified ASTER data alone and OBIA classified ASTER data alone

A3

		Reference Data					
		NF	P	AF	S	FG	Row total
Classified Data	NF	13	3	4	0	0	20
	P	0	16	1	0	1	18
	AF	0	3	21	0	1	25
	S	0	1	0	3	0	4
	FG	0	0	0	0	0	0
	Column Total	13	23	26	3	2	**67**

A4

		Reference Data					
		NF	P	AF	S	FG	Row Total
Classified Data	NF	12	1	3	0	1	17
	P	0	15	1	0	1	17
	AF	1	7	20	0	0	28
	S	0	0	0	3	0	3
	FG	0	0	2	0	0	2
	Column Total	13	23	26	3	2	**67**

A5 and A6: Error matrices of MLC classified combined ASTER+SAR data and OBIA classified combined ASTER+SAR data

A5

		Reference Data					
		NF	P	AF	S	FG	Row Total
Classified Data	NF	13	2	2	0	1	18
	P	0	17	2	0	1	20
	AF	0	3	22	0	0	25
	S	0	0	0	3	0	3
	FG	0	1	0	0	0	1
	Column Total	13	23	26	3	2	**67**

A6

		Reference Data					
		NF	P	AF	S	FG	Row Total
Classified Data	NF	13	3	4	0	0	20
	P	0	17	3	0	1	21
	AF	0	2	16	0	1	19
	S	0	1	2	3	0	6
	FG	0	0	1	0	0	1
	Column Total	13	23	26	3	2	**67**